Pontificia Universidad Católica de Chile
Facultad de Ciencias Biológicas
Programa Doctorado en Ciencias Biológicas
Mención Biología Celular y Molecular

TESIS DOCTORAL:

"LA INHIBICIÓN DE LA QUINASA ABL ACTIVA AL FACTOR TFEB Y PROMUEVE LA LIMPIEZA CELULAR EN LA ENFERMEDAD LISOSOMAL DE NIEMANN-PICK C"

Por

PABLO ANDRÉS CONTRERAS SOTO

Enero 2019

Pontificia Universidad Católica de Chile
Facultad de Ciencias Biológicas
Programa Doctorado en Ciencias Biológicas
Mención Biología Celular y Molecular

TESIS DOCTORAL:

"LA INHIBICIÓN DE LA QUINASA ABL ACTIVA AL FACTOR TFEB Y PROMUEVE LA LIMPIEZA CELULAR EN LA ENFERMEDAD LISOSOMAL DE NIEMANN-PICK C"

Tesis entregada a la Pontificia Universidad Católica de Chile en cumplimiento parcial de los requisitos para optar al grado de Doctor en Ciencias Biológicas Mención en Biología Celular y Molecular

Por

PABLO ANDRÉS CONTRERAS SOTO

Director de tesis:	Dra. Alejandra Álvarez R.
Co-tutor de tesis:	Dra. Silvana Zanlungo M.
Comisión de tesis:	Dra. María Paz Marzolo C.
	Dra. María Isabel Yuseff S.
	Dra. Eugenia Morselli
	Dra. María Soledad Matus M.

Enero 2019

A mi abuela por enseñarme a vivir

A mi madre por su fuerza, constancia y amor

A mi hermana por mostrarme nuevos caminos

A mi esposa Lila por ser el mejor hallazgo de mi vida.

AGRADECIMIENTOS

Quisiera agradecer a todas las personas e instituciones que han permitido llevar a cabo esta tesis doctoral. En primer lugar quiero agradecer a las personas que confiaron en mis capacidades durante estos años y me dieron la oportunidad única de aprender y desarrollarme, incluso más allá de la ciencia, mis tutoras, la Dra. Alejandra Álvarez y la Dra. Silvana Zanlungo. Siento fortuna de haber sido parte de sus laboratorios, los que marcaron profundamente mi formación profesional.

También quiero agradecer a mis compañeros de laboratorio, quienes fueron fundamentales durante estos años y quienes a través de discusiones y sonrisas, me han ayudado e inspirado a seguir adelante. En especial quiero agradecer al Dr. Marcelo González y a la Dra. Lisbell Estrada, por sus sabios consejos, amistad y su infinita ayuda. A Pablo Tapia, al Dr. Alexis Martínez, Macarena de las Heras, Nancy Leal y Juan Castro por su apoyo fundamental para el desarrollo de esta tesis. También quiero agradecer a la Dra. María José Yañez, a Juan Esteban Oyarzún y Tamara Marín, por sus constantes colaboraciones y apoyo.

Quisiera también agradecer a David Chamorro, Juan Osorio, Adrián González, Cristián Valls y nuevamente al Dr. Marcelo González, quienes además de ser buenos compañeros de laboratorio, se convirtieron en los amigos que me acompañaron en este importante camino.

A Víctor Troncoso, Vanessa Morales, Paula Rivera, Ludwig Amigo, Paula García, Dra. Graciela Arguello, Marisol Oyarzún, Catalina De La Fuente, Rilda León, Dra. Lina Vargas, Diego Guzmán, Álvaro Cáceres, Esteban Asunción, y Pablo Jiménez, quienes agradezco su colaboración, disposición a escuchar mis presentaciones y todas esas conversaciones que más de alguna vez tuvimos y que me ayudaron a mejorar día a día.

También quiero agradecer a mi comisión de tesis, a la Dra. María Paz Marzolo, Dra. María Isabel Yuseff, Dra. Eugenia Morselli y a la Dra. María Soledad Matus, quienes desde un principio han sido fundamental en la discusión y estructuración de esta tesis.

Por otro lado, agradezco a mis colaboradores, al Dr. Andrea Ballabio, por permitirme ser parte de su laboratorio y por entregarme sus sabios concejos a la hora de desarrollar mi tesis. En especial quiero agradecer al Dr. Diego Medina, Dr. Gennaro Napolitano, Valerio Benedetti, Angela Zampelli, Nicolina Zampelli, Maria Matarese, Ciro Talotti, Rafaelle Pastore, Dra. Alessia Calcagni, Alessandra Esposito, Dra. Qing Yang, Ivana Peluso, Dra. Jlenia Monfregola, Dra. Chiara Di Malta, Dr. Mickael Decressac, Dr. Carmine Spampanato y al Dr. Carmine Settembre, quienes apoyaron mi trabajo en Italia. Además agradezco a los buenos amigos y amigas que descubrí en este camino en el extranjero; al Dr. Andrés Klein y su familia, al Dr. Leandro Soria, a la Dra. Sandra Pisonero y a María Belén Demattei, quienes me acompañaron y apoyaron en innumerables ocasiones e hicieron de mi estadía en Italia una experiencia maravillosa. Agradezco además a nuestra colaboradora, la Dra. Frances Platt, por su infinita amabilidad y sabiduría, que me permitieron no sólo desarrollar de buena manera mi tesis, si no que también aprender muchísimo en la universidad de Oxford, Inglaterra. Quisiera destacar a la Dra. María Fernández, Dawn Shepherd, Dra. Kerri Wallon y Ecem Kaya, quienes me ayudaron en

mis experimentos y fueron pacientes y muy amables. En especial quisiera agradecer a Claire Smith, David Smith y al Dr. David Priestman quienes fueron los amigos que hicieron de mi estadía en Inglaterra una experiencia muy enriquecedora.

A mis amigos de toda la vida, Nelson Guaman, Camilo Guaman y toda la familia Guaman, quienes agradezco su amistad y cariño incondicional.

Agradezco a la Comisión Nacional de Investigación Científica y Tecnológica (CONICYT), a la Pontificia Universidad Católica de Chile, al CARE, a la University of Pennsylvania Orphan Disease Center y al European Union's Horizon 2020 research and innovation programme (RISE), por el soporte financiero que permitieron realizar este trabajo.

Finalmente, agradezco profundamente a quienes dedico este trabajo, mi familia. A los González-Hódar, por su compañía, cariño y humor. A mi madre Erica, a mi abuela Carmen y mi hermana Francisca, gracias por su incondicional apoyo, esfuerzo y amor que hoy me tienen feliz alcanzando mis metas junto a ustedes. A mi esposa, Lila, por su amor incondicional, compañía y esfuerzo. Gracias por permitirme estar a tu lado. Te lo dedico con todo mi amor.

INDEX

FIGURE INDEX

ABBREVIATIONS

AD: Alzheimer disease

BBB: Blood-Brain Barrier

ABL: Non-receptor tyrosine kinase

CoIP: Co-immunoprecipitation

DIV: Days in vitro

DMEM: Dulbecco's modified Eagle's medium

DMSO: Dimethyl sulfoxide

DNA: Deoxyribonucleic Acid

F: Phenylalanine

GFP: Green Fluorescent Protein

HDAC: Histone Deacetylase

HPDC: Hydroxypropyl-ß-Cyclodextrin

IF: Immunofluorescence

IP: Immunoprecipitation

KO: knock Out

mRNA: messenger RNA

mTORC1: Mechanistic Target of Rapamycin Complex 1

NPC: Niemann-Pick type C

NPC1: Niemann-Pick type C 1 Protein

NPC2: Niemann-Pick type C 2 Protein

PBS: Phosphate buffered Saline

qPCR: Quantitative Polymerase Chain Reaction

RIPA: Radioimmunoprecipitation Assay Buffer

RNA: Ribonucleic acid

S or Ser: Serine

SDS: Sodium dodecyl sulfate

siRNA: Small interference RNA

TFEB: Transcription factor EB

WB: Western blot

WT: Wild type

Y or Tyr: Tyrosine

Y75F: Mutated TFEB, tyrosine residue 75 was mutated to phenylalanine residue

Y173F: Mutated TFEB, tyrosine residue 173 was mutated to phenylalanine residue

RESUMEN

Los lisosomas son organelos celulares que juegan un rol fundamental en la homeostasis celular al estar involucrados en procesos tales como: la reparación de la membrana plasmática, la degradación y el reciclaje de nutrientes, el metabolismo de macromoléculas y la autofagia. Deficiencias en proteínas lisosomales generan la acumulación de diversos tipos de moléculas en este organelo y son la causa de diferentes enfermedades lisosomales, tales como Niemann-Pick tipo C (NPC), la cual se caracteriza por presentar acumulación de colesterol lisosomal debido a mutaciones en los genes que codifican para las proteínas NPC1 ó NPC2.

Interesantemente, en el último tiempo se ha descrito al factor de transcripción EB (TFEB) como el regulador maestro de la biogénesis lisosomal y de la expresión de genes involucrados en la autofagia. La actividad de TFEB y su translocación al núcleo depende de su estado de fosforilación en las serinas 211 y 142, las que son fosforiladas principalmente por la serina/treonina quinasa mTORC1. En condiciones basales, TFEB está fosforilado en las serinas mencionadas anteriormente y se mantiene en el citoplasma debido a su acoplamiento a la chaperona citosólica 14-3-3.

En nuestro laboratorio se ha descrito previamente la activación de la tirosina quinasa ABL en la enfermedad NPC. La inhibición de ABL usando Imatinib, un inhibidor específico de la quinasa, previene la muerte neuronal en el cerebelo, y promueve una mejora de las habilidades motoras y la sobrevida de los ratones modelo de la enfermedad.

Adicionalmente, se ha descrito que el uso de inhibidores farmacológicos de ABL inducen el flujo autofágico y el incremento en la cantidad de lisosomas. Sin embargo, el

mecanismo celular por el cual la inhibición de ABL estaría induciendo estos cambios aún se desconoce.

Tomando en cuenta esta información y resultados preliminares, nos planteamos la siguiente hipótesis: *"La señalización de ABL promueve la localización citoplasmática de TFEB inhibiendo la limpieza celular y contribuyendo a la patogenia de la enfermedad lisosomal de Niemann-Pick C".*

Para corroborar nuestra hipótesis, primero evaluamos la translocación de TFEB al núcleo mediante la técnica de high-content screening utilizando distintos inhibidores de ABL. Encontramos que la inhibición de ABL mediante distintos inhibidores promueven la translocación de TFEB al núcleo. Encontramos los mismos resultados mediante fraccionamiento núcleo citoplasma, y al evaluar TFEB endógeno. Adicionalmente, al utilizar un siRNA contra ABL1 observamos el mismo fenómeno de translocación al núcleo y un incremento de la expresión de los genes blanco de TFEB. Estos resultados indican que la inhibición de ABL promueve la activación de TFEB.

Luego, evaluamos procesos biólogiocos descritos rio abajo de la activación de TFEB en condiciones de inhibición de ABL. Observamos que la inhibición de ABL incrementa el flujo autofágico en células H4 que sobreexpresan establemente el plásmido LC3-GFP-mRFP. Además, la inhibición de ABL utilizando Imatinib o un siRNA contra ABL1, incrementó los niveles proteicos de los lisosomas, lo que fue evaluado siguiendo los niveles de LAMP1 y la tinción de lysotracker. Interesantemente, observamos que los lisosomas se acoplan a la membrana plasmática al inhibir ABL, sugiriendo un incremento en el proceso de exocitosis lisosomal. Estos resultados indican que el incremento tanto del flujo autofágico, la cantidad de lisosomas como la de exocitosis lisosomal, procesos

regulados por la activación de TFEB, son eventos rio abajo de la inhibición ABL.

Por otro lado, evaluamos si esta activación de TFEB por la inhibición de ABL era dependiente o independiente de mTORC1. Para ello, evaluamos los niveles de fosforilación de las serinas 142 y 211 de TFEB utilizando anticuerpos específicos para estas serinas fosforiladas. Encontramos que el inhibidor de ABL no produce cambios en los niveles de fosforilación de la serina 142, y si reduce los niveles en la serina 211 de TFEB. Evaluamos la actividad de mTORC1 analizando la fosforilación de proteínas blanco de mTORC1, y en forma coherente con los resultados anteriores observamos que inhibidores de ABL, Imatinib o Nilotinib, no generan cambios en la actividad de mTORC1. Estos resultados indican que la inhibición de ABL activa a TFEB independiente de la actividad mTORC1.

Posteriormente, evaluamos si la tirosina quinasa ABL podría fosforilar en tirosina a TFEB. Mediante inmmunoprecipitación de TFEB y un ensayo de fosforilación in vitro, encontramos que la actividad de ABL es suficiente para promover un incremento en los niveles de fosforilación en tirosina de TFEB. Por otro lado, encontramos mediante mutaciones sitio dirigidas de TFEB que la tirosina 173 es relevante para mantener a TFEB en el citoplasma e impacta en los niveles fosforilación en S211. Nuestros resultados muestran por primera vez que ABL fosforila a TFEB en tirosina y que estas fosforilaciones son relevantes para su localización citoplasmática.

Debido a que ABL fosforila a TFEB en tirosina y su inhibición promueve su translocación al núcleo, quisimos evaluar si esta vía de señalización tendría un impacto en la limpieza celular, un fenómeno regulado por TFEB. En distintos modelos celulares en los cuales primero se promovió la acumulación de colesterol lisosomal, observamos que la inhibición

de ABL promueve la limpieza celular de este colesterol acumulado. Interesantemente, este fenómeno no ocurre al utilizar células nulas para TFEB, indicando que la inhibición de ABL promueve la limpieza celular a través de la activación de TFEB.

Posteriormente, evaluamos si esta vía de señalización ABL/TFEB participa en la acumulación de colesterol lisosomal en modelos de la enfermedad lisosomal de NPC. Encontramos en fibroblastos de pacientes de NPC que la quinasa ABL está activa, y que su inhibición promueve tanto la reducción en la acumulación de colesterol como la translocación de TFEB al núcleo. Esto se correlacionó con un incremento en los niveles de lysotracker y Lamp1 y de la expresión de genes blanco de TFEB en fibroblastos de pacientes NPC tratados con Imatinib y Nilotinib.

Finalmente, corroboramos mediante modelos in vivo de la enfermedad que la inhibición o ausencia de ABL promueve la reducción de acumulación de colesterol y la translocación de TFEB al núcleo en las neuronas de purkinje.

En resumen, hemos encontrado una nueva vía de señalización que involucra a ABL y TFEB. La inhibición de ABL promueve la translocación de TFEB al núcleo, incrementando la expresión de genes lisosomales y promoviendo la limpieza celular de colesterol en modelos de la enfermedad de NPC. De esta manera, la inhibición de la vía de señalización ABL/TFEB emerge como un blanco terapéutico no sólo para NPC, sino que también para las diversas enfermedades en las que la función lisosomal se ve disminuida.

ABSTRACT

Lysosomes are cellular organelles that play a fundamental role in cellular homeostasis because they are involved in different process such as: membrane repair, degradation and recycling of nutrients, macromolecules metabolism and autophagy. Deficiencies in lysosomal proteins promote the accumulation of different molecules in the organelle causing multiples lysosomal diseases, such as Niemann-Pick type C (NPC), which is characterized by lysosomal cholesterol accumulation due to mutations in the genes encoding for the NPC1 and NPC2 proteins.

Interestingly, in the last time the transcription factor EB (TFEB) has been described as the master regulator of lysosomal biogenesis and gene expression related to autophagy. The activity and nuclear translocation of TFEB depends on its phosphorylation status in serine 211 and 142, which are regulated by the serine/threonine kinase mTORC1. At basal conditions, TFEB is phosphorylated in these serines and is retained in the cytoplasm due to its attachment to the cytosolic chaperone 14-3-3.

Previously, our lab described that the tyrosine kinase ABL is activated in NPC disease. The Inhibition of this kinase using Imatinib, an ABL specific inhibitor, prevents the neuronal death in the cerebellum and improves the locomotor function and survival of the NPC mice.

In addition, it has been described that the use of pharmacological ABL inhibitors induces the autophagy flux and an increase in the lysosomal levels. Nevertheless, the cellular mechanism by which ABL inhibition induces these changes are still unknown.

Considering this data, the hypothesis of this thesis is the following: “ABL signaling promotes TFEB cytoplasmic localization, inhibiting cellular clearance and contributing to the pathogenesis of the lysosomal storage disease Niemann-Pick type C”.

To test our hypothesis, first we evaluated TFEB nuclear translocation by the high-content screening technique, using different ABL inhibitors. We found that ABL inhibition by these inhibitors promotes TFEB nuclear translocation. The same results were obtained analyzing nuclear-cytoplasmic fractions, as well as evaluating endogenous TFEB cellular localization. In addition, we observed the same results; TFEB nuclear translocation and an increase in the expression of TFEB target genes, using a siRNA against ABL1. These results indicate that ABL inhibition activates TFEB.

Then, we evaluated TFEB downstream cell biological process in conditions of ABL inhibition. We observed that ABL inhibition increases the autophagy flux in the stable H4 LC3-GFP-mRFP cell line. In addition, the results show that ABL inhibition, using Imatinib or a siRNA against ABL1 increases Lamp1 lysosomal protein levels and lysotracker staining. In addition, we found that under ABL inhibition lysosomes are attached to the plasma membrane,, suggesting an increase in lysosomal exocytosis. Thus, our results support the idea that the increase in autophagy flux, quantity of lysosomes and lysosomal exocytosis, all of them biological process that are regulated by TFEB, are downstream events of ABL inhibition.

On the other hand, we evaluated if TFEB activation induced by ABL inhibition is dependent or independent of mTORC1. To do that, we evaluated the phosphorylation levels in TFEB serine 142 and 211, using specific antibodies for them. We found that ABL inhibition does not change the levels of phosphorylated serine 142 and decreases the levels of

phosphorylated serine 211 on TFEB. Due to these results, we then evaluated the activity of mTORC1 following the phosphorylation of an mTORC1 target protein. We found that the ABL inhibitors, Imatinib or Nilotinib, do not change the activity of mTORC1. These results demonstrate that ABL inhibition activates TFEB independent of mTORC1.

Then, we assessed whether the tyrosine kinase ABL phosphorylates TFEB on tyrosine. Using TFEB immunoprecipitation and an in vitro phosphorylation assay, we found that the activity of ABL was enough to promote an increase in the TFEB tyrosine phosphorylation levels. Concordantly, site directed mutagenesis showed that TFEB tyrosine 173 is relevant for maintaining TFEB cytoplasmic localization and impact on the S211 phosphorylation levels. These results demonstrate that ABL phosphorylates TFEB on tyrosine and these phosphorylations are important to retain TFEB in the cytoplasm.

Subsequently, because ABL phosphorylates TFEB on tyrosine and its inhibition promotes TFEB nuclear translocation, we asked if this signaling pathway could have a role in cellular clearance, a phenomena that is regulated by TFEB. The results show that in different models in which cholesterol accumulation was promoted, ABL inhibition promotes cellular clearance cholesterol accumulated in lysosomes. This clearance effect was not observed in TFEB knock out cells, demonstrating that ABL inhibition promotes cellular clearance in a TFEB dependent way.

The next step was to evaluate if the ABL/TFEB signaling pathway was relevant in the NPC lysosomal disease, which is characterized by lysosomal cholesterol accumulation. Our data show that in fibroblast from NPC patients, ABL kinase is active, and its inhibition promotes a reduction in cholesterol accumulation and TFEB nuclear translocation. These results correlates with an increase in Lamp1 and lysotracker levels and in TFEB target

gene expression, measured in fibroblast from NPC patients treated with the ABL inhibitors, Imatinib and Nilotinib.

Finally, we corroborated using in vivo models of the disease, that the inhibition or absence of ABL promotes a reduction in cholesterol accumulation and TFEB translocation to the nucleus in the purkinje neurons.

In summary, we found a novel-signaling pathway, which involves the ABL kinase and TFEB. The inhibition of ABL promotes TFEB nuclear translocation, increasing lysosomal gene expression and causing an increase in cellular clearance in NPC models. Therefore, inhibition of ABL/TFEB signaling pathway arises as a therapeutic target not only for NPC disease, but also for different diseases that are characterized by lysosomal dysfunction.

1. INTRODUCTION

1.1 Niemann-Pick type C disease.

Niemann-Pick type C (NPC) disease is a lysosomal cholesterol storage disorder resulting from loss-of-function mutations in either the *NPC1* or *NPC2* genes (Carstea et al., 1997; Naureckiene et al., 2000). Both genes encode the NPC1 or NPC2 cholesterol transport proteins, and their deficiency leads to the pathogenic accumulation of cholesterol within the late endosomal/lysosomal compartment (Kwon et al., 2009; Schulze and Sandhoff, 2011; Walkley and Suzuki, 2004). In addition to cholesterol, other lipids are accumulated in NPC cells, among them, lactosylceramide, glucosylceramide, GM2 and GM3 glycosphingolipids and sphingosine (Lloyd-Evans et al., 2008; Pentchev et al., 1984; Sturley et al., 2004).

Patients with NPC disease present liver and pulmonary damage and progressive neurodegeneration that lead to an early death (Patterson et al., 2012).

95% of NPC cases arise from mutations of the gene that codes for the NPC1 protein, and mutations in the NPC2 gene are responsible for the remaining 5% of NPC cases (Patterson et al., 2012). A variety of mutations have been described in NPC patients, with a marked correlation between the loss of NPC1 or NPC2 function and the severity of the disease symptoms (Park et al., 2003; Vanier, 2010). The most common form of NPC disease is the juvenile or classic in which the patient usually live until their pre-teens and is characterized by the presence of several neurological and motor symptoms, progressive ataxia and dementia in later stages of the disease (Patterson et al., 2012). Recent

estimates indicate a prevalence of NPC of 1:120,000 live births, but this likely represents an underestimate, as the disease may be under-diagnosed due to its highly heterogeneous presentation (Mengel et al., 2013; Patterson et al., 2012).

NPC is characterized by neurodegeneration in the Central Nervous System (CNS) and the presence of several neurological and motor symptoms, including vertical supranuclear gaze palsy (VSPG), dystonia, progressive ataxia and dementia in later stages of the disease. These symptoms are associated with CNS damage, including hipomyelination, swollen meganeurite formation, neuroaxonal dystrophy and extensive growth of new ectopic dendrites as well as formation of neurofibrillary tangles (NFTs) (Paul et al., 2004; Walkley and Suzuki, 2004). Several regions of the CNS are affected, such as the hippocampus, basal ganglia and the cerebral cortex (Walterfang et al., 2010). As the disease progresses, neuronal cell death is particularly evident in Purkinje cells of the cerebellum (Lopez and Scott, 2013; Walkley and Suzuki, 2004). The loss of cerebellar Purkinje neurons has been extensively reported in NPC animal models, including the NPC cat and mouse models (Alvarez et al., 2008; Ko et al., 2005; Walkley and Suzuki, 2004; Zhou et al., 2011), being the NPC1 malfunction the main responsible for this cell death (Lopez et al., 2011).

Although NPC disease etiology has been previously investigated, treatments today are basically symptomatic. Currently, there is no curative treatment for this devastating and fatal neurodegenerative disorder, nevertheless, the NPC researchers heavily focuses on therapies that help to improve two central hallmarks: i) promotes the clearance of the cholesterol accumulated into the lysosomes and ii) decrease the neuronal damage.

1.2 Promoting cellular clearance in NPC.

Regarding the main hallmark in NPC research, lysosomal cholesterol accumulation, several therapeutics approaches are currently been tested for the disease. Among the cholesterol-binding agents, hydroxypropyl-ß-cyclodextrin (HPCD) appears to be the most promising drug (Sturley et al., 2009). However, it is necessary to consider data that shows limited or no blood-brain barrier (BBB) penetration of HPCD followed by its systemic administration (Calias, 2017).y The treatment of NPC mice with HPCD significantly reduces neurodegeneration and hepatic disease and increase lifespans of the mice, suggesting a potential therapeutic approach for the treatment of individuals with NPC (Vance and Peake, 2011). Although the mechanisms by which HPCD mediates these beneficial effects are still unknown, is known that the liberated cholesterol flow into the cytosolic ester pool, thereby suppressing sterol synthesis and reducing the expression of macrophage-associated inflammatory genes. However, although HPCD has displayed promising effects on the brain and liver, it has had little to no effect on lung dysfunction, which constitutes another important issue in NPC pathology (Muralidhar et al., 2011). Regrettably, the first results of a clinical trial on NPC patients conducted by National institute of health (NIH) were not very encouraging. (https://www.sciencemag.org/news/2018/11/drug-rare-disease-disappoints-key-trial).

On the other hand, the Miglustat (N-butyldeoxynojirimycin) is currently approved in the European Union for the treatment of progressive neurological manifestations in patients with NPC. Miglustat inhibits glucosylceramide synthase enzyme, which catalyzes the first step in glycosphingolipid synthesis (Butters et al., 2003; Platt et al., 1994). Miglustat can cross the BBB (Treiber et al., 2007), and treatment of NPC mouse and cat models with this drug reduces glycosphingolipid accumulation and pathology in the brain, delays the onset

of neurological symptoms and increases survival (Zervas et al., 2001). In human patients, Miglustat treatment reduces pathological lipids storage, improves endosomal uptake and normalizes lipids trafficking in peripheral blood B-lymphocytes (Lachmann et al., 2004).

Most recently, a new approach to reduce the cholesterol accumulation in NPC involves the use of histone deacetylase (HDAC) inhibitors (HDACi). HDACs are a group of eighteen proteins with deacetylase activity, which are responsible for histone deacetylation, promoting a more compact chromatin conformation, inaccessible to the transcriptional machinery (Yang and Seto, 2003, 2008). The first report concerning NPC and HDACs showed that treatment with pan-HDACs inhibitors, such as TSA, LBH-589 and SAHA, reduces cholesterol accumulation in NPC human fibroblasts due to an increased NPC1 protein expression (Munkacsi et al., 2011; Pipalia et al., 2011). Interestingly, TSA treatment increases the mRNA levels of proteins responsible for intracellular cholesterol transport and metabolism and lipoprotein endocytosis, such as, Npc1, ApoE, ABCA1 and CYP46A1 (Nunes et al., 2013; Pipalia et al., 2011). In addition, the neuroblastoma cell line SH-SY5Y treated with TSA, reduces the expression of the genes responsible for the cholesterol synthesis and uptake (Nunes et al., 2013) and the treatment with the HDAC inhibitor valproic acid of neuronal stem cells from Npc1 KO mice, showed improved neuronal differentiation, neuronal gene expression and cholesterol accumulation compared with the NPC control cells (Kim et al., 2007).

The potential use of HDAC inhibitors for NPC is under investigation and their capacity to cross BBB has to be evaluated. However, based on that its effect depends on NPC1 expression, it could be visualized that it may not work for all NPC patients, especially on that suffer NPC2 mutations or NPC1 null mutations.

Interestingly, an improvement in the cross of the BBB of HDACi and HPCD using polyethylene glycol (PEG) was recently published (Alam et al., 2016). Treatment of NPC mice with this combination comprising the HDACi Vorinostat, HPCD and PEG, increased histone acetylation, preserved neuritis and Purkinje cells, delayed symptoms of neurodegeneration, and extended mouse life span from 4 to almost 9 months. Nevertheless, results related with cholesterol accumulation are not shown in this study (Alam et al., 2016).

1.3 The ABL tyrosine kinase involvement in NPC.

Regarding the second hallmark in NPC research, that is to decrease the neuronal damage and death, our laboratory has shown that the tyrosine kinase ABL plays a key role in the neurodegenerative process observed in NPC.

ABL is a non-receptor tyrosine kinase involved in a variety of cell biology process, such as, cytoskeleton regulation, cell cycle and apoptosis (Schlatterer et al., 2011a). ABL activation and its autophosphorylation can be induced, by DNA damage, ER stress and oxidative stress among others, and as consequence, ABL nuclear translocation is triggered. Indeed, ABL has three nuclear localization signals and one nuclear export signal, with allow a dynamic transport between the cytosol and nucleus in response to different stimuli (Hantschet et al., 2004; Greuber et al., 2013). Nevertheless, in basal conditions, ABL is retained in the cytoplasm by the chaperone cytosolic 14-3-3 (Yoshida et al., 2005).

ABL in addition to Arg are members of the ABL family. The *ABL1* gene was first identified as the cellular homolog of the oncogene in Abelson murine leukemia virus genome (Goff et

al., 1980; Greuber et al., 2013). Later, was identified as the oncogene associated with the development of chronic myelogenous leukemia (CML), which is an oncogene formed by the translocation between chromosome 9 and 22, producing the Bcr-Abl fusion protein, also known as Philadelphia chromosome (Ben-Neriah et al., 1986; Greuber et al., 2013).

The ABL family is organized into three-homology domains: i) SH1 (tyrosine kinase catalytic core); ii) SH2 (docking motif for phosphorylated tyrosine residues); and iii) SH3 (which binds to sequences rich in proline). The carboxy-terminal portion of ABL has proline-rich motifs that interacts with the SH3 domains of other proteins, such as p53 (Goga et al., 1995), and motifs to interact with globular (G) and filamentous (F)-actin (Van Etten et al., 1994), and DNA (David-Cordonnier et al., 1999).

In addition, alternative splicing produces two ABL isoforms: isoform 1a which is cytosolic and isoform 1b, which is myristoylated in the N-terminal region and is associated with membranes (Hantschel et al., 2003) (Figure 1).

The activation of ABL can be induced by tyrosine phosphorylation. Tyrosine 412, within the catalytic domain and tyrosine 245, within the SH2-kinase domain linker, which when phosphorylated produce the self-activation of ABL (Hantschel et al., 2003). In fact, these phosphorylation reactions can be catalyzed by members of the family of Src kinases or by trans-phosphorylation between ABL proteins (Brasher and Van Etten, 2000).

The tyrosine kinase ABL has been implicated in several neurodegenerative processes, and its activity is increased in several animal models of Alzheimer Disease (AD) (Alvarez et al., 2004; Cancino et al., 2008), Parkinson Disease (Ko et al., 2010), Amyotrophic Lateral Sclerosis (Katsumata et al., 2012) and NPC (Alvarez et al., 2008). In addition, ABL-overexpressing mice show severe neurodegeneration (Schlatterer et al., 2011b).

Figure 1

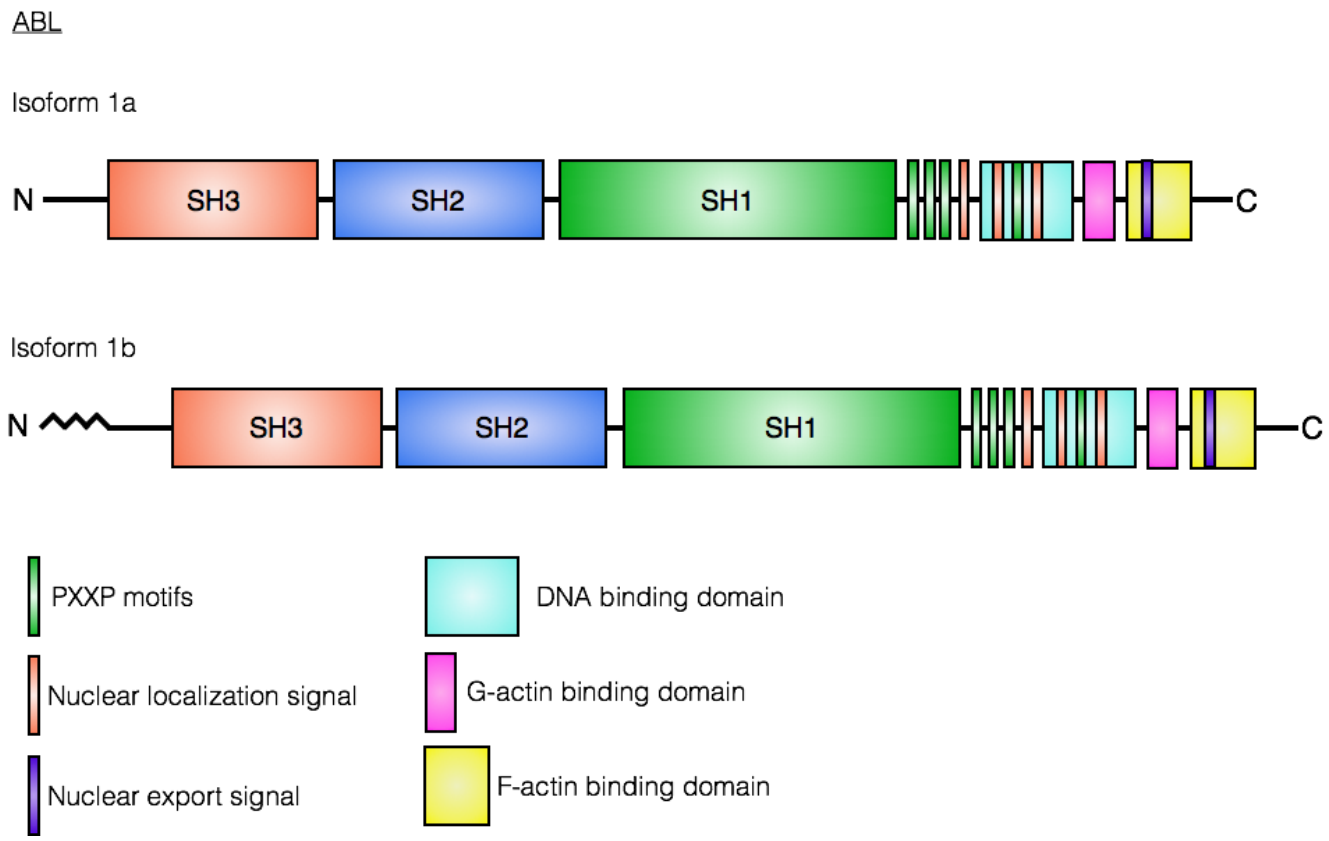

Figure 1. Molecular structure of ABL. ABL tyrosine kinase has a modular structure arranged in three domains: SH1 (tyrosine kinase domain), SH2 (to dock to phosphorylated tyrosine residues) and SH3 (binds to sequences rich in proline). In addition, in the carboxyl-terminal region ABL has proline-rich motifs (PXXP motifs) and binding domains to DNA, G-actin and F-actin. Also, ABL has two isoforms produced by alternative splicing; ABL 1b can be myristoylated, which is crucial for ABL acquires an inactive conformation.

Furthermore, activated ABL was found to be more abundant in hippocampus and also is involved in the signal cascade that regulates neuronal death in brain from AD mice models (Estrada et al., 2011; Jing et al., 2009).

The proapoptotic ABL/p73 pathway has been extensively studied and implicated in neurodegeneration (Estrada et al., 2011; Jacobs et al., 2006). In this pathway, ABL phosphorylates and activates the proapoptotic p73 transcription factor, leading to an increase in the expression of several proapoptotic target genes, such as NOXA, Scotin and PUMA (Klein et al., 2011). Interestingly, our lab found that both ABL and p73 are expressed in the cerebellum of the Npc1 KO mouse model (Alvarez et al., 2008). The expression of p73 target genes were also increased, and pro-apoptotic phosphorylated-p73 co-localized with both ABL and active caspase 3 in Purkinje cells. In NPC neuronal cultures, ABL/p73 mediated apoptotic neuronal death (Klein et al., 2011). Concordantly, inhibition of ABL with Imatinib, an FDA approved drug, decreased weight loss, neurological symptoms and cerebellar apoptosis, increasing the number of Purkinje cells and the survival of NPC mice (Alvarez et al., 2008).

Previously, our lab published that oxidative stress is an upstream event activating the ABL/p73 pro-apoptotic pathway. Indeed, treatment with the antioxidants N-acetyl-cystein (NAC) or vitamin E prevented apoptosis and the activation of the ABL /p73 pathway in NPC neuronal models (Klein et al., 2011; Marin et al., 2014; Yevenes et al., 2012). Moreover, our lab showed that a vitamin E-rich diet increased Purkinje cell survival, the gain of weight, locomotor coordination and survival of the NPC mice (Marin et al., 2014).

On the other hand our research group has published that, in both Alzheimer disease (Gonzalez-Zuniga et al., 2014) and in NPC models (Contreras et al., 2016), ABL activation

leads to increased histone deacetylase 2 (HDAC2) protein levels and activity. This over-activation of HDAC2 in NPC promotes a reduction in the expression of neuronal genes that express proteins involved in synaptic function and axogenesis. Interestingly, ABL inhibition reduces HDAC2 protein levels and activity, reverting gene repression of neuronal genes (Contreras et al., 2016).

In summary, our results and others show that, treatment with HDAC inhibitors increases the clearance of accumulated cholesterol in NPC human fibroblast (Pipalia et al., 2011) and treatment with ABL inhibitors improves neuronal death and reduces HDAC2 protein levels and activity in NPC mice (Alvarez et al., 2008; Contreras et al., 2016; Klein et al., 2011). Considering these antecedents, we wondered if ABL inhibition could mediate cholesterol clearance in NPC disease.

1.4 TFEB a master regulator of cellular clearance.

The master regulator of lysosomal biogenesis is the transcription factor that recognizes and bound to the E-box sequences (5'-CANNTG-3') (TFEB). The transcription factor TFEB is member of the microphthalmia family of basic helix-loop-helix– leucine-zipper (bHLH-Zip) transcription factors (MiT family). The MiT family also includes the transcription factors MITF, TFE3 and TFEC (Steingrimsson et al., 2004).

TFEB controls the expression of more than 50 genes. These genes conform the CLEAR network (Coordinated Lysosomal Enhancement And Regulation) (Settembre et al., 2013).

TFEB overexpression or activation leads to an increase in the number and degradative function of lysosomes, autophagic flux and lysosomal exocytosis, leading to clearance of

substrates stored in lysosomes (Medina et al., 2011; Sardiello and Ballabio, 2009; Settembre et al., 2011). This is particularly relevant in lysosomal storage diseases in which the degradative capacity of the cells is compromised.

It has been shown that TFEB induction ameliorates substrate accumulation in diverse models of lysosomal storage diseases such as, Pompe, Mucopolisacaridosis type IIIA and Mucosulfatosis (Medina et al., 2011; Spampanato et al., 2013; Wang et al., 2015). TFEB over-expressed in neuronal stem cells isolated from both mucopolysaccharidosis type IIIA (MPS-IIIA) and multiple sulfatase deficiency (MSD) mice, promotes a reduction in the glycosaminoglycans (GAGs) accumulation, a key characteristic found in this two lysosomal disorders (Medina et al., 2011). In addition, the degradation of GAGs is elevated in Hela cells that over-expresed TFEB (Sardiello et al., 2009), a process that requires the concerted action of different lysosomal hydrolases (Sardiello et al., 2009).

Interestingly, it has been reported that TFEB overexpression promotes cellular clearance ameliorating the phenotypes in a variety of neurodegenerative diseases with miss-folding proteins accumulation such as Alzheimer, Parkinson, and Huntington (Ballabio, 2016; Decressac et al., 2013; Napolitano and Ballabio, 2016; Polito et al., 2014; Sardiello et al., 2009; Tsunemi et al., 2012; Xiao et al., 2014; Xiao et al., 2015). As an example of this, the over-expression of TFEB in Huntington cell lines increased the mutant Huntingtin protein degradation (Sardiello et al., 2009).

Nevertheless the relevance of TFEB in NPC disease has not been totally explored yet.

1.5 TFEB regulation.

Due to the importance of TFEB for lysosomal homeostasis, having a better understanding of TFEB biology and regulation, could led us to find a promising therapeutic strategy for lysosomal and neurodegenerative diseases.

Interestingly, TFEB activity is regulated by phosphorylation; under basal conditions TFEB is found in the cytoplasm and highly phosphorylated on serine (Ser) 211 and Ser142 (Roczniak-Ferguson et al., 2012; Settembre et al., 2011). TFEB phosphorylation on Ser211 and Ser142 is mainly regulated by mTORC1, a kinase that controls cell growth and negatively regulates autophagy (Medina et al., 2011; Settembre et al., 2013; Wang et al., 2015). TFEB phosphorylated on Ser211 interacts with the cytosolic chaperone 14-3-3 and is retained in the cytoplasm. Dephosphorylation of TFEB on Ser 211 results in the loss of the interaction between 14-3-3 and TFEB, and promotes TFEB nuclear translocation (Medina et al., 2015; Roczniak-Ferguson et al., 2012; Settembre et al., 2012). Recently, it has been described that phosphorylation in Ser142 primes the phosphorylation in Ser138 on TFEB. The relevance of Ser138 phosphorylation is highlighted by its localization in a functional nuclear export signal (NES) of TFEB that was recently described (Li et al., 2018; Napolitano et al., 2018). TFEB phosphorylation in Ser142 and Ser138 promotes the TFEB nuclear export whereas phosphorylation of Ser211 regulates TFEB cytosolic retention, indicating that TFEB subcellular localization is finely controlled via modulation of its shuttling kinetics (Li et al., 2018; Napolitano et al., 2018).

In addition, it has been described that Calcineurin phosphatase is responsible for Ser211 dephosphorylation on TFEB. Activation of Calcineurin leads to TFEB dephosphorylation on TFEB Ser211 and its translocation to the nucleus (Medina et al., 2015) (Figura 2).

Interestingly, in NPC1 null CHO cells TFEB is preferentially localized in the cytoplasm, finding that correlates with overactivation of mTORC1 (Castellano et al., 2017). Congruently, mTORC1 Inhibition with Torin1 promotes clearance of accumulated cholesterol (Wang et al., 2015). Nevertheless, Torin1 has been shown to be toxic, probably due to the pleiotropic mTORC1 function in cells. In the context of this thesis, it is relevant to mention that the specific regulation of TFEB in different cellular conditions, such as, oxidative stress, lysosomal dysfunction and/or alterations in cholesterol homeostasis remains elusive. Indeed, the relevance of tyrosine phosphorylation on TFEB localization has not been explored yet.

Figure 2

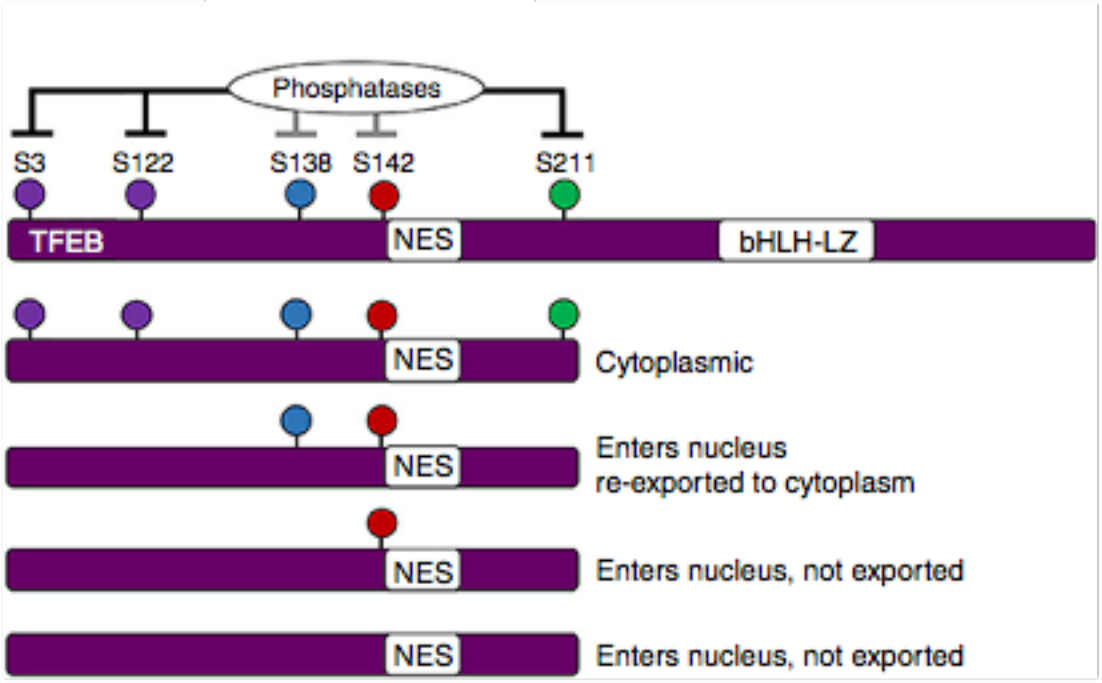

Figure 2. TFEB regulation: implications on its subcellular localization. Increased phosphatase activity targeting S211 will release TFEB from its cytoplasmic anchor. Absence of phosphorylation of S138 or S142 will lead to nuclear retention. In this model dephosphorylation of S142 or S138 is not a necessary pre-requisite for nuclear entry as it was recently described (Li et al., 2018; Napolitano et al., 2018).

1.6 ABL as a possible regulator of TFEB.

Interestingly, It has been published that the use of the ABL inhibitor, Imatinib, promotes an increase in the lysosomal number and autophagy flux in *in vitro* mammalian models (Ertmer et al., 2007). In addition, the second-generation ABL inhibitor, Nilotinib, promotes clearance of the alpha-synuclein protein by induction of autophagy flux in Parkinson's disease models (Hebron et al., 2013).

Several evidences suggest that the ABL and TFEB signaling pathways could be connected. Indeed, a recent study in dendritic cells shows that the ABL inhibitors, Imatinib and Nilotinib, promote nuclear translocation of MITF, a transcription factor that belongs to the same family of TFEB transcription factors (Gutknecht et al., 2015). In addition, its was recently shown that the treatment of BV2 microglial cells with lipopolysaccharide and rotenone reduces TFEB protein levels, and that pre-treatment with the ABL inhibitor, Dasatinib, prevents this reduction (Lawana et al., 2017).

In search of a connection between ABL and TFEB, we performed an in-silico analysis using both the netphos 2.0 and GPS 2.1.2 platforms looking for tyrosine consensus phosphorylation sites and ABL-specific phosphorylation sites on TFEB, with the idea to analyze which tyrosine on TFEB could be phosphorylated by ABL. Two tyrosine residues with the highest probability to be phosphorylated by ABL were identified; tyrosine (Tyr) 75 and Tyr 173. Interestingly, these two tyrosine identified on TFEB are highly conserved in different species.

Remarkable, a small clinical trial performed at Georgetown University Medical Center showed that the ABL inhibitor Nilotinib improves cognition, motor skills and non-motor

function in patients with Parkinson's disease (https://gumc.georgetown.edu/news/Researchers-Report-First-Therapy-Appearing-to-Reverse-Decline-in-Parkinsons). However, how ABL inhibition is clinically improving these patients and if the mechanism is related to the induction of clearance and lysosomal exocytosis mediated by TFEB is unknown.

Considering these data, the goal of this thesis was to evaluate how ABL activity affects lysosomal function through TFEB in the lysosomal NPC storage disorder.

Based on the literature and our previous data, we propose that ABL is involved in TFEB cellular localization. Then, our first goal is to evaluate if the activity of ABL prevents TFEB nuclear translocation. To do that, our strategy is to analyze in cells treated with ABL inhibitors and a siRNA against ABL1: i) Nuclear localization of both TFEB-GFP and endogenous TFEB ii) TFEB-target gene expression by qPCR and iii) mTORC1 activity. In addition, to analyze: iv) if ABL phosphorylates TFEB on tyrosine.
Our next goal is to understand the functional consequences of this signaling. If ABL inhibition induces TFEB nuclear translocation, we expect to observe a promotion of cellular clearance. To do that we will evaluate in cells with accumulation of cholesterol in lysosomes induced by the U18666A drug and ABL inhibitors: i) cellular clearance , ii) TFEB localization and iii) the relevance of TFEB on the cellular clearance response.

Finally, if ABL inhibition is promoting cellular clearence throught TFEB, we propose to evaluate this functional consequence in the lysosomal NPC storage disorder. To do that, we will evaluate: vi) TFEB localization and cellular clearance in human fibroblasts from NPC1 patients, vii) lysosomal number and exocytosis and vii) participation of the ABL/TFEB axis in *in vivo* NPC models.

1.7 Hypothesis and Objectives.

Hypothesis

ABL promotes TFEB cytoplasmic localization, inhibiting cellular clearance and contributing to the pathogenesis of Niemann-Pick C disease.

Objectives

Aim:

To evaluate the role of ABL on TFEB cytoplasmic localization and its impact in the cellular clearance of cholesterol in Niemann-Pick C disease models.

Specific Objectives.

1. To evaluate if ABL prevents TFEB nuclear translocation and the mechanism involved.

2. To demonstrate that TFEB nuclear localization promoted by ABL inhibition induces cellular clearance.

3. To demonstrate that ABL inhibition promotes TFEB mediated cholesterol accumulation reduction in Niemann-Pick C models.

2. RESULTS: PAPER

The next section presents the results that support the specific objectives 1, 2 and 3.

This work is entitled: "*ABL inhibition activates TFEB and promotes cellular clearance in a lysosomal disorder*"

from the authors: Pablo S. Contreras, Pablo J. Tapia, Lila González-Hódar, Ivana Peluso, Chiara Soldati, Gennaro Napolitano, Maria Matarese, Macarena Las Heras, Alexis Martinez, Juan Castro, Nancy Leal, Frances M. Platt, Andrzej Sobota, Dominic Winter, Andrés D. Klein, Diego L. Medina, Andrea Ballabio, Alejandra R. Alvarez, Silvana Zanlungo.

In this work we establish that: ABL inhibition promotes clearance of cholesterol in NPC models depending on TFEB, revealing a novel axis between ABL and TFEB. We demonstrate that ABL inhibition promotes an increase in TFEB nuclear localization —independently of mTORC1— and in the expression of TFEB-target genes. This TFEB activation was associated with an increase in autophagy flux, lysosomes number and exocytosis. We found that ABL phosphorylates TFEB on tyrosine, describing a novel post-translational modification for TFEB. In addition, we show that the treatment with several ABL inhibitors promote cellular clearance in both *in vitro* and *in vivo* NPC models. Our results position the ABL/TFEB axis as a therapeutic target for the treatment of patients with diseases in which the lysosomes are compromised.

ABL inhibition activates TFEB and promotes cellular clearance in a lysosomal disorder

Pablo S. Contreras[1,2,3], Pablo J. Tapia[3], Lila González-Hódar[3], Ivana Peluso[4], Chiara Soldati[4], Gennaro Napolitano[4], Maria Matarese[4], Macarena Las Heras[3], Alexis Martinez[1,2], Juan Castro[3], Nancy Leal[1,2], Frances M. Platt[5], Andrzej Sobota[6], Dominic Winter[7], Andrés D. Klein[4], Diego L. Medina[4], Andrea Ballabio[4,8,9,10], Alejandra R. Alvarez*[#1,2,], Silvana Zanlungo*[#3].

1. Department of Cell & Molecular Biology, Biological Sciences Faculty, Pontificia Universidad Católica de Chile, Santiago, Chile. 2. CARE UC Pontificia Universidad Católica de Chile, Santiago, Chile. 3. Departament of Gastroenterology, Faculty of Medicine, Pontificia Universidad Católica de Chile, Santiago, Chile. 4. Telethon Institute of Genetics and Medicina (TIGEM), Via Campi Flegrei 34, 80078 Pozzuoli, Naples, Italy. 5. Department of Pharmacology, University of Oxford, Oxford, UK. 6. Department of Cell Biology, Nencki Institute of Experimental Biology, 3 Pasteur St., 02-093 Warsaw, Poland. 7. Institute for Biochemistry and Molecular Biology, Rheinische-Friedrich-Wilhelms-University, Bonn, Germany. 8. Medical Genetics, Department of Pediatrics, Federico II University, Via Pansini 5, 80131 Naples, Italy. 9. Department of Molecular and Human Genetics, Baylor College of Medicine, Houston, TX 77030, USA. 10. Jan and Dan Duncan Neurological Research Institute, Texas Children's Hospital, Houston, TX 77030, USA.

* Both are corresponding authors.

Both are lead contact

Address correspondence to:

Alejandra R. Alvarez, Facultad de Ciencias Biológicas, Pontificia Universidad Católica de Chile, Alameda 340, Santiago 8331010, Chile. Tel.: +56-2-26862926; Fax: +56-2-6862959; E-mail: aalvarez@bio.puc.cl

Silvana Zanlungo, Facultad de Medicina, Pontificia Universidad Católica de Chile, Alameda 340, Santiago 8331010,Chile. Tel.: +56-2-23543833; Fax: +56-2-26397780; E-mail: szanlungo@uc.cl

Running title: ABL down-regulates TFEB

Abstract

Lysosomes fulfill multiple functions involved in cellular homeostasis and their dysfunction leads to lysosomal storage disorders (LSD), characterized by substrate accumulation. The transcription factor EB (TFEB) has emerged as a master regulator of lysosomal biogenesis, exocytosis and autophagy. We previously demonstrated that the activation of the tyrosine kinase ABL leads to neuronal dysfunction and neurodegeneration in the Niemann-Pick type C (NPC) LSD. Here, we show that ABL inhibition promotes cellular clearance in both pharmacological NPC models and human fibroblasts from NPC patients. Under pharmacological and genetic ABL inhibition, TFEB translocates into the nucleus — independently of its well-known regulator: target of rapamycin complex 1 (mTORC1) — and promotes the expression of its target genes. Active ABL1 phosphorylates TFEB on tyrosine and the inhibition of this kinase promotes lysosomal biogenesis, exocytosis and a reduction in lysosomal cholesterol accumulation in *in vitro* and *in vivo* NPC models. We propose the modulation of this novel ABL/TFEB axis using the FDA-approved drugs Imatinib or Nilotinib, as a therapeutic strategy to treat LSD.

Keywords

Tyrosine kinase ABL, Transcription Factor EB (TFEB), Niemann-Pick type C (NPC), Lysosomal Storage Disorders (LSD), Cellular clearance.

Introduction

Lysosomes are essential organelles for the degradation of complex substrates and therefore necessary for maintaining cellular homeostasis. Moreover, in recent years the lysosome has emerged as a signaling organelle able of sensing its external environment and thereby regulating fundamental processes such as cellular clearance and autophagy (Fraldi et al., 2016; Settembre and Ballabio, 2014; Settembre et al., 2013). Therefore, lysosomes are involved in vital cell functions and their dysfunction, due to mutations in genes that encode lysosomal proteins, result in more than 50 different LSD (Fraldi et al., 2016; Parenti et al., 2015).

A key element of lysosome signaling is the basic helix-loop-helix (bHLH) leucine zipper transcription factor EB (TFEB). TFEB is the master regulator of the coordinated lysosomal expression and regulation (CLEAR) network, covering genes related to autophagy, exocytosis and lysosomal biogenesis (Palmieri et al., 2011; Sardiello and Ballabio, 2009; Sardiello et al., 2009). TFEB overexpression or activation leads to increased number of lysosomes, autophagic flux and lysosomal exocytosis, triggering cellular clearance of substrates stored in cells (Medina et al., 2011; Napolitano and Ballabio, 2016; Settembre and Ballabio, 2011; Settembre et al., 2011). This is relevant in diseases in which the degradative capacity of the cells is compromised. In fact, it has been reported that TFEB overexpression promotes cellular clearance ameliorating the phenotypes in a variety of neurodegenerative diseases such as Alzheimer's, Parkinson's, and Huntington's (Ballabio, 2016; Decressac et al., 2013; Napolitano and Ballabio, 2016; Polito et al., 2014; Sardiello et al., 2009; Tsunemi et al., 2012; Xiao et al., 2014; Xiao et al., 2015).

Due to the large number of diseases where lysosomal function is compromised, recent

research has focused on elucidating the mechanisms by which TFEB is regulated. TFEB activity is regulated by phosphorylation, mainly by the mammalian target of rapamycin complex 1 (mTORC1), a serine/threonine kinase that controls cell growth and negatively regulates autophagy (Martina et al., 2012; Roczniak-Ferguson et al., 2012; Settembre et al., 2013; Settembre et al., 2012). In the presence of nutrients, mTORC1 basally phosphorylates TFEB on serine 142 (S142) (Settembre et al., 2011; Settembre et al., 2012) and serine 211 (S211) (Martina et al., 2012; Roczniak-Ferguson et al., 2012), which are in turn dephosphorylated by calcineurin phosphatase in the absence of nutrients (Medina et al., 2015). TFEB phosphorylated at S211 interacts with the cytosolic chaperone 14-3-3 and is retained in the cytoplasm (Martina et al., 2012; Roczniak-Ferguson et al., 2012). In the absence of nutrients, mTORC1 is inactive, and dephosphorylated TFEB translocates into the nucleus promoting the expression of the CLEAR gene network. More recently, other serine/threonine kinases such as Akt (protein kinase B) and protein kinase C (PKC) have been described as regulators of TFEB activation (Li et al., 2016; Palmieri et al., 2017). Nevertheless, the mechanism of TFEB regulation under different stress conditions such as those present in different lysosomal storage diseases, are still not well understood (Martina et al., 2016; Raben and Puertollano, 2016). In relation to this lack of evidence, the possible TFEB regulation by tyrosine phosphorylation has not been explored.

Enormous effort has been made to find the signaling pathways that regulate TFEB. However, there are still few pharmacological alternatives for the activation of TFEB that can be proposed as an alternative for the treatment of those diseases in which TFEB activation has been shown to alleviate the symptoms (Palmieri et al., 2017). In this sense, the inhibition of mTORC1 does not seem to be a good therapeutic option because this

kinase fulfills pleiotropic cellular functions.

Previously, our laboratory demonstrated that the tyrosine kinase ABL is activated in the Niemann-Pick type C (NPC) lysosomal storage disorder (Alvarez et al., 2008; Klein et al., 2011). NPC is characterized by lysosomal cholesterol accumulation due to *NPC1* or *NPC2* gene mutations (Carstea et al., 1997; Naureckiene et al., 2000). ABL is a tyrosine kinase implicated in a variety of processes such as cytoskeleton regulation, cell cycle and apoptosis (Schlatterer et al., 2011). ABL activation and autophosphorylation can be induced through a variety of stimuli including DNA damage, endoplasmic reticulum stress and oxidative stress (Hantschel and Superti-Furga, 2004). These stimuli trigger the nuclear translocation of ABL. However, in the absence of a stimulus ABL is retained in the cytoplasm by the 14-3-3 chaperone (Yoshida et al., 2005).

ABL activity is induced in NPC neurons promoting dysfunction and death through several signaling pathways including the activation of the proapoptotic p73 transcription factor (Alvarez et al., 2008; Klein et al., 2011) and the histone desacetylase 2 (HDAC2) (Contreras et al., 2016). This situation triggers the expression of proapoptotic p73-target genes and the repression of neuronal genes, respectively. In addition, ABL activation promotes APP (Amyloid precursor protein) processing and increased amyloid β-peptide levels in NPC models (Yanez et al., 2016). The inhibition of ABL with the classic inhibitor Imatinib decreases neuronal death in the cerebellum and improves motor skills and survival of NPC mice (Alvarez et al., 2008), which confirms the relevance of ABL activation in NPC disease.

The evidence suggests that ABL and TFEB signaling pathways could be connected. For example, a recent study in dendritic cells shows that the ABL inhibitors Imatinib and

Nilotinib promote nuclear translocation of MITF, a transcription factor that belongs to the same family of TFEB transcription factor (Gutknecht et al., 2015). In addition, it was recently shown that treatment of BV2 microglial cells with lipopolysaccharide and rotenone decreases TFEB protein levels, and that pre-treatment with the ABL inhibitor Dasatinib prevents this reduction (Lawana et al., 2017).

The goal of this study was to evaluate how the activation of ABL affects lysosomal function through TFEB in the lysosomal NPC storage disorder. Our data show that the inhibition of ABL promotes clearance of cholesterol in NPC models. This increased clearance dependent on TFEB, reveals a novel axis between ABL and TFEB. We demonstrate that ABL inhibition promotes increased TFEB nuclear localization — independent of mTORC1—, and the expression of TFEB-target genes. This effect was associated with increased autophagy, lysosome number and exocytosis. We also found that ABL phosphorylates TFEB on tyrosine, a novel post-translational modification for TFEB. In addition, the treatment with several ABL inhibitors promotes cellular clearance in both *in vitro* and *in vivo* NPC models. Our results position the ABL/TFEB axis as a therapeutic target for the treatment of patients with diseases in which the lysosomes are compromised.

Results

ABL inhibition promotes TFEB activity

The transcription factor EB (TFEB) has been characterized as the master regulator of lysosomal biogenesis and autophagy (Sardiello et al., 2009; Settembre et al., 2011). Because ABL inhibition induces the process of autophagy and lysosomal biogenesis (Ertmer et al., 2007), we hypothesized that the tyrosine kinase ABL could regulate TFEB nuclear translocation.

To evaluate this hypothesis, we first examined TFEB-GFP nuclear localization in Hela TFEB-GFP cells treated with different ABL inhibitors. Imatinib and Nilotinib are classic first and second generation ABL inhibitors. Dasatinib is a tyrosine kinase inhibitor, also used as an ABL inhibitor, but it is less specific; the three are FDA approved drugs (Capdeville et al., 2002; Druker et al., 1996; Hantschel et al., 2008; Maekawa et al., 2007). GNF-2 and its analog, GNF-5, are allosteric inhibitors of ABL (Iacob et al., 2011). We measured TFEB-GFP nuclear localization using a high-content nuclear translocation assay in a confocal automated microscope. As a positive control for TFEB nuclear translocation we used 0.3 μM Torin1, a mTORC1 inhibitor, for 3h. Fig. 1a-b shows that the different concentrations of ABL inhibitors as well as Torin1, promote a significantly increase in TFEB-GFP nuclear signal compared to control conditions (DMSO), being Imatinib and Nilotinib the most effective at lower concentrations. We observed the same result at 6h, 12h, and 24h (Supplementary Fig. 1a). Treatment with 10 μM Imatinib for 3h promoted TFEB nuclear translocation in Hela TFEB-GFP cells measured by nucleus cytoplasm fractionation (Fig. 1c), confirming our analysis of the high-content nuclear translocation assay. In addition, we tested Imatinib in HT22 (a cell line derived from mice hippocampal neurons) and in HEK293 cells (derived from human embryonic kidney) that had been transiently transfected with TFEB-GFP. As expected, we observed that Imatinib promoted TFEB nuclear localization (Supplementary Fig. 1b-c). These experiments clearly show an increase in TFEB-GFP nuclear translocation when ABL is inhibited.

Next, we evaluated the effect of ABL inhibition on endogenous TFEB. We treated wild type human fibroblasts with Imatinib 10 μM for 24h and then performed a nucleus cytoplasm fractionation assay. ABL inhibition clearly increased the levels of endogenous TFEB in the nucleus (Fig. 1d). In addition, we performed immunofluorescence experiments to explore

FIGURE 1

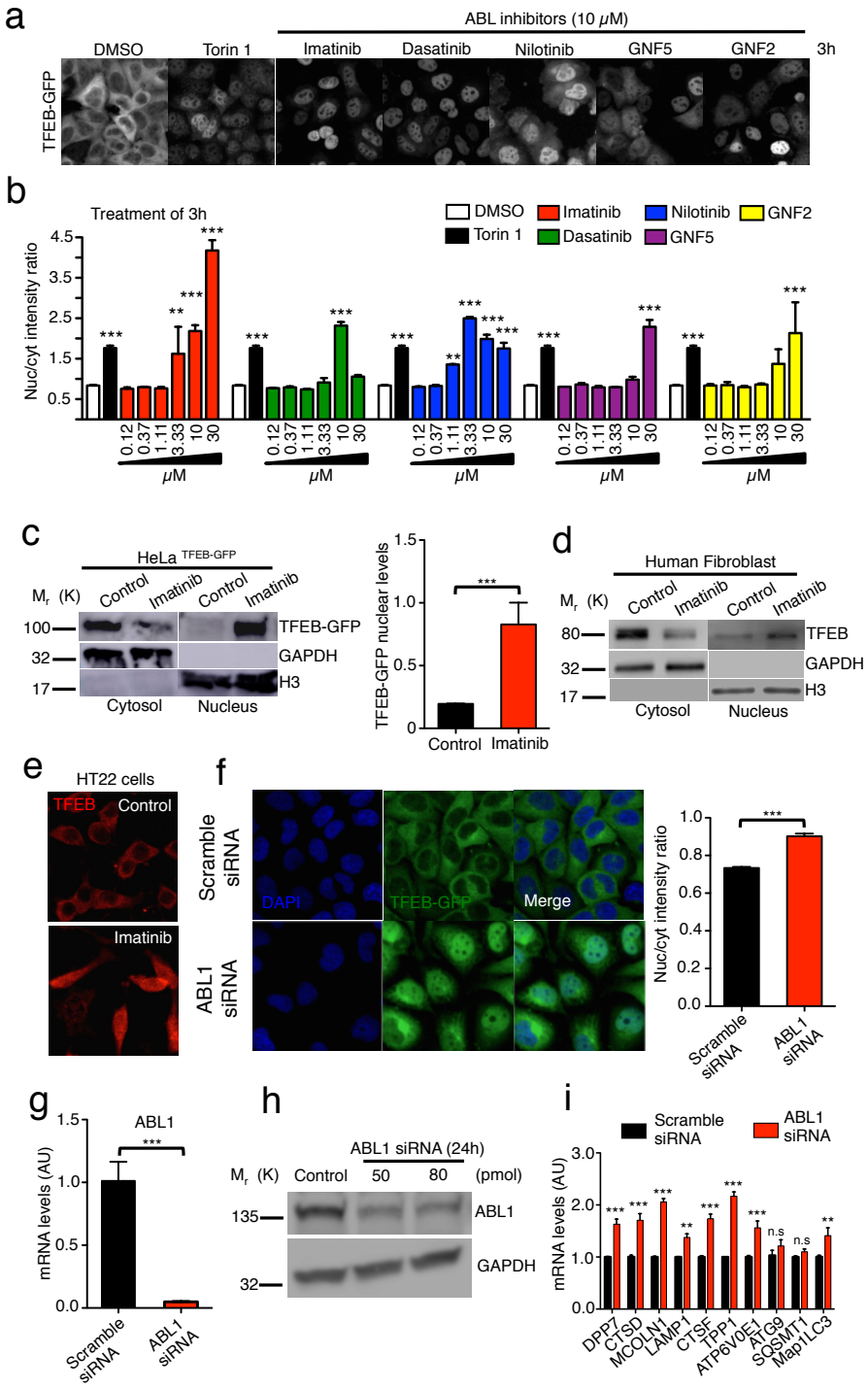
a
ABL inhibitors (10 μM)
DMSO
Torin 1
Imatinib
Dasatinib
Nilotinib
GNF5
GNF2
3h
TFEB-GFP
b
Treatment of 3h
DMSO
Torin 1
Imatinib
Dasatinib
Nilotinib
GNF5
GNF2
Nuc/cyt intensity ratio
μM
c
HeLa TFEB-GFP
Control
Imatinib
Control
Imatinib
Mr (K)
100
32
17
TFEB-GFP
GAPDH
H3
Cytosol
Nucleus
TFEB-GFP nuclear levels
Control
Imatinib
d
Human Fibroblast
Control
Imatinib
Control
Imatinib
Mr (K)
80
32
17
TFEB
GAPDH
H3
Cytosol
Nucleus
e
HT22 cells
TFEB
Control
Imatinib
f
Scramble siRNA
ABL1 siRNA
DAPI
TFEB-GFP
Merge
Nuc/cyt intensity ratio
Scramble siRNA
ABL1 siRNA
g
ABL1
mRNA levels (AU)
Scramble siRNA
ABL1 siRNA
h
ABL1 siRNA (24h)
Mr (K)
Control
50
80
(pmol)
135
32
ABL1
GAPDH
i
Scramble siRNA
ABL1 siRNA
mRNA levels (AU)
n.s
DPP7
CTSD
MCOLN1
LAMP1
CTSF
TPP1
ATP6V0E1
ATG9
SQSMT1
Map1LC3

Figure 1. ABL inhibition increases TFEB nuclear translocation and activity. Hela TFEB-GFP cells were treated with DMSO (control), Torin1 0.3 μM (positive control) and ABL inhibitors at different concentrations for 3h. Then, the cells were fixed and stained with DAPI. (a) Representative images of the TFEB-GFP translocation assay obtained by confocal automated microscopy and (b) graph of the ratio value resulting from the average intensity of nuclear TFEB–GFP fluorescence divided by the average cytosolic intensity of TFEB–GFP fluorescence. Black bars represent Torin1 treatment (positive control). Differences are statistically significant compared to control conditions (DMSO). For each condition, 450-800 cells were analyzed (two wells x 7 images). (c) Western blot and quantification of TFEB-GFP normalized with histone 3 (H3), in a nuclear/cytoplasmic fractionation of Hela TFEB-GFP cells treated with Imatinib 10μM for 3h. *n*=3 independent experiments. (d) Representative western blot of endogenous TFEB in a nuclear/cytoplasmic fractionation assay of control human fibroblast treated with Imatinib 10μM for 24h. *n*=3 independent experiments. (e) Representative images of endogenous TFEB in HT22 cells treated with Imatinib 10 μM for 24h. (f) Hela TFEB-GFP cells were treated with a scramble siRNA and ABL1siRNA for 72h. Representative images of the TFEB-GFP translocation assay and quantification. For each condition 3,000-5,000 cells were analyzed (five wells x 16 images). (g,h) The left graph represents q-PCR analysis of ABL1 mRNA levels in Hela cells treated with the scramble siRNA and siRNA against ABL1 for 24h. The western blot confirms the reduction of ABL1 protein levels in Hela cells treated with siRNA against ABL1 for 24h. (i) The graph shows q-PCR analysis of mRNA levels of different TFEB target genes in Hela cells treated with the scramble siRNA and a siRNA against ABL1. *n*=3 independent experiments. *$p < 0.05$, **$p < 0.01$,***$p < 0.001$. Data represent mean ± SEM.

the effect of ABL inhibition on TFEB nuclear translocation. In the HT22 cell line treated with Imatinib for 24h, we observed that ABL inhibition increased TFEB nuclear signal (Fig. 1e). Therefore, ABL inhibition promotes endogenous TFEB nuclear translocation.

To confirm that the pharmacological inhibition of ABL mediates the increase in TFEB nuclear localization, we used a pool of siRNA against ABL1. We transfected Hela TFEB-GFP cells with the siRNAs against ABL1 for 72h and then analyzed TFEB nuclear localization using a high-content nuclear translocation assay. The cells treated with the siRNAs against ABL1 show increased TFEB-GFP nuclear localization compared with cells transfected with a scramble siRNA (Fig. 1f). The effectiveness of the siRNAs was tested following the levels of ABL1 mRNA and protein (Fig. 1g-h). Importantly, Hela cells treated with siRNAs against ABL1, showed an increased mRNA levels for several TFEB-target genes measured by q-PCR (Fig. 1i). Similar results on TFEB-target genes were observed in wild type human fibroblasts treated with the ABL inhibitors, Imatinib and Nilotinib, for 24h (Supplementary Fig. 1d).

Altogether, these experiments demonstrate that under basal conditions ABL inhibition promotes TFEB nuclear localization inducing its transcriptional function.

To elucidate how the inhibition of ABL activates TFEB we first corroborated some of the cellular readouts of TFEB activation (Settembre et al., 2013; Settembre and Medina, 2015).

On the one hand, we measured autophagy flux using the stable H4 GFP-mRFP-LC3 cell line (Fig. 2a-b). Under conditions that induce the fusion between lysosomes and autophagosomes, the lower pH of lysosomes degrades the GFP signal, being the mRFP-LC3 signal a marker of autophago-lysosome formation. We treated these cells with

Imatinib for 3h, and then we quantified the induction of autophagy using confocal automated microscopy (Fig. 2a-b). We observed an increased in the mRFP-LC3 signal in the Imatinib treated cells as well as in the Torin1 positive control, compared with control conditions. As expected, the induction of this phenotype is inhibited in co-treatments with Imatinib and bafilomycin A1, a well-known autophagy inhibitor (Fig. 2a-b).

On the other hand, we analyzed the effect of ABL inhibition on lysosomes. We found increased Lamp1 levels by western blot in HT22 cell lines treated with Imatinib 10 μM for 24h (Fig. 2c). In addition, we found increased lysotracker red marker using FACs in both Hela cells and in wild type human fibroblast treated with Imatinib (Fig. 2d & 2e respectively). Concordantly, we observed increased Lamp1 staining by immunofluorescence in human fibroblast treated with both Imatinib 10μM for 24h and with a siRNA against ABL1 (Fig. 2f).

Next, we analyzed the effect of inhibiting ABL on lysosome distribution. We treated Hela cells with Imatinib for 24h and, using an antibody that recognizes the luminal domain of Lamp1, we found that ABL inhibition promoted an increase in the lysosomes that are attached to the plasma membrane, suggesting an increase in the exocytic process (Fig. 2g).

These results show that ABL inhibition induces autophagy flux and increases acidic organelles and lysosomal protein levels in cells, and suggest increased lysosomal exocytosis, all effects that correlate with TFEB nuclear translocation and activation.

FIGURE 2

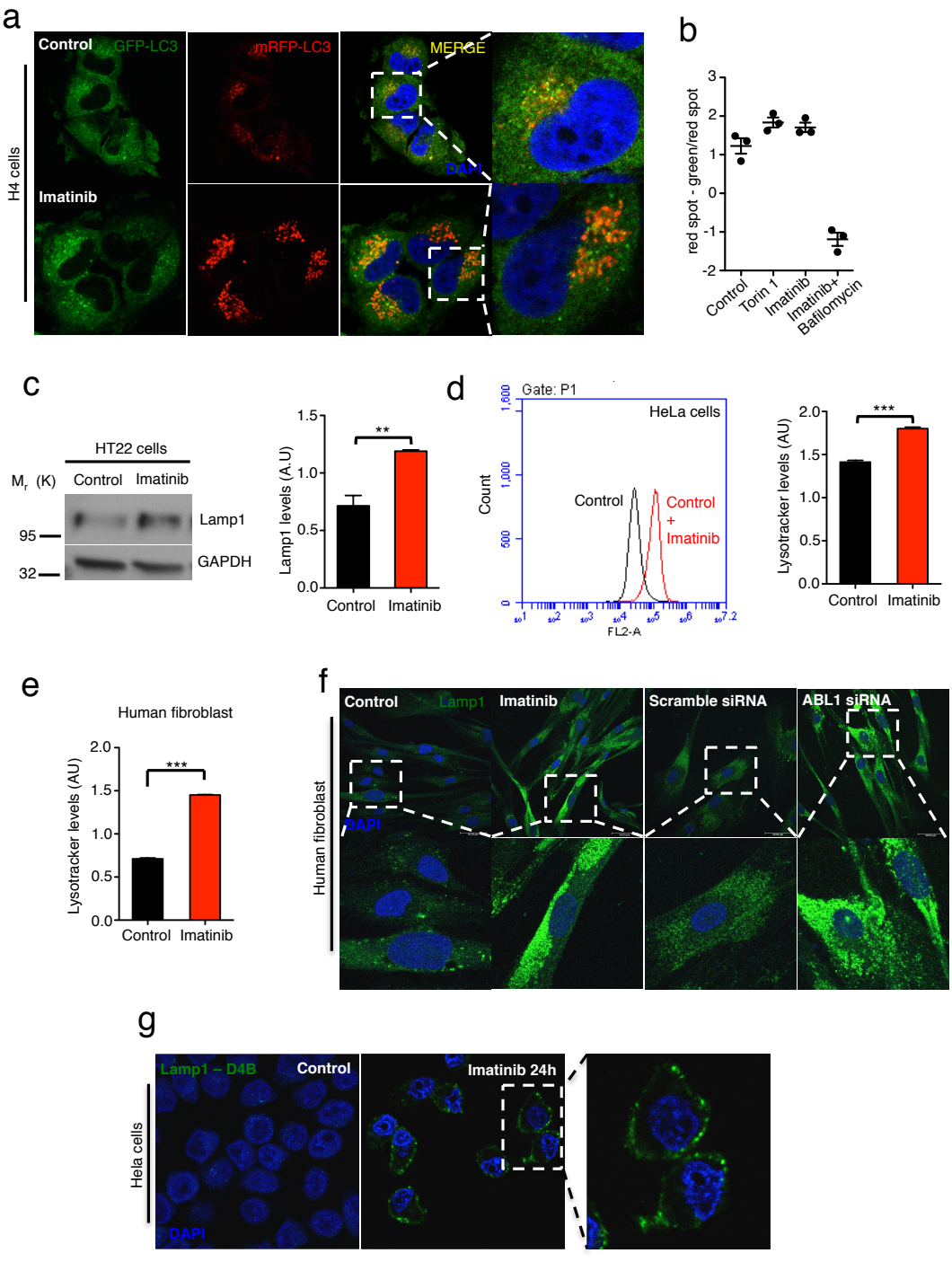
a
Control
GFP-LC3
mRFP-LC3
MERGE
DAPI
Imatinib
H4 cells
b
red spot - green/red spot
Control
Torin 1
Imatinib
Imatinib+ Bafilomycin
c
HT22 cells
Mr (K)
Control
Imatinib
95
32
Lamp1
GAPDH
Lamp1 levels (A.U)
**
d
Gate: P1
HeLa cells
Count
Control
Control + Imatinib
FL2-A
Lysotracker levels (AU)
***
e
Human fibroblast
f
Control
Lamp1
Imatinib
Scramble siRNA
ABL1 siRNA
DAPI
Human fibroblast
g
Lamp1 – D4B
Control
Imatinib 24h
Hela cells
DAPI

Figure 2. ABL inhibition induces autophagy flux and increases acidic organelles and lysosomal protein levels. H4 cells were treated with DMSO (control), Torin1 0.3 μM (positive control), ABL inhibitor Imatinib 10 μM for 3h and/or Bafilomycin A1 0.4 μM for 3h. The cells were then fixed and stained with DAPI. (a) Representative confocal microscopy images. (b) Graph of the value resulting from the following substraction: red spot fluorescence intensity minus green-red spots fluorescence intensity. For each condition 450-800 cells were analyzed (three wells x 19 images). (c) Representative Western blot and quantification of HT22 cells treated with Imatinib 10μM for 24h using a Lamp1 antibody. *n*=3 independent experiments. (d) Quantitative flow cytometry analysis of lysotracker in Hela cells treated with Imatinib 10μM for 24h. *n*=10,000 cells per conditions. (e) Quantitative flow cytometry analysis of lysotracker in the human wild type fibroblasts treated with Imatinib 10μM for 24h. *n*=10,000 cells per conditions. (f) Representative immunofluorescence images of lysosomes using Lamp1 antibody in human fibroblast treated with Imatinib 10μM for 24h, or transfected with a scramble siRNA or a siRNA against ABL1 for 48h. (g) Representative immunofluorescence images of lysosomes attached to the plasma membrane using the antibody Lamp1-DB4 in Hela cells treated with Imatinib 10μM for 24h. *$p < 0.05$, **$p < 0.01$,***$p < 0.001$. Data represent mean ± SEM.

ABL inhibition activates TFEB independently of mTORC1 activity

The regulation of TFEB nuclear localization mediated by mTORC1 serine phosphorylation is well characterized. Active mTORC1 phosphorylates TFEB on S142 and S211, promoting TFEB cytoplasmic retention by chaperone 14-3-3 (Martina et al., 2012; Roczniak-Ferguson et al., 2012). Conversely, TFEB serine de-phosphorylation promotes its translocation into the nucleus. Therefore, our next question was if TFEB nuclear translocation mediated by inhibition of ABL is dependent or independent on mTORC1.

To elucidate if the effect of ABL on TFEB depends on mTORC1, we first analyzed the phosphorylation status of endogenous TFEB in cells treated with ABL inhibitors by western blot. As expected, Torin1 promoted an electrophoretic shift on TFEB compared to control condition. This electrophoretic mobility is due to its de-phosphorylation on S142 and/or S211 as result of the inhibition of mTORC1 (Martina et al., 2012; Martina and Puertollano, 2013; Roczniak-Ferguson et al., 2012; Settembre et al., 2012) (Fig. 3a). Concordantly, in cells under nutrient deprivation induced by starvation media (STV), a condition under which mTORC1 inhibition is promoted, we observed the same electrophoretic shift of the endogenous TFEB compared to control condition (Fig 3a). Interestingly, Imatinib, which promoted TFEB nuclear translocation, also induced an electrophoretic shift of the endogenous TFEB compared with control condition (Fig. 3a). Nevertheless, the electrophoretic shift promoted by the inhibition of ABL is smaller compared to the conditions in which mTORC1 is inhibited (Fig 3a). Similar results were observed in Hela TFEB-GFP cells treated with Imatinib, in which the electrophoretic shift is induced and there is not a change in TFEB-GFP levels (Supplementary Fig. 2a). These results suggest that ABL inhibition promotes TFEB translocation into the nucleus in spite of a TFEB de-phosphorylation status different from that generated by mTORC1 inhibition.

Next, we followed the effect of ABL inhibition on the levels of TFEB phosphorylated on S142 (TFEB p-S142) by western blot. As expected, in TFEB-GFP Hela cells treated with STV, TFEB p-S142 levels were reduced (Fig. 3b). We obtained the same results when were treated with Torin1 (Supplementary Fig. 2b). However, we did not observe decreased levels of TFEB p-S142 when we treated the cells with Imatinib or used a siRNA against ABL1, indicating that ABL inhibition promotes TFEB nuclear translocation independent of S142 phosphorylation levels (Fig. 3b). In addition, we measured the levels of S211 phosphorylated TFEB (TFEB p-S211) in Hela TFEB-GFP cells. We accomplished this by following the binding of 14-3-3 chaperone to this phosphorylated residue using a specific antibody (Roczniak-Ferguson et al., 2012). Unlike S142 phosphorylation, we observed a decrease in S211 phosphorylation in both Torin1 as well as in Imatinib treated TFEB-GFP cells (fig. 3c). In addition, we measured the phosphorylation of Serine 138 (S138) on TFEB, since it was recently shown that phosphorylation in this position promotes TFEB nuclear export (Li et al., 2018; Napolitano et al., 2018). As expected, we observed that mTORC1 inhibition promotes full de-phosphorylation in Ser138 (Supplementary Fig. 2c). Interestingly, although ABL inhibition promotes a slight decrease in TFEB Ser138 phosphorylation levels (Supplementary Fig. 2c), TFEB was localized mainly in the nucleus.

These results indicate that ABL inhibition with Imatinib, promotes a partial and different TFEB de-phosphorylation status compared with the inhibition of mTORC1; S142 phosphorylation is not affected, S138 phosphorylation is partially decreased, while S211 phosphorylation decreases. These results suggest that ABL controls TFEB nuclear translocation through a different mechanism than that mediated by mTORC1.

To further analyze if TFEB nuclear translocation induced by inhibition of ABL is independent on mTORC1 inhibition we measured the phosphorylation levels of p70 S6

FIGURE 3

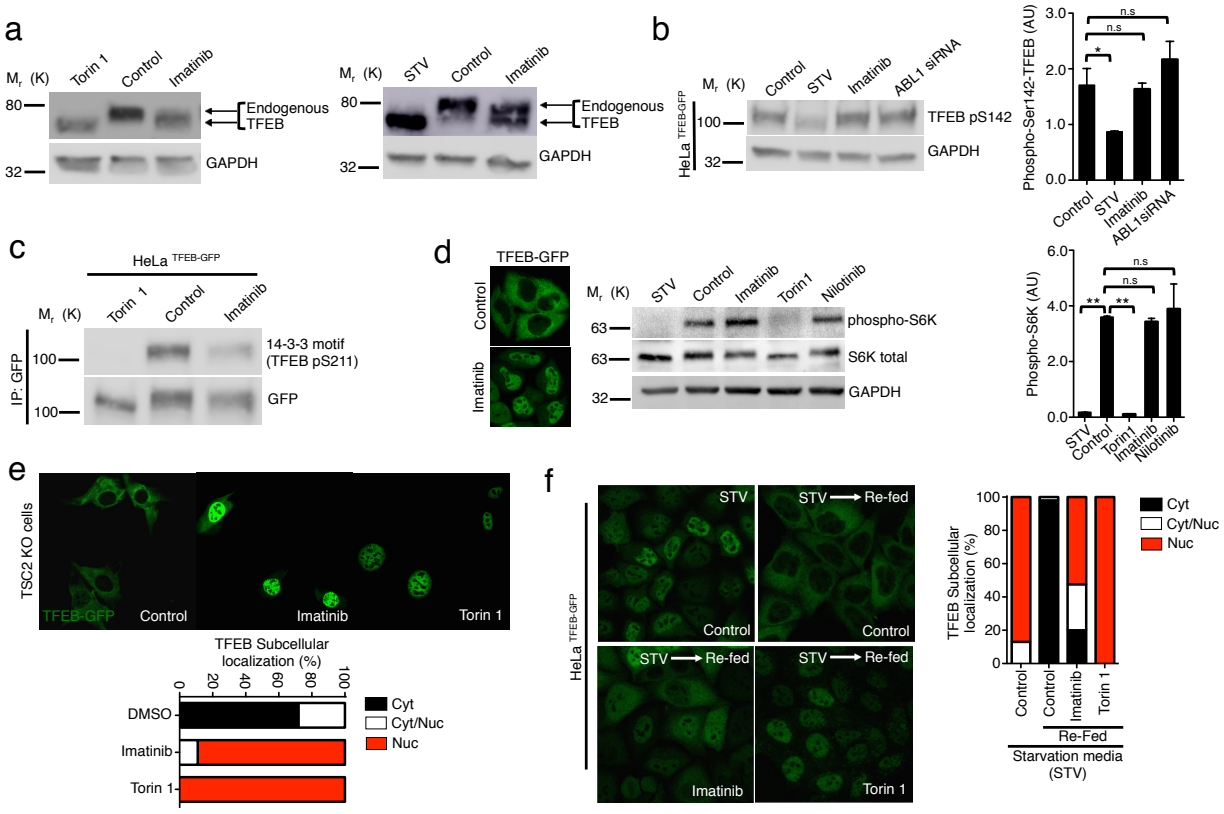
a
Mr (K)
Torin 1
Control
Imatinib
80
32
Endogenous TFEB
GAPDH
Mr (K)
STV
Control
Imatinib
80
32
Endogenous TFEB
GAPDH
b
Mr (K)
Control
STV
Imatinib
ABL1 siRNA
HeLa TFEB-GFP
100
32
TFEB pS142
GAPDH
Phospho-Ser142-TFEB (AU)
3.0
2.0
1.0
0.0
n.s
n.s
*
Control
STV
Imatinib
ABL1siRNA
c
HeLa TFEB-GFP
Mr (K)
Torin 1
Control
Imatinib
IP: GFP
100
100
14-3-3 motif (TFEB pS211)
GFP
d
TFEB-GFP
Control
Imatinib
Mr (K)
STV
Control
Imatinib
Torin1
Nilotinib
63
63
32
phospho-S6K
S6K total
GAPDH
Phospho-S6K (AU)
6.0
4.0
2.0
0.0
n.s
n.s
**
**
STV
Control
Torin1
Imatinib
Nilotinib
e
TSC2 KO cells
TFEB-GFP
Control
Imatinib
Torin 1
TFEB Subcellular localization (%)
0
20
40
60
80
100
DMSO
Imatinib
Torin 1
Cyt
Cyt/Nuc
Nuc
f
HeLa TFEB-GFP
STV
STV → Re-fed
Control
Control
STV → Re-fed
STV → Re-fed
Imatinib
Torin 1
TFEB Subcellular localization (%)
100
80
60
40
20
0
Cyt
Cyt/Nuc
Nuc
Control
Control
Imatinib
Torin 1
Re-Fed
Starvation media (STV)

Figure 3. ABL regulates TFEB independent of mTORC1 activity. (a) Western blots of endogenous TFEB in Hela cells treated with Imatinib 10μM for 3h. Torin1 0.3μM and starvation media (STV) for 3h were used as a positive control. (b) Representative Western blot and quantification of TFEB phosphorylated on S142 normalized against GAPDDH in Hela TFEB-GFP cells treated with Imatinib 10μM for 3h and siRNA ABL1 for 48h. STV media for 3h was used as positive control. *n*=3 independent experiments. (c) Representative Western blot using the 14-3-3 antibody that binds to phosphorylated TFEB on S211. For immunoprecipitated GFP from Hela TFEB-GFP, cells treated with Imatinib 10 μM and Torin1 0.3 μM for 3h. *n*=3 independent experiments. (d) Representative Western blot and quantification of phospho p70-S6K normalized against GAPDH in Hela cells treated with Imatinib and Nilotinib 10μM for 3h. Torin1 0.3μM and STV media treatment for 3h were used as positive controls. *n*=3 independent experiments. (e) Representative confocal microscopy images and quantification of TSC2 KO cells transfected with the TFEB-GFP plasmid. Cells were treated with Imatinib 10μM for 3h and with Torin1 0.3μM for 3h as a positive control. *n*=40 cells per conditions. (f) Representative images and quantification of percentage of nuclear TFEB-GFP in Hela TFEB-GFP cells synchronized with STV media for 1h. Then, cells were treated with Imatinib 10μM for 1h and Torin1 0.3 μM for 1h as a positive control and re-fed with normal media plus Imatinib and Torin1 for 2h. *n*=3 independent experiments. *$p < 0.05$, **$p < 0.01$,***$p < 0.001$. Data represent mean ± SEM.

Kinase (phospho-S6K) a well-known mTORC1 target protein. Interestingly, we observed that treatment with ABL inhibitors for 3h did not change the phosphorylation status of S6K (phospho-S6K) in Hela cells and in Hela cells that over-expressed TFEB-GFP (Fig. 3d and Supplementary Fig. 2d respectively). We obtained similar results when Hela cells were treated with Imatinib for 3h, 6h and 24h (Supplementary Fig. 2e), confirming that ABL is not modulating mTORC1 activity.

Altogether these results suggest that ABL inhibition contributes to TFEB nuclear translocation by a mechanism that neither involves S142 phosphorylation nor mTORC1 activity.

Indeed, in TSC2 KO cells, which have a constitutively active mTORC1, Imatinib treatment induced TFEB-GFP nuclear translocation as well as with Torin 1 treatment, in spite of mTORC1 over-activation (Fig. 3e). Moreover, Imatinib prevented TFEB-GFP cytoplasmic return in synchronized cells using starvation media and re-fed. TFEB was retained in the nucleus compared with control conditions (Fig. 3f).

These experiments demonstrate that ABL inhibition promotes TFEB nuclear translocation in spite of mTORC1 over-activation, revealing a novel mTORC1-independent TFEB regulatory pathway mediated by ABL tyrosine kinase.

ABL phosphorylates TFEB on tyrosine

Because our results demonstrated that inhibition of the tyrosine kinase ABL promotes TFEB activation independent of its classic regulator mTORC1, we assessed if this tyrosine kinase could phosphorylate TFEB.

To this end, we used a plasmid encoding a fusion ABL1-ERT2 protein that contains the ABL1 kinase domain fused to the ligand-binding domain of the estrogen receptor (ER), which binds to tamoxifen with high affinity. When this fusion protein is expressed in cells it associates with HSP90 chaperones. Upon tamoxifen treatment, the ABL1-ERT2 protein dissociates from HSP90 and its activity is de-repressed. As a control we used a plasmid containing an ABL1 kinase death-ERT2 (ABL1-ERT2 KD) fusion protein. We overexpressed this ABL1-ERT2 construction in Hela TFEB-GFP cells. Remarkably, the TFEB-GFP protein immunoprecipitated from tamoxifen treated cells, in which ABL1-ERT2 is active, showed a clear band corresponding in size to TFEB-GFP phosphorylated in tyrosine (Fig. 4a). This band, corresponding to tyrosine phosphorylated TFEB, was not observed in cells transfected with the control plasmid containing the ABL1 ERT2 KD fusion protein and treated with tamoxifen (Fig. 4a). More importantly, in an *in vitro* phosphorylation assay using TFEB-Flag, recombinant human active ABL1 and ATP-γ-^{32}P, we observed the incorporation of radioactivity in TFEB-Flag in a time dependent manner (Fig. 4b). As a positive control for ABL1 dependent phosphorylation we used the well-known ABL1 target CRKII (Supplementary Fig. 3a).

These experiments demonstrate, for the first time, that TFEB is phosphorylated on tyrosine by ABL kinase.

Then, to analyze which tyrosine on TFEB could be phosphorylated by ABL1, we performed an in-silico analysis on TFEB. We used the platforms netphos 2.0. to search for tyrosine consensus phosphorylation sites (Blom et al., 1999) and GPS 2.1.2 to find possible ABL1-specific phosphorylation sites (Xue et al., 2011). We identified two tyrosine residues with the highest probability to be phosphorylated by ABL1: tyrosine 75 and 173 (Y75 and Y173) (Fig. 4c). Remarkably, these two tyrosines identified on TFEB are highly conserved in

different species (Fig. 4c). Then, we carried out site-directed mutagenesis of the TFEB-GFP plasmid in order to change Y75 and Y173 to phenylalanine (F), and analyzed the sub-cellular localization of the Y75F and Y173F TFEB-GFP mutant proteins. The localization of TFEB-GFP when is transfected into cells is usually cytoplasmic. Interestingly, we observed that the Y173F TFEB-GFP mutant protein has a constitutive nuclear localization compared to the wild type and Y75F TFEB-GFP proteins (Fig. 4d). Next, we performed *in vitro* phosphorylation assays using active ABL1 and wild-type (WT) and mutant TFEBs. Even though we expected decreased incorporation of radioactivity in TFEB mutants, the Y173F TFEB-GFP and Y75F TFEB-GFP proteins incorporated radioactivity at levels similar to that of the wild type TFEB-GFP, probably due to basal phosphorylation of other tyrosines. Slightly less radioactivity was detected in the Y75F TFEB-GFP protein suggesting that ABL1 phosphorylates TFEB on Y75. However, the construct Y75F TFEB-GFP showed lower expression levels in cells transfected for the *in vitro* phosphorylation assays (Supplementary Fig. 3b). Then, because S211 is key to retain TFEB in the cytoplasm, we analyzed this serine phosphorylation on the mutant TFEBs by western blot using a specific antibody against phosphorylated TFEB in S211. Interestingly, and in accordance with our previous results of cells treated with ABL inhibitors (Fig. 3), we observed a reduction of S211 phosphorylation in the Y173 TFEB-GFP protein (Fig. 4e), suggesting a relevant role of Y173 on TFEB cellular localization by influencing S211 phosphorylation.

These results strongly suggest that ABL1 mediates TFEB tyrosine phosphorylation and that TFEB Y173 is relevant for its retention in the cytoplasm.

FIGURE 4

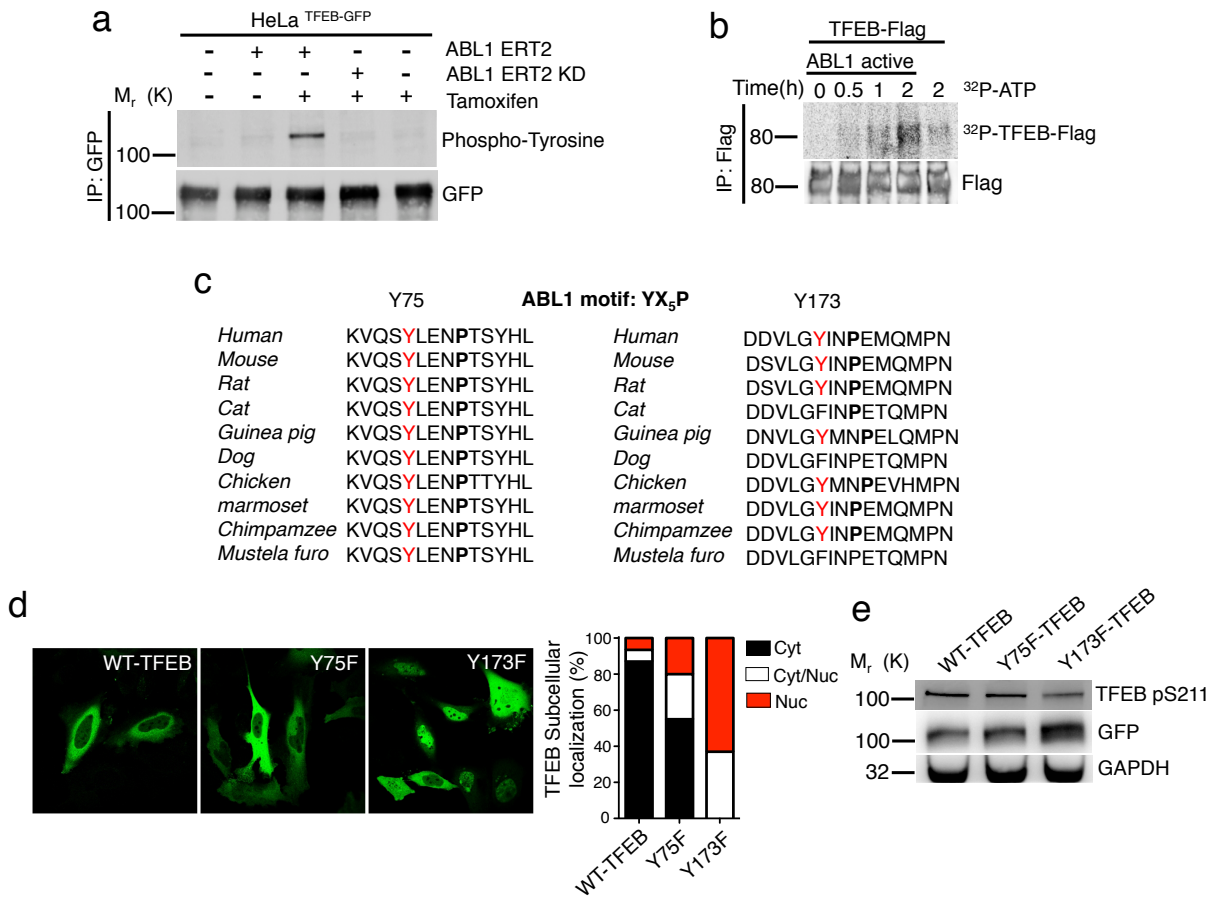
a
HeLa TFEB-GFP
ABL1 ERT2
ABL1 ERT2 KD
Tamoxifen
Mr (K)
IP: GFP
100
100
Phospho-Tyrosine
GFP
b
TFEB-Flag
ABL1 active
Time(h) 0 0.5 1 2 2
32P-ATP
IP: Flag
80
80
32P-TFEB-Flag
Flag
c
Y75
ABL1 motif: YX5P
Y173
Human KVQSYLENPTSYHL DDVLGYINPEMQMPN
Mouse KVQSYLENPTSYHL DSVLGYINPEMQMPN
Rat KVQSYLENPTSYHL DSVLGYINPEMQMPN
Cat KVQSYLENPTSYHL DDVLGFINPETQMPN
Guinea pig KVQSYLENPTSYHL DNVLGYMNPELQMPN
Dog KVQSYLENPTSYHL DDVLGFINPETQMPN
Chicken KVQSYLENPTTYHL DDVLGYMNPEVHMPN
marmoset KVQSYLENPTSYHL DDVLGYINPEMQMPN
Chimpamzee KVQSYLENPTSYHL DDVLGYINPEMQMPN
Mustela furo KVQSYLENPTSYHL DDVLGFINPETQMPN
d
WT-TFEB
Y75F
Y173F
TFEB Subcellular localization (%)
100
80
60
40
20
0
Cyt
Cyt/Nuc
Nuc
WT-TFEB
Y75F
Y173F
e
Mr (K)
WT-TFEB
Y75F-TFEB
Y173F-TFEB
100
100
32
TFEB pS211
GFP
GAPDH

Figure 4. Active ABL1 phosphorylates TFEB on tyrosine. (a) Representative western blot of Hela TFEB-GFP cells transfected with ABL1 ERT2 and ABL1 ERT KD plasmids and treated with Tamoxifen for 8h. GFP was immunoprecipitated using beads-anti-GFP and then used a anti-phospho-tyrosine antibody. *n*=3 independent experiments. (b) Autoradiography of an *in vitro* phosphorylation assay. TFEB-Flag IP was incubated with human recombinant ABL1 active and ATP-γ-^{32}P for 0h, 0.5h, 1h and 2h. (c) Tyrosine 75 (Y75) and Y173 are highly conserved across different species and are included in the ABL1 phosphorylation motif YX_5P. (d) Representative confocal microscopy images and quantification of subcellular localization of TFEB-GFP mutants and control plasmids. *n*=3 independent experiments. (e) Western blot of Hela cells transfected with a TFEB-GFP wild type plasmid or with plasmids carrying the Y75 or Y173 mutations. Western blot membranes were incubated with a specific antibody against S211.

ABL inhibition promotes cellular clearance through activation of TFEB

When TFEB is active in the nucleus is crucial for the expression of genes encoding proteins that promote cellular clearance of substrates accumulated in the lysosomes in different LSD (Medina et al., 2011; Spampanato et al., 2013), positioning TFEB as an excellent therapeutic target (Ballabio, 2016; Napolitano and Ballabio, 2016). It has been previously described that ABL inhibition promotes the clearance of alpha-synuclein in models of Parkinson's disease (Hebron et al., 2013). Therefore, because ABL phosphorylates TFEB and its inhibition induces TFEB activity, we analyzed if ABL inhibition promotes cellular clearance.

To evaluate cellular clearance we decided to load lysosomes with a substrate. The U18666A drug induces lysosomal cholesterol accumulation by inhibiting the lysosomal protein NPC1 (Lu et al., 2015). Then, we evaluated the effect of Imatinib in Hela cells treated with U18666A for 24h. Cholesterol accumulation was followed using the recombinant protein perfringolysin O, a cholesterol-binding bacterial toxin, fused to glutathione S-transferase (GST-PFO). This strategy allowed us to measure cholesterol accumulation in immunofluorescence using anti GST antibodies. This novel method for cholesterol visualization has been previously validated (Kwiatkowska et al., 2014).

As expected, we observed intracellular cholesterol accumulation in Hela cells treated with U18666A (Fig. 5a). However, pre-treatment with Imatinib, decreased the GST-PFO signal, suggesting a reduction in cholesterol accumulation induced by U18666A (Fig. 5a). Then, to quantify the effect of Imatinib on cholesterol accumulation we used confocal automated microscopy and performed a high-content GST-PFO assay. Interestingly, U18666A-treated Hela cells that had been pre-treated with Imatinib showed significantly less cholesterol

accumulation (Fig. 5b). We also observed that Imatinib decreased cholesterol accumulation, followed by GST-PFO staining, in U18666A-treated HEK293T cells (Supplementary Fig. 4a).

To confirm the cholesterol cellular clearance induced by ABL inhibition, we treated HT22 (neuronal cell line) and Hepa 1-6 (hepatocyte derived cell line) cells with the U18666A drug and Imatinib. Then, we analyzed cholesterol accumulation using the well-known cholesterol-marker filipin (Fig. 5c). In agreement with our previous results, we observed that Imatinib decreased filipin staining. All these results confirm the Imatinib cholesterol-lowering effect in different U18666A-treated cell lines using two different techniques to detect cholesterol accumulation (Fig. 5c). In addition, GNF-2, an allosteric ABL inhibitor, also reduced cholesterol accumulation in HT22 cells, demonstrating that two inhibitors that act on different ABL sites have the same effect. These results support the hypothesis that the cholesterol-lowering effects are mediated by ABL inhibition (Supplementary Fig. 4b).

Although Imatinib and GNF2 are well-known ABL inhibitors, to further evaluate if the cellular clearance of cholesterol is effectively mediated by ABL1 inhibition, we cultured hippocampal neurons from ABL1 null (ABL1 KO) and wild type mice embryos. 7 DIV neurons were treated with U18666A and, as expected, we observed increased filipin staining in wild type neurons. Interestingly, in the ABL1 KO hippocampal neurons we observed a decreased filipin staining in spite of U18666A treatment (Fig. 5d).

These results demonstrate that ABL inhibition promotes cellular clearance in cells loaded with cholesterol using the U18666A drug.

Then, we analyzed the relevance of TFEB on accumulation of cholesterol in U18666A-treated cells using wild type Hela (control), Hela TFEB-GFP and Hela TFEB-Knock out

FIGURE 5

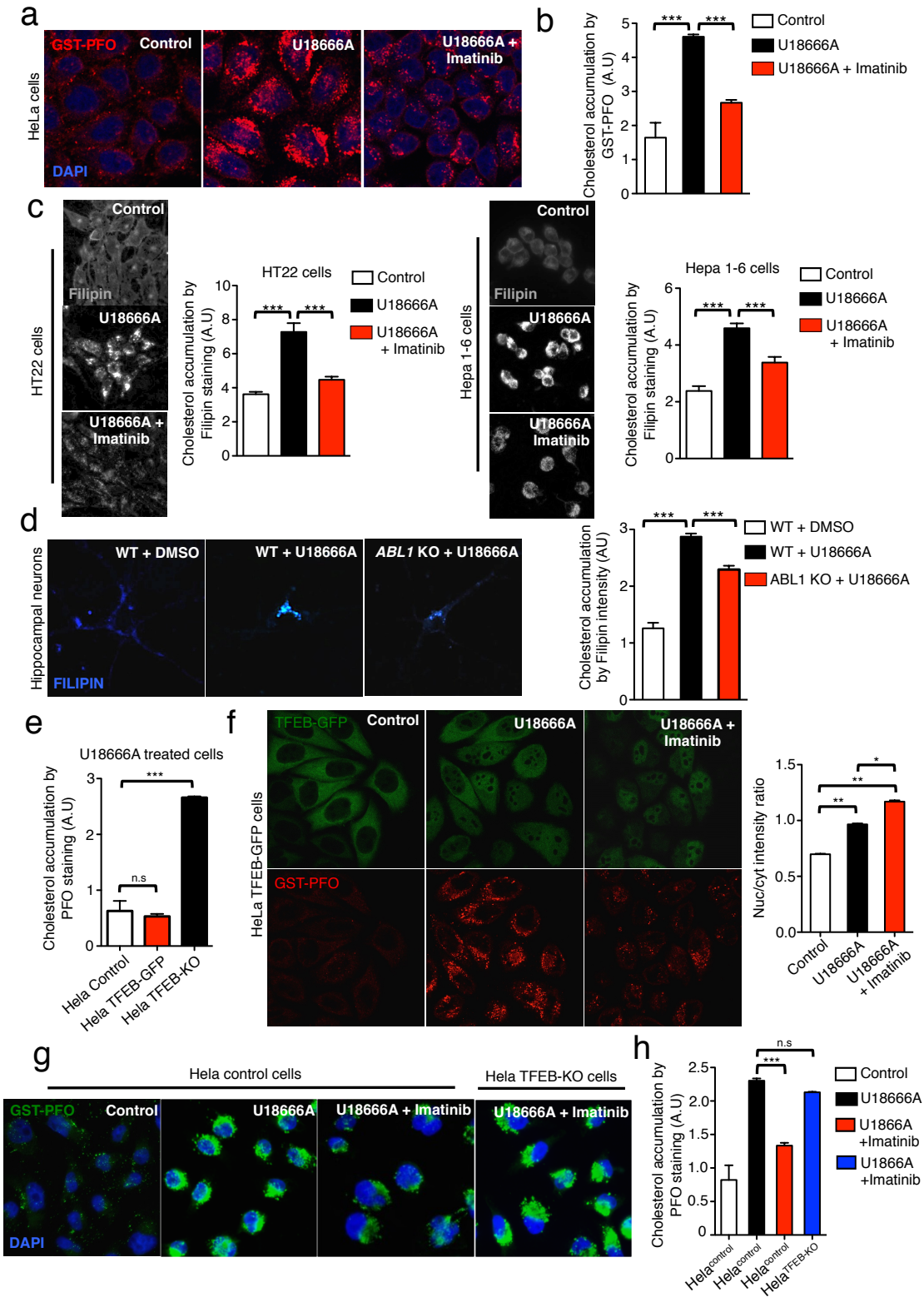
a
GST-PFO
Control
U18666A
U18666A + Imatinib
HeLa cells
DAPI
b
Cholesterol accumulation by GST-PFO (A.U)
***
***
Control
U18666A
U18666A + Imatinib
c
HT22 cells
Control
Filipin
U18666A
U18666A + Imatinib
Cholesterol accumulation by Filipin staining (A.U)
HT22 cells
Hepa 1-6 cells
Hepa 1-6 cells
d
Hippocampal neurons
WT + DMSO
WT + U18666A
ABL1 KO + U18666A
FILIPIN
Cholesterol accumulation by Filipin intensity (AU)
e
U18666A treated cells
Cholesterol accumulation by PFO staining (A.U)
n.s
Hela Control
Hela TFEB-GFP
Hela TFEB-KO
f
TFEB-GFP
GST-PFO
HeLa TFEB-GFP cells
Nuc/cyt intensity ratio
Control
U18666A
U18666A + Imatinib
g
Hela control cells
Hela TFEB-KO cells
h
Cholesterol accumulation by PFO staining (A.U)
U1866A +Imatinib

Figure 5. ABL inhibitors reduce cholesterol accumulation in a TFEB-dependent manner. (a) Representative confocal microscopy images showing cholesterol accumulation. Hela cells were treated with U18666A 0.5μg/mL and/or Imatinib 10μM for 24h. Then, GST-PFO (red) immunofluorescence and DAPI (blue) staining were performed. (b) Quantification of cholesterol accumulation from (a). A high-content GST-PFO assay using confocal automated microscopy was performed. *n*=3 independent experiments. (c) Representative images and quantification of cholesterol accumulation by filipin staining in HT22 cells and Hepa 1-6 cells treated with U18666A 0.5μg/mL and/or Imatinib 10μM for 24h. *n*=3 independent experiments. (d) Representative images and quantification of cholesterol accumulation by filipin staining on hippocampal neurons cultures of 7 DIV from Wild type (WT) mice and ABL1 KO mice (ABL1 KO) treated with U18666A 0.5μg/mL and/or Imatinib 10μM for 24h. *n*=40 neurons per conditions. (e) Hela cells; Hela TFEB-GFP cells and Hela TFEB-KO were treated with U18666A 0.5 μg/mL for 24h and cholesterol accumulation was analyzed by the high-content GST-PFO assay. For each condition 450-800 cells were analyzed (two wells x 7 images). (f) Representative images of cholesterol by GST-PFO and quantification of TFEB-GFP translocation assay in Hela TFEB-GFP cells treated with U18666A 0.5μg/mL and/or Imatinib 10μM for 24h. For each condition 450-800 cells were analyzed (two wells x 7 images). (g-h) Representative images and quantification of cholesterol accumulation using GST-PFO of Hela and Hela TFEB-KO cells treated with U18666A 0.5 μg/mL and/or Imatinib 10 μM for 24h. *n*=3 independent experiments. *$p < 0.05$, **$p < 0.01$,***$p < 0.001$. Data represent mean ± SEM.

(TFEB-KO) cells (Supplementary Fig. 4c). High-content GST-PFO assays showed that TFEB-KO cells have higher cholesterol accumulation than cells that express TFEB, indicating that TFEB absence worsens the effect of U18666A (Fig. 5e).

To analyze the effect of ABL inhibition on TFEB subcellular localization in cells that accumulate cholesterol, we treated Hela TFEB-GFP cells with U18666A and Imatinib and followed TFEB localization using the high-content nuclear translocation assay. We observed that U18666A treatment effectively promotes cholesterol accumulation compared to controls and that it also increases the TFEB nuclear signal (Fig. 5f). However, addition of Imatinib induces a large increase in TFEB nuclear translocation (Fig. 5f). Remarkably, in cells exposed to U18666A, Imatinib treatment induces a clear reduction in the accumulation of cholesterol that correlates with TFEB-GFP nuclear translocation (Fig. 5f and Supplementary Fig. 4d).

Interestingly, we observed that Imatinib did not decrease cholesterol accumulation in Hela TFEB-KO cells treated with U18666A (Fig. 5g-h), demonstrating that cellular cholesterol clearance triggered by ABL inhibition depends on the presence of TFEB. Moreover, Hela cells exposed to U18666A showed increased lysotracker red marker analyzed by FACs (Supplementary Fig. 4e), but co-treatment with Imatinib further increased lysotracker levels. Remarkably, we did not observe this increment in Hela TFEB KO cells treated with U18666A plus Imatinib, suggesting that this increase in lysotracker levels depends on TFEB (Supplementary Fig. 4e).

These results demonstrate that the increase in lysosomal cholesterol clearance induced by ABL inhibition is mediated by TFEB translocation into the nucleus.

ABL inhibition reduces cholesterol accumulation in NPC1 human fibroblasts

The cholesterol accumulation inducer U18666A has been used as a pharmacological model for the LSD Niemann-Pick type C (NPC). This disease is characterized by mutations in the *NPC1* or *NPC2* genes that encode cholesterol transporter proteins, leading to the pathogenic accumulation of cholesterol and other lipids within the late endosomal/lysosomal compartments (Kwon et al., 2009; Lloyd-Evans et al., 2008; Pentchev et al., 1984; Sturley et al., 2004).

To address the relevance of the novel ABL/TFEB axis in NPC pathology, we decided to use fibroblasts from NPC1 patients. We first analyzed the activation of ABL1 in these cells following phosphorylated-ABL1 (p-ABL1) and phosphorylated-CRKII (p-CRKII). Interestingly, we observed an increase of both phosphorylated proteins in different NPC1 patient's fibroblasts compared to wild type human fibroblasts (Fig. 6a). Next, we treated the different NPC1 patient fibroblasts with two ABL inhibitors, Imatinib and Nilotinib, for 24h and analyzed cholesterol accumulation with filipin staining. Remarkably, we observed that cholesterol accumulation was reduced in NPC1 patient fibroblasts carrying different mutations, when ABL was inhibited (Fig. 6b). The same cholesterol lowering-effect was observed in longer treatments (48h) with the ABL inhibitors (Supplementary Fig. 5a).

Concordantly, we observed a reduction in the GST-PFO signal in Npc1 knock out (KO) mouse fibroblasts, which accumulate cholesterol at basal levels, treated with Imatinib (Supplementary Fig. 5b). This result supports the idea that ABL inhibition promotes cellular clearance in NPC disease. Consequently, GNF2 treatment also reduced filipin staining in Npc1 KO fibroblasts (Supplementary Fig. 5c).

In addition, we decided to analyze in more detail the effect on ABL inhibition in V1165M

FIGURE 6

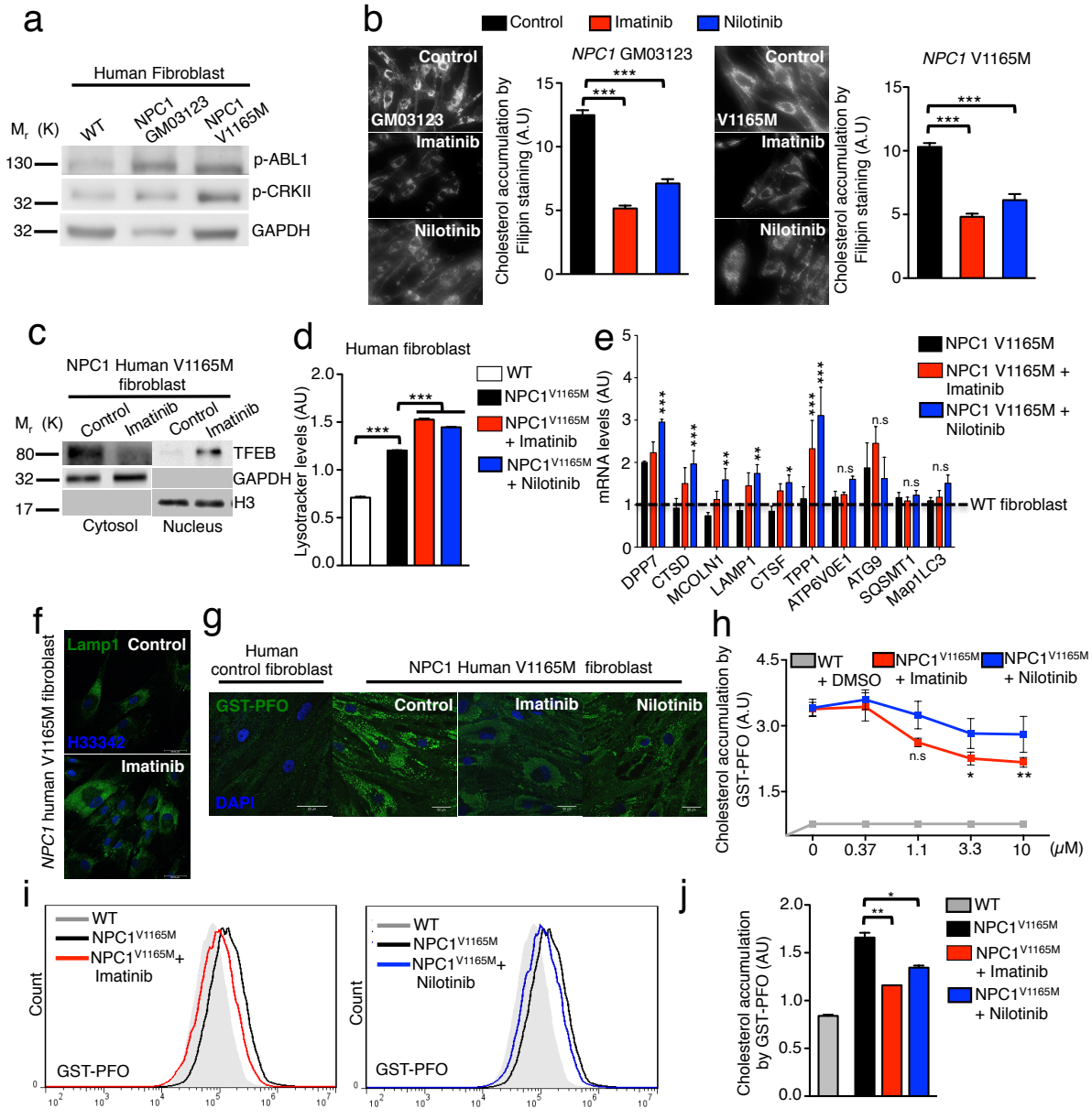
a
Human Fibroblast
WT
NPC1 GM03123
NPC1 V1165M
Mr (K)
130
p-ABL1
32
p-CRKII
32
GAPDH
b
Control
Imatinib
Nilotinib
Control
GM03123
Imatinib
Nilotinib
NPC1 GM03123
Cholesterol accumulation by Filipin staining (A.U)
Control
V1165M
Imatinib
Nilotinib
NPC1 V1165M
c
NPC1 Human V1165M fibroblast
Control
Imatinib
Control
Imatinib
Mr (K)
80
TFEB
32
GAPDH
17
H3
Cytosol
Nucleus
d
Human fibroblast
Lysotracker levels (AU)
WT
NPC1V1165M
NPC1V1165M + Imatinib
NPC1V1165M + Nilotinib
e
mRNA levels (AU)
NPC1 V1165M
NPC1 V1165M + Imatinib
NPC1 V1165M + Nilotinib
WT fibroblast
DPP7
CTSD
MCOLN1
LAMP1
CTSF
TPP1
ATP6V0E1
ATG9
SQSMT1
Map1LC3
f
NPC1 human V1165M fibroblast
Lamp1
Control
H33342
Imatinib
g
Human control fibroblast
NPC1 Human V1165M fibroblast
GST-PFO
DAPI
Control
Imatinib
Nilotinib
h
Cholesterol accumulation by GST-PFO (A.U)
WT + DMSO
NPC1V1165M + Imatinib
NPC1V1165M + Nilotinib
n.s
(μM)
i
Count
WT
NPC1V1165M
NPC1V1165M+ Imatinib
GST-PFO
Count
WT
NPC1V1165M
NPC1V1165M+ Nilotinib
GST-PFO
j
Cholesterol accumulation by GST-PFO (AU)
WT
NPC1V1165M
NPC1V1165M + Imatinib
NPC1V1165M + Nilotinib

Figure 6. Reduction of cholesterol accumulation by ABL inhibition in NPC1 human V1165M fibroblasts. (a) Representative western blot of phospho-ABL (p-ABL) and phosphor-CRKII (p-CRKII) in wild type and NPC1 human fibroblasts. GAPDH was used as loading control. (b) Representative images and quantification of cholesterol accumulation detected through filipin staining in NPC1 human fibroblast treated with Imatinib 10μM and Nilotinib 10μM for 24h. *n*=80 cells per conditions. (c) Representative western blot of endogenous TFEB in a nuclear/cytoplasmic fractionation assay of NPC1 patient V1165M fibroblasts treated with Imatinib 10μM for 24h. *n*=3 independent experiments. (d) Quantitative analysis of lysotracker in NPC1 patient V1165M fibroblasts treated with Imatinib and Nilotinib with 10μM for 24h using flow cytometry. *n*=10,000 cells per conditions. (e) q-PCR analysis of different mRNA TFEB target genes in NPC1 patient V1165M fibroblasts treated with Imatinib and Nilotinib 10 μM for 24h. *n*=3 independent experiments. (f) Representative immunofluorescence images of Lamp1 in NPC1 patient V1165M fibroblasts treated with Imatinib 10μM for 24h. (g-h) Representative images and quantification of cholesterol accumulation by high-content GST-PFO assay in NPC1 human fibroblasts treated with Imatinib and Nilotinib at different concentrations for 24h. For each condition 450-800 cells were analyzed (three wells x 7 images). (i-j) Quantitative analysis by flow cytometry of GST-PFO (cholesterol) in NPC1 human fibroblasts treated with Imatinib and Nilotinib with 10μM for 24h. *n*=10,000 cells per conditions. *$p < 0.05$, **$p < 0.01$,***$p < 0.001$. Data represent mean ± SEM.

NPC1 patient fibroblasts, because it was one of the NPC1 mutants where the effect on cholesterol clearance was more clearly seen. We treated the NPC1 patient V1165M fibroblasts with Imatinib for 24h and performed a nucleus-cytoplasm fractionation to analyze TFEB subcellular localization. We observed that this mutant presents low basal levels of TFEB in the nucleus and that Imatinib treatment clearly induced TFEB translocation to the nucleus (Fig. 6c). Concordantly, we observed that in NPC1 patient V1165M fibroblasts both ABL inhibitors, Imatinib and Nilotinib increased the lysotracker red signal compared with the control condition (Fig. 6d). Interestingly, both inhibitors significantly increased the expression of several TFEB-target genes such as *CTSD, MCOLC1, Lamp1 and TPP1* in this NPC1 patient fibroblast measured by q-PCR (Fig. 6e). Remarkably, we found that the most important changes were in the genes related to lysosomal biogenesis and exocytosis (Fig. 6e), an effect that correlates with increased LAMP1 signal measured by immunofluorescence in NPC1 patient V1165M fibroblasts treated with Imatinib (Fig. 6f).

Then, we treated this mutant with different concentrations of Imatinib and Nilotinib. Remarkably, using the high-content GST-PFO assay, we observed that the inhibitors promote a reduction in cholesterol accumulation in a concentration-depending manner, being Imatinib the most effective (Fig. 6 g-h). Concordantly, we observed the reduction of cholesterol accumulation in fibroblasts from NPC1 patient V1165M treated with these two ABL inhibitors measuring the GST-PFO signal by FACs (Fig. 6 i-j). It is important to mention that in Npc1 KO hippocampal neuronal cultures that clearly show cholesterol accumulation by GST-PFO staining, treatment with Imatinib reduced this accumulation (Supplementary Fig. 5d).

Remarkably, we observed that the ABL inhibitors Imatinib and Nilotinib, which are FDA

approved drugs, promote a reduction in cholesterol accumulation in NPC models.

ABL inhibition reduces cholesterol accumulation in vivo

Finally, in order to analyze the *in vivo* relevance of the ABL/TFEB axis, we treated $Npc1^{-/-}$ (NPC1 KO) mice with Imatinib by administering daily intraperitoneal injections (12.5 mg/Kg) and measured cholesterol accumulation in cerebellum sections by GST-PFO staining. As expected, we observed a clear accumulation of cholesterol in the soma of Purkinje neurons from NPC1 KO mice compared with wild type (WT) mice (Fig. 7a). Notably, NPC1 KO mice treated with Imatinib showed less cholesterol accumulation in Purkinje neurons (Fig. 7a).

To strengthen our data, we treated NPC1 KO mice with GNF-2, an allosteric ABL inhibitor. First, we corroborated that this ABL inhibitor improved the behavioral tests of NPC1 KO mice as we had previously demonstrated for NPC mice treated with Imatinib (Alvarez et al., 2008). Daily intraperitoneal injections of GNF-2 (5 mg/Kg) in NPC1 KO mice increased motor coordination, measured by the beam test (Fig. 7b); improved weight gain (Fig. 7c); and prevented Purkinje cell death in the cerebellum, measured by calbindin staining (Supplementary Figure 6 a-b). More importantly, filipin staining of cerebellum and liver sections showed that NPC1 KO mice treated with GNF-2 accumulate less cholesterol than NPC1 KO mice treated with saline solution (Fig. 7d).

Finally, we decided to promote cholesterol accumulation in cerebellum in an *in vivo* ABL1 deficient model. To do that, we treated wild type (WT) and ABL1 KO mice with U18666A (10 mg/kg) by intraperitoneal injection. We observed that WT mice treated with U18666A show increased cholesterol accumulation in Purkinje neurons compared with the control mice (Fig. 7e). Concordantly, ABL1 KO mice treated with U18666A showed decreased

cholesterol accumulation (Fig. 7e). Interestingly, and in accordance with our *in vitro* results, we observed a greater signal for endogenous TFEB in the nucleus of Purkinje cells in ABL1 KO mice treated with U1866A compared with WT mice treated with saline or U18666A. (Fig. 7e).

Altogether, these results demonstrate that inhibition of the novel signaling pathway ABL/TFEB promotes a reduction in the accumulation of cholesterol in *in vitro* and *in vivo* models of NPC disease.

FIGURE 7

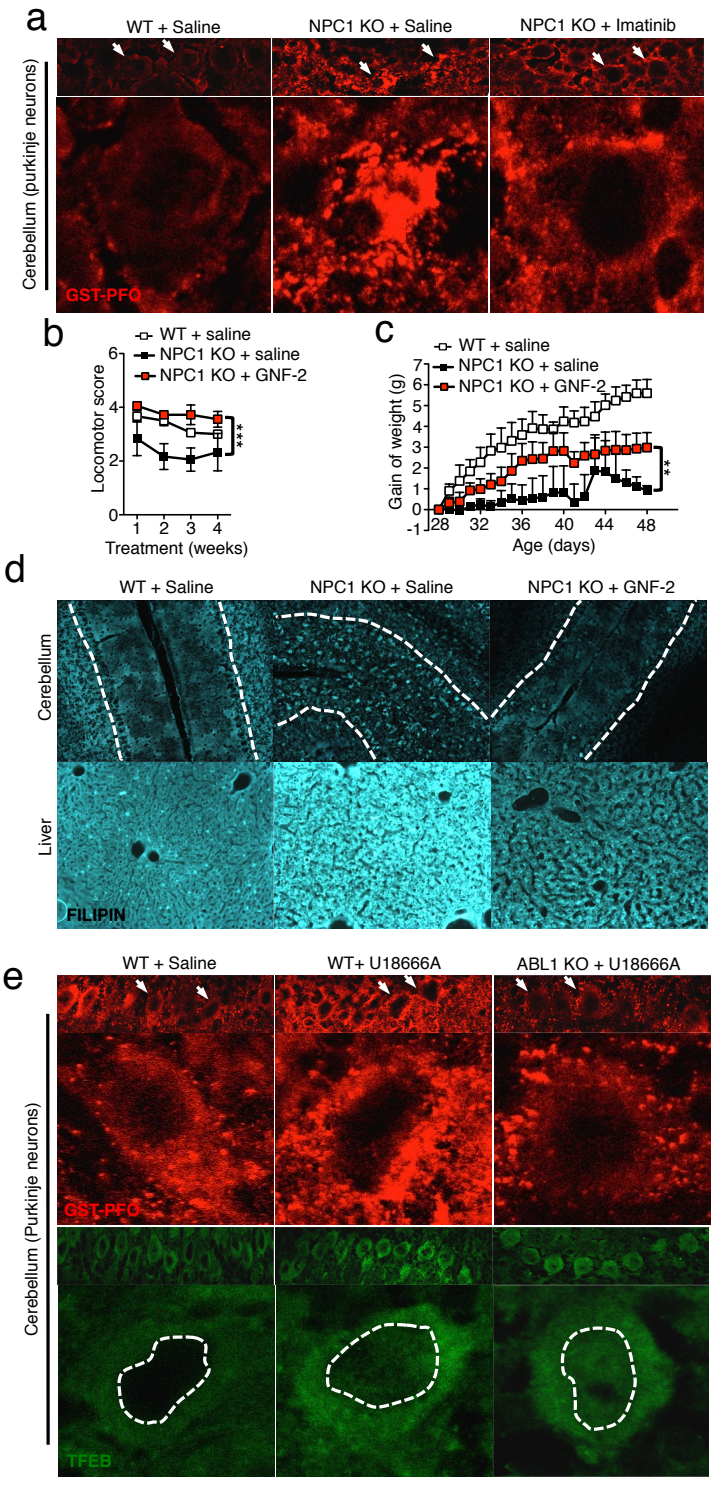
a
WT + Saline
NPC1 KO + Saline
NPC1 KO + Imatinib
Cerebellum (purkinje neurons)
GST-PFO
b
WT + saline
NPC1 KO + saline
NPC1 KO + GNF-2
Locomotor score
Treatment (weeks)
***
c
WT + saline
NPC1 KO + saline
NPC1 KO + GNF-2
Gain of weight (g)
Age (days)
**
d
WT + Saline
NPC1 KO + Saline
NPC1 KO + GNF-2
Cerebellum
Liver
FILIPIN
e
WT + Saline
WT+ U18666A
ABL1 KO + U18666A
Cerebellum (Purkinje neurons)
GST-PFO
TFEB

Figure 7. ABL deficiency reduces cholesterol accumulation in *in vivo* models of NPC. (a) Representative immunofluorescence showing cholesterol by GST-PFO staining (red) in cerebellum sections from 8 month-old wild type (WT) and NPC1 KO mice treated with vehicle or Imatinib 12.5 mg/Kg, every day for 2 weeks by intraperitoneal injections. (b-c) WT and NPC1 KO mice were treated for 4 weeks with vehicle and GNF-2 5 mg/Kg starting at p28. Motor coordination was assessed weekly by beam test (b) and weight was registered during the treatment (c) (n=5). (d) WT and NPC1 KO mice were treated with GNF-2 (5 mg/Kg) for three weeks starting at p28. Upper panels show filipin staining of cerebellum sections and lower panels show filipin staining of liver sections. (e) Representative immunofluorescence showing cholesterol by GST-PFO (red) and endogenous TFEB (green) in cerebellum sections from 8-month-old wild type (WT) and ABL1 KO mice treated with vehicle or U18666A 10 mg/Kg, for 2 days by intraperitoneal injections.

Discussion

Our results identified a novel mTORC1-independent axis between TFEB and the tyrosine kinase ABL and therefore a new potential therapeutic target for the treatment of lysosomal storage disorders. We demonstrated that the inhibition of this ABL/TFEB axis promotes cellular clearance and plays a key role in the reduction of cholesterol accumulation in the Niemann Pick-type C lysosomal storage disorder. Remarkably, we found that inhibition of the tyrosine kinase ABL promotes a cholesterol-lowering effect in several NPC1 pharmacological and genetic models (Fig. 4,5,7). Interestingly, the effect of the different ABL inhibitors was independent of cell type, including Hela, hepatic and neuronal cell lines.

To demonstrate that ABL controls the translocation of TFEB to the nucleus we used different strategies (Fig. 1). First, we used several pharmacological inhibitors, including Imatinib, Nilotinib and Dasatinib, designed to bind to the ATP binding site of ABL1 in the BCR-ABL1 fusion protein produced in patients with chronic myeloid leukemia (CML). In wild type cells, ABL1 is the primary target of these drugs. In addition, we included the more recently developed inhibitors GNF2 and GNF5, which bind to the allosteric site of ABL1 (Iacob et al., 2011). We found that all the inhibitors we tested increased TFEB nuclear localization. The more effective inhibitors that promoted TFEB nuclear translocation at lower concentrations were Nilotinib and Imatinib. Nilotinib was developed based on the chemical structure of the first and classic BCR-ABL1 inhibitor Imatinib, optimizing cellular potency and selectivity (Manley et al., 2010). As a second strategy, we used a siRNA against ABL1 and found that two readouts of TFEB activation, nuclear translocation and the induction of mRNA levels of lysosomal genes were increased. Importantly, our results also show that ABL inhibition not only activates overexpressed transfected TFEB but also

the endogenous TFEB, indicating that the ABL/TFEB axis is a relevant signaling pathway under physiological conditions.

Our results suggest that inhibition of ABL promotes several readouts of TFEB activation (Fig. 2). We observed an increase in autophago-lysosome formation, lysotracker and Lamp-1 signals and lysosome localization near the plasma membrane. These results suggest an increase in autophagic flux, lysosomal biogenesis and exocytosis in cells treated with Imatinib. Concordantly, it has been demonstrated that the inhibition of ABL promotes autophagy (Can et al., 2011; Ertmer et al., 2007; Lim et al., 2014), a process that is dysregulated in different lysosomal storage disorders such as NPC, Pompe disease and MPSIIIA (Lieberman et al., 2012). Because TFEB regulates lysosomal biogenesis, exocytosis and autophagy (Settembre et al., 2013; Settembre and Medina, 2015), inhibition of the ABL/TFEB axis could promote cholesterol clearance through these 3 biological processes (Medina et al., 2011).

Our results demonstrated that TFEB nuclear translocation, promoted by inhibition of ABL, is independent of mTORC1 (Fig. 3). Interestingly, the inhibition of ABL was able to induce the translocation of TFEB to the nucleus under conditions in which mTORC1 is fully active, including re-fed conditions after nutrient starvation and in cells deficient for TSC2, the negative regulator of mTORC1. This is of great relevance in pathological conditions in which mTORC1 signaling could be compromised such as in certain NPC1 mutations found in patients, in which a negative feed-back is lost between NPC1 and mTORC1 because it requires an intact sterol-sensing domain site in NPC1 (Castellano et al., 2017). Moreover, this result is encouraging because the inhibition of mTORC1 is not a good strategy for the treatment of diseases with compromised lysosomes, since this kinase fulfills multiple cellular functions. Recent studies have shown that inhibition of Akt kinase by compounds

such as trehalose induces the nuclear translocation of TFEB independent of mTORC1 (Palmieri et al., 2017). Therefore, regulation of TFEB translocation seems to respond to more than one signaling system, increasing the possibilities for its modulation.

Our study demonstrates, for the first time, that TFEB activity is negatively regulated by tyrosine phosphorylation. We found that the activity of ABL1 is sufficient to promote TFEB tyrosine phosphorylation (Fig. 4). Indeed, our results showed that the Y173F TFEB-GFP mutant protein has a constitutive nuclear localization, suggesting that Y173 is relevant to retain TFEB in the cytoplasm. This tyrosine is highly conserved in TFEB from different species.

Notably, we found that under conditions in which ABL is inhibited, TFEB translocates into the nucleus when it is phosphorylated no S142 and S138 but not on S211. This difference would probably reflect a decrease in the interaction between TFEB and the 14-3-3 chaperone, which retains TFEB in the cytoplasm when TFEB is phosphorylated on S211 (Roczniak-Ferguson et al., 2012). It is possible to propose that the reduction of TFEB tyrosine phosphorylation, as a consequence of ABL inhibition, would favor de-phosphorylation on TFEB-S211. Indeed, we found that the Y173F TFEB-GFP protein exhibit less phosphorylation on S211 compared with the wild type TFEB-GFP protein and the mutant Y73F TFEB-GFP protein. However, additional studies are required to solve this point and to determine how ABL inhibition promotes TFEB de-phosphorylation on S211. Nevertheless, these findings reinforce the idea that tyrosine phosphorylation state could have an impact on the serine phosphorylation state of signaling proteins. This priming phenomenon has been previously described in other contexts (Kosten et al., 2014).

The relevance of TFEB in NPC disease has not been totally explored yet. Previously, it was shown that the mTORC1 inhibitor Torin1 promotes clearance of cholesterol accumulated in lysosomes (Wang et al., 2015). However, Torin1 has been shown to be toxic, probably due to the pleiotropic mTORC1 functions in cells. In addition, mTORC1 has been shown to be over-activated in NPC cells (Castellano et al., 2017), and TFEB preferentially localized in the cytoplasm of NPC null CHO cells (Castellano et al., 2017). Our results in figure 5 show that in Hela cells overexpressing TFEB, U18666A treatment slightly increases TFEB nuclear translocation. However, after Imatinib treatment, TFEB nuclear localization is increased further. Most importantly, in NPC1 human fibroblasts, the ABL inhibitors promoted a reduction in cholesterol accumulation, independent of the specific NPC1 mutation (Fig. 6). Further studies are required to evaluate the effect of ABL inhibition on *NPC2* mutants, which are responsible for 5% of NPC cases (Patterson et al., 2012) as well as in models of other lysosomal disorders, to find the relevance of this axis in other diseases. In any case, inhibiting ABL seems to be a good therapeutic option not only for lysosomal storage disorders but also for other diseases such as Alzheimer's, Parkinson's and ALS, where lysosomal function is also compromised (Cancino et al., 2011; Cancino et al., 2008; Estrada et al., 2016; Estrada et al., 2011; Hebron et al., 2013; Imam et al., 2013; Imamura et al., 2017; Karuppagounder et al., 2014; Katsumata et al., 2012; Pagan et al., 2016; Rojas et al., 2015; Tanabe et al., 2014; Vargas et al., 2018). Remarkably, under basal conditions, NPC1 human fibroblasts show very low levels of TFEB in the nucleus, which are greatly increased after ABL inhibition. These experiments demonstrate that in the context of NPC disease, ABL inhibition promotes TFEB nuclear translocation (Fig. 6) promoting an increase in Lamp1 protein levels and a TFEB-dependent increase in lysotracker red staining in Hela-U18666A treated cells. Concordantly, mRNA levels of several TFEB-target genes, most of them related with

lysosomal biogenesis and exocytosis, were recovered in NPC1 human fibroblasts treated with Imatinib or Nilotinib. Furthers studies are needed to analyze if in specific contexts, TFEB promotes the fine-tune regulation of particular genes (Fig. 6). Remarkably, we demonstrated that the cholesterol-lowering effect of ABL inhibition is abolished in Hela TFEB KO cells. These results confirm the relevance of TFEB in cellular clearance induced by ABL inhibition in NPC cells (Fig. 5).

Importantly, we observed similar results in NPC *in vivo* models (Fig. 7) and also that Imatinib treatment prevented cholesterol accumulation in Npc1 KO mice. We described previously that this ABL inhibitor prevents neuronal death and improves performance in different behavioral test and increases lifespan of this NPC mice model (Alvarez et al., 2008). Therefore, the cholesterol-lowering effect of Imatinib could be crucial to this improvement in the Npc1 KO mice. Then, it was important to corroborate these results with a novel ABL inhibitor. We chose GNF-2, because even though is not an approved FDA drug, our analysis showed that it has a better penetrance of the blood brain barrier (data no shown) than Imatinib. In agreement with our previous data with Imatinib, we observed that Npc1 KO mice treated with GNF-2 have a better performance in the behavioral tests. Importantly, this improved performance correlates with decreased cholesterol accumulation in Purkinje neurons. Similar results on cholesterol accumulation were observed in ABL1 KO mice treated with U18666A, in which endogenous TFEB was found mainly in the nucleus of Purkinje cells (Fig. 7).

Interestingly, because ABL is a tyrosine kinase that participates in several signaling pathways that induce neuronal dysfunction and death, its inhibition also generates beneficial effects in neurodegenerative diseases including decreased activation of the proapoptotic p73 transcription factor, HDAC2 activity and APP processing, as it has

already been shown in AD and NPC models (Cancino et al., 2008; Contreras et al., 2016; Estrada et al., 2016; Gonzalez-Zuniga et al., 2014; Klein et al., 2011; Yanez et al., 2016). In addition, the inhibition of ABL decreases protein accumulation of misfolded α-synuclein and mutant SOD1 in Parkinson and ALS (Imamura et al., 2017), respectively. Imatinib and Nilotinib are FDA approved ABL inhibitors and their chronic use in patients with CML is safe and has few side effects. Moreover, the results from a small group of patients with Parkinson's disease and Dementia with Lewy bodies that had been treated with Nilotinib for 24 weeks, suggested a possible beneficial effect of this drug in neurodegenerative diseases (Pagan et al., 2016). Altogether, these results position ABL inhibitors as a novel strategy for the treatment of diseases in which lysosomes and TFEB have been proposed as therapeutic targets, such as Pompe, Gaucher, MPSIV and Batten disease, among others (Ballabio, 2016; Napolitano and Ballabio, 2016).

Finally, our data revealed a new mTORC1-independent mechanism for lysosomal clearance through the activation of TFEB by inhibiting the tyrosine kinase ABL. Our results show that ABL is a very good target for treatment of neurodegenerative lysosomal diseases. This mechanism is relevant in the context of the NPC lysosomal storage disorder in which this kinase is active. The inhibition of ABL using FDA approved drugs promotes the activation of TFEB and cellular clearance, opening the possibility of treating NPC patients as well as other patients suffering from other neurodegenerative lysosomal storage disorders.

Material and methods

Animals, antibodies and reagents: Npc1$^{+/-}$ BALB/c mice carrying a heterozygous mutation in the NPC1 gene were kindly obtained from Jackson laboratory (Sacramento, CA, USA) . Genotypes were identified using a PCR-based screening as described previously (Amigo et al., 2002). ABL1 KO mice were bred from ABL1^{loxp}/ABL1^{loxp} and Nestin-Cre^{+} was purchased from Jackson laboratory. The animal protocols used were reviewed and approved by the animal studies board at our institution. Rabbit anti-TFEB #4240, rabbit anti-ABL #2862, rabbit anti-Histone H3 #9715, rabbit anti-phospho-P70 S6 Kinase #9205, rabbit anti-P70 S6 Kinase #9202, phospho-(Ser) 14-3-3 Binding Motif #9601 (Detection of TFEB phosphorylation at Ser211), anti-phosho-CRKII #3491 were purchased from Cell Signaling Technology (Danvers, Massachusetts, USA). Antibody for Mouse TFEB was purchased from Proteintech (13372-1-AP). Rabbit anti-GFP (A11122), Hoechst 33342 (H3570), LysoTracker red DND-99 (L7528) and Fluoromont-G with DAPI (00-4959-52) were purchased from Thermo Fischer Scientific (Waltham, Massachusetts, USA). Anti-GST (24-4577-01) was purchased from GE Healthcare. Mouse anti-ABL (sc-23), mouse anti-GAPDH (sc-32233), anti-rat Lamp1-D4B (sc-19992) were purchased from Santa Cruz Biotechnology (Dallas, United States of America). Anti-mouse Lamp1 (ab25630) was purchased from abcam (Cambridge, UK). Rabbit anti-TFEB AB1 (AV100809) Rabbit anti-phospho-ABL (C4240), Filipin, ANTI-FLAG M2 affinity gel (A2220), ANTI-FLAG (F7425) and Tamoxifen (T5648) were purchased from Sigma-Aldrich. Agarose anti-GFP (MB-0732) was purchased from Vector laboratories. Imatinib mesylate (13139), Nilotinib, Dasatinib were purchased from Cayman Chemical Company (Ann Arbor, USA). Torin1 (4247) was purchased from Tocris (Minneapolis, USA). GNF2 and GNF5 were obtained from the

National Center for Advancing Translational Sciences (Center at the National Institutes of Health (NIH). U18666A (U18) drug was purchased from Enzo Life Sciences Inc. (Farmingdale, NY, USA). Mouse anti-phospho-tyrosine antibody (4G10), anti-MAP2 (MAB3418) was purchased from Merck Millipore. Anti-p-Ser-142-TFEB was produced as described previously (Settembre et al., 2012). Anti-p-Ser-138-TFEB was produced as described previously (Napolitano et al., 2018). GST-PFO recombinant protein was produced as described previously (Kwiatkowska et al., 2014).

Cell Culture: Hela cells, Hela TFEB-GFP cells, TFEB-3xFlag cells, TFEB-KO cells and TSC2 KO cells were obtained from the Andrea Ballabio's lab (TIGEM, Italy). Hepa 1-6 cells, HEK293T and NPC1 mouse fibroblasts were obtained from ATCC (Virginia, USA) and from Peter Lobel (Rutgers University, New Yersey, USA). NPC1 human fibroblast V1165M (c.2795+1G>C c.3493G>A p.V1165M) were donated by Andrea Dardis (Coordinator Centre for Rare Diseases, Academic Hospital Santa Maria della Misericordia, Udine, Italy) and GM03123 (c.709C>T p.P237S c. 3182T>C p. I1061T) were obtained from Coriell Institute (USA). HT22 cells were kindly donated by Elena Pasquale (Sanford-Burnham Medical Research Institute, La Jolla, California, USA). H4 GFP-mRFP-LC3 cells were obtained from Patricia Burgos's lab (Universidad Austral de Chile and Universidad San Sebastián, Chile). All the cells were maintained in Dulbecco's modified Eagle's medium (DMEM) supplemented with 10% fetal bovine serum, 100 IU/mL penicillin, and 100 μg/ml streptomycin.

Mice hippocampal neuron cultures: Hippocampi from ABL1$^{floxo/floxo}$ Nestin Cre (ABL1 KO) and ABL$^{floxo/floxo}$ (wild-type) mice were removed on postnatal day 1 (the genotype of the animals (ABL1$^{+/+}$ (WT) or ABL1$^{-/-}$ (ABL1 KO) was determined 1 day later) or from NPC1 KO mice, were dissected in Ca^{2+}/Mg^{2+}-free Hank's balanced salt solution (HBSS) and rinsed twice with HBSS. Then, the tissue was re-suspended in HBSS containing 0.25% trypsin and incubated for 15 min at 37°C. After three rinses with HBSS, the tissue was mechanically dissociated in DMEM, supplemented with 10% horse serum (Invitrogen, Waltham, MA, USA), 100 U/mL penicillin, and 100 μg/mL streptomycin. Dissociated hippocampal cells were seeded onto poly-Lysine coated coverslips. Cultures were maintained at 37°C in 5% CO_2 for 2 h before the plating medium was replaced with Neurobasal growth medium (Invitrogen) supplemented with B27 (Invitrogen), 2 mM L-glutamine, 100 U/mL penicillin, and 100 μg/mL streptomycin. On day 2, cultured neurons were treated with AraC 2μM for 24 h; this method resulted in cultures highly enriched in neurons (approximately 5% glia).

Imatinib, Nilotinib, Dasatinib, GNF2, GNF5, U18666A (U18), Torin1, treatments: All the cell lines were treated as indicated in the manuscript. Cells were treated with Imatinib 10μM or Nilotinib 10μM and later, cells were treated with U18 0.5 μg/mL for 24 h when is indicated. ABL1 KO hippocampal neurons were treated with U18 0.5 μg/mL for 24h.

Plasmids and siRNA: TFEB-GFP and TFEB-3xFlag were obtained from Andrea Ballabio's Lab (TIGEM, Italy). Non-targeting siRNA Pool (scramble), On-Target plus Human siRNA anti-ABL1 were purchased from Dharmacon (GE Healthcare, USA). ABL1 ERT2 and ABL1

ERT2 KD, were generated in the Douglas R. Green lab (St. Jude Children's Research Hospital, Memphis, USA). TFEB-GFP, TFEB-3xFLag, ABL ERT2 and ABL ERT2 KD were transfected into cells using: TransIT-LT1 transfection reagent was purchased from Mirus Bio LCC (USA) and Lipofectamine 2000 reagent Thermo Fischer Scientific (Waltham, Massachusetts, USA). siRNA scramble and On-Target plus Human siRNA anti-ABL1 were transfected into cells using Lipofectamine RNAiMAX transfection reagent Thermo Fischer Scientific (Waltham, Massachusetts, USA). 48 h or 72h after transfection, the cells were lysed in RIPA buffer and used for Immunoprecipitation and/or immunoblot analysis.

TFEB tyrosine phosphorylation assay: Hela cells were transfected with ABL1 ERT2 and ABL1 ERT2 KD plasmid. The cells were then treated with Tamoxifen 0.1 μM for 6h. Then cells were lysed in immunoprecipitation buffer plus protease and phosphatase inhibitors. We used agarose beads anti-GFP for the immunoprecipitations. TFEB tyrosine phosphorylation was evaluated with an anti-phospho-Tyr antibody (4G10, Millipore).

Immunofluorescence procedures: Cell lines and hippocampal neurons were seeded onto poly-Lysine coated coverslips in 24-well culture plates at a density of 3.0 x 10^4 cells per well. After treatment, cells were washed twice with PBS, fixed in 4% paraformaldehyde in PBS for 20 min, and permeabilized for 10 min in 0.2% Triton X-100 in PBS. After 2 washes with PBS, the cells were incubated in 3% BSA in PBS for 30 min at room temperature, followed by incubation with primary antibodies against Lamp1 or TFEB at 4°C overnight. For the GST-PFO assay, cells were incubated (2 times) with 3% fish gelatin in PBS 1X (30 min each incubation). Then, cells were treated with 5 μg/ml GST-PFO for 45 min at RT and washed five times in 0.2% fish gelatin/PBS 1X followed by incubation with primary antibodies against GST goat at 4°C overnight. The cells were washed four times with PBS and then incubated with anti-mouse/anti-goat Alexa 488 and anti-rabbit/anti-goat Alexa

555 antibodies (Life Technologies, Carlsbad, United States of America) at room temperature for 1h. The fluorescence images were captured with Opera high content system; Perkin-Elmer. For confocal imaging, the samples were examined under a Zeiss LSM 700 confocal microscope or with an Olympus BX51 microscope and analyzed and quantified with the ImageJ software

Luminal Lamp1: Cells were seeded in a coverslips. After 24 hours were washed with MEM + 10mM HEPES and Treated with Imatinib 10 μM for 24 hours followed by incubation with primary antibody (Lamp1-D4B) in MEM + 10 mM Hepes +1% BSA for 20 min at 4°C. Then PFA 4% for 20 min and Washed once in PBS followed by incubation with secondary antibody (Alexa Fluor 488) in PBS + 1% BSA for 1h at RT. The cells were washed, incubated with Hoechst for 10 min at RT. Images were obtained with Zeiss a LSM 700 confocal microscope.

High-Content TFEB-GFP Translocation, GST-PFO and GFP-mRFP-LC3 assays: Hela cells, HeLa TFEB-GFP cells, H4 cells, NPC1 human fibroblast were seeded in 96- or 384-well plates and treated as indicated in the text, washed, fixed and stained with DAPI or Hoechst. The acquisition of the images was by using confocal automated microscopy (Opera high-content system; Perkin-Elmer). A dedicated script was developed to perform the analysis of TFEB localization, GST-PFO and GFP-mRFP-LC3 puncta on the different images (Harmony and Acapella software; Perkin-Elmer) (Medina et al., 2015).

In vitro phosphorylation assay: Kinase assay mixtures contained 25 mM HEPES, pH 7.25, 100 mM NaCl, 5 mM MgCl2, 5% glycerol, 100 ng/μL of bovine serum albumin, 1 mM sodium orthovanadate, TFEB-Flag or GST–CrkII, 5 μM ATP, and 0.5 μCi of [γ^{32}P]ATP. After a 5 min preincubation at 30°C, 25 µL reactions were initiated by the addition of 10 nM ABL1 T315I kinase. All reaction mixtures were incubated at 30°C for different periods of time. Then the TFEB-Flag or GST-CrkII proteins were pulled down, washed, and analyzed by autoradiography.

Flow Cytometry: For GST-PFO analysis, confluent cells transfected were trypsinized and washed with PBS before incubation with PFA 4% for 20 min. Then cells were washed with PBS, centrifuged and re-suspended in PBS/Triton X-100 0.05% (v/v) for 5 min. Then cells were centrifuged and re-suspended in gelatin fish 3% for 15 min. Cells were centrifuged and re-suspended in GST-PFO 10 μg/mL in gelatin fish 1% for 45 min. Then, cells were treated with Anti-GST Alexa fluor-647 in gelatin fish 1% for 1 h. Finally, cells were resuspended in 0.3 mL PBS and analyzed on a FACS (BD FACSCanto II Flow Cytometer). For lysotracker red analysis, confluent cells were trypsinized for 5 min, centrifuged and re-suspended in DMEM 1% FBS. Then cells were incubated with Lysotracker red DND-99 for 5 min, washed and then analyzed on a FACS (BD FACSCanto II Flow Cytometer).

Nuclei-cytoplasmic fractions: Cells were seeded and treated as indicated in the text, washed and scraped gently. Then, cells were centrifuged and supernatant was discard and pellet was diluted an incubated for 2 minutes at RT with buffer A (20 mM Tris-HCL 7.6; 0.1 mM EDTA; 2 mM MgCl2 6H20; 0.5 mM NaF; 0.5 mM Na3 OV4) and then was incubated for 10 minutes on ice. Then NP-40 1% was added and samples were passes trough a syringe 20G 3 times. After this, samples were centrifuged 500 g for 3 minutes at 4ºC. Supernatant correspond to cytoplasmic fraction. Cell pellet was washed 3 times with

buffer A + 1% NP-40 centrifuging at 500 g for 3 minutes at 4ºC. Then were treated with buffer B (20 mM Hepes pH 7.9; 400 mM NaCl; 2.5% (V/V) Glicerol; 1 mM EDTA; 0.5 mM DTT; 0.5 mM NaF; 0.5 mM Na3 OV4) and incubated in liquid nitrogen and then at 37ºC. Then samples were incubated on ice for 20 minutes, centrifuged at 20.000 g for 20 minutes and the supernatant corresponded to nuclear fraction.

Filipin staining: Cells lines or hippocampal neurons were fixed in 4% paraformaldehyde/4% sucrose in PBS for 30 min. Then, cells were washed in PBS and treated with 1.5 mg/mL glycine for 20 min. Finally cells were treated with 25 μg/mL Filipin (Sigma) for 30 min, washed with PBS and covered with Fluoromount-G (Southern Biotech, Birmingham, AL, USA). Images were captured with an Olympus BX51 microscope and analyzed with the ImageJ software.

Immunoblot analysis: Cells were lysed in RIPA buffer (25mM Tris-HCl pH 7.6, 150mM NaCl, 1% NP-40, 1% sodium deoxycholate, 0.1% SDS) supplemented with cocktail of protease inhibitors (Roche): Na_3VO_4, NaF, PMSF and Aprotinina. The homogenates were maintained on ice for 30 min and then they were centrifuged at 10,000g for 10 min. The supernatant was recovered, and protein concentration was determined with the Pierce BCA protein assay kit (23225) purchased from Thermo Scientific (Waltham, United States of America). Proteins were resolved in SDS-PAGE, transferred to Nitrocellulose membranes (Thermo Scientific), and probed with primary antibodies against TFEB, GFP, ABL, p-ABL, p-CRKII, GAPDH and p-P70 S6 Kinase, total-P70 S6 Kinase. The reactions were followed by incubation with HRP labeled secondary antibodies and developed using the ECL technique (Thermo Scientific).

Quantitative Real-Time PCR: Total RNA from Hela cells and human fibroblasts was extracted using an RNeasy Mini Kit (Qiagen), and reverse-transcribed to cDNA using the QuantiTect Reverse Transcription Kit (Qiagen). Real-time quantitative PCR assays were performed in triplicate using LightCycler 480 SYBR Green I Master in a LightCycler System 2.0 (Rocher Applied Science). The oligonucleotides used were as follows: GAPDH; fw: 5'-attgttcgtcatgggtgtgaa-3', rev: 5'-aggggtgctaagcagttggt-3', DPP7; fw: 5'-gattcggaggaacctgagtg-3', rev: 5'-cggaagcaggatcttctgg-3', CTSD; fw: 5'-cttcgacaacctgatgcagc-3', rev: 5'-tacttggagtctgtgccacc-3', MCOLN1; fw: 5'-gagtccctgcgacaagtttc-3', rev: 5'-tgttctcttcccggaatgtc-3', LAMP1; fw: 5'-ccaacttctctgctgccttc-3', rev: 5'-agcaatcaacgagactgggg-3'. CTSF; fw: 5'-acagaggaggagttccgcacta-3', rev: 5'-gcttgcttcatcttgttgcca-3', TPP1; fw: 5'-gatcccagctctcctcaatacg-3', rev: 5'-gccatttttgcaccgtgtg-3', ATP6V0E1; fw: 5'-cattgtgatgagcgtgttctgg-3', rev: 5'-aactccccggttaggaccctta-3', ATG9; fw: 5'-ttcctttgcccttatgcatg-3', rev: 5'-aaccgcatcaaagaaagctc-3', SQSTM1; fw: 5'-caggtcttccaaggttgagg-3', rev: 5'-ataaaaacacggccatttgc-3', ABL1; fw: 5'-ctgcaaatccaagaaggggct-3', rev: 5'-ctgaggctcaaagtcagatgcta-3', Map1LC3; fw: 5'-agcgctacaagggtgagaa-3', rev: 5'-gttcaccagcaggaagaag-3'. The relative quantities of cDNA were calculated using the comparative CT method. Data were derived from three independent amplifications.

Site-directed mutagenesis: TFEB Tyr mutants were generated by PCR using the proofreading Pfu polymerase (Stratagene, Santa Clara, United States of America), followed by DpnI (New England Biolabs, Massachusetts, United States of America) digestion of the methylated parental plasmid. Oligonucleotides used were as follows: Y75F; fw: 5'-gttgaaggtgcagtccttcctggagaatcccac-3', rev: 5'-

gtgggattctccaggaaggactgcaccttcaac-3', Y173F; fw: 5'-gacgatgtccttggcttcatcaatcctgaaatgc-3', rev: 5'-gcatttcaggattgatgaagccaaggacatcgtc-3'. Each clone was verified by automated sequencing.

Histological analysis: Mice were perfused with 4% paraformaldehyde in PBS. Brains were removed and post-fixed overnight at 4°C, placed in 20% sucrose in PBS at 4°C overnight, and then cut in 25 ìm thick sagital sections using a cryostat (Leika) at -20°C. Slices were permeabilized with 0.1% Triton X-100, blocked in 5% BSA or Gelatin in PBS and incubated overnight with the antibody rabbit anti-TFEB and GST in 5% BSA in PBS. For GST-PFO staining, tissues were treated with GST-PFO after gelatin block. The primary antibody was visualized with anti-rabbit Alexa-Fluor 555 or Alexa-Fluor 488.

Statistical analysis: Mean and SEM values and the number of experiments are indicated in each figure legend. One-way ANOVA tests were performed followed by Bonferroni post-test using the Prisma Software.

Statement of ethics: All protocols were approved and followed local guidance documents generated by the *ad hoc* committee of the Chilean Science and Technology Council (CONICYT) and were approved by the Scientific Ethics Committee for the care of animals and the environment, Pontificia Universidad Católica de Chile #160321008 (exCEBA 14-038). Protocols are in agreement with the US Public Health Service Policy on Humane Care and Use of Laboratory Animals recommended by the Institute for Laboratory Animal Research in its Guide for Care and Use of Laboratory Animals.

Abbreviations

NPC: Niemann-Pick type C; LSD: Lysosomal storage diseases;

Competing interests

The authors declare that they have no conflicts of interest.

Author Contributions

P.S.C., A.R.A., and S.Z. conceived of the study. P.S.C., D.L.M., A.B., A.R.A and S.Z designed experiments. P.S.C., P.J.T., L.G-H., I.P., Ch.S., G.N., M.M., M.LH., D.W and A.D.K. performed experiments. P.S.C., P.J.T., L.G-H., I.P., M.LH., and Ch.S. performed quantitative analysis of the results. P.S.C., A.M., F.M.P., J.C., N.L. and A.S. generated reagents. P.S.C., A.B., A.R.A. and S.Z wrote the manuscript.

Acknowledgments

We thank Douglas Green (St. Jude Children's Research Hospital, Memphis, TN, USA) and Patricia Burgos (Universidad Austral de Chile, Valdivia and Universidad San Sebastián, Santiago, Chile) for the donation of the ABL1 ERT2 and ABL1 ERT2 KD plasmids and the H4 GFP-mRFP-LC3 cells, respectively.

This study was supported by grants from the Fondo Nacional de Desarrollo Científico y Tecnológico (FONDECYT) (grant numbers 1161065 to A.R.A, and 1150186 to S.Z); from Conicyt-Chile Grant Redes 150082 (SZ); from the University of Pennsylvania Orphan Disease Center and a donation from the University of Notre Dame's Warren Family Research Center for Drug Discovery. From European Union's Horizon 2020 research and innovation programme (RISE) under the Marie Skłodowska-Curie grant agreement Nº

734825 (P.S.C, A.D.K, F.M.P and S.Z) From de Fomento al Desarrollo Científico y Tecnológico FONDEF D10E1077 to A.R.A and S.Z and Projecto Basal PFB12/2007, 2013-2017 to A.R.A. P.S.C acknowledges support from CONICYT, Beca doctorado nacional 21140469.

References

Alvarez, A.R., Klein, A., Castro, J., Cancino, G.I., Amigo, J., Mosqueira, M., Vargas, L.M., Yevenes, L.F., Bronfman, F.C., and Zanlungo, S. (2008). Imatinib therapy blocks cerebellar apoptosis and improves neurological symptoms in a mouse model of Niemann-Pick type C disease. FASEB journal : official publication of the Federation of American Societies for Experimental Biology *22*, 3617-3627.

Amigo, L., Mendoza, H., Castro, J., Quinones, V., Miquel, J.F., and Zanlungo, S. (2002). Relevance of Niemann-Pick type C1 protein expression in controlling plasma cholesterol and biliary lipid secretion in mice. Hepatology *36*, 819-828.

Ballabio, A. (2016). The awesome lysosome. EMBO molecular medicine *8*, 73-76.

Blom, N., Gammeltoft, S., and Brunak, S. (1999). Sequence and structure-based prediction of eukaryotic protein phosphorylation sites. Journal of molecular biology *294*, 1351-1362.

Can, G., Ekiz, H.A., and Baran, Y. (2011). Imatinib induces autophagy through BECLIN-1 and ATG5 genes in chronic myeloid leukemia cells. Hematology *16*, 95-99.

Cancino, G.I., Perez de Arce, K., Castro, P.U., Toledo, E.M., von Bernhardi, R., and Alvarez, A.R. (2011). c-Abl tyrosine kinase modulates tau pathology and Cdk5 phosphorylation in AD transgenic mice. Neurobiology of aging *32*, 1249-1261.

Cancino, G.I., Toledo, E.M., Leal, N.R., Hernandez, D.E., Yevenes, L.F., Inestrosa, N.C., and Alvarez, A.R. (2008). STI571 prevents apoptosis, tau phosphorylation and behavioural

impairments induced by Alzheimer's beta-amyloid deposits. Brain : a journal of neurology *131*, 2425-2442.

Capdeville, R., Buchdunger, E., Zimmermann, J., and Matter, A. (2002). Glivec (STI571, imatinib), a rationally developed, targeted anticancer drug. Nature reviews. Drug discovery *1*, 493-502.

Carstea, E.D., Morris, J.A., Coleman, K.G., Loftus, S.K., Zhang, D., Cummings, C., Gu, J., Rosenfeld, M.A., Pavan, W.J., Krizman, D.B.*, et al.* (1997). Niemann-Pick C1 disease gene: homology to mediators of cholesterol homeostasis. Science *277*, 228-231.

Castellano, B.M., Thelen, A.M., Moldavski, O., Feltes, M., van der Welle, R.E., Mydock-McGrane, L., Jiang, X., van Eijkeren, R.J., Davis, O.B., Louie, S.M.*, et al.* (2017). Lysosomal cholesterol activates mTORC1 via an SLC38A9-Niemann-Pick C1 signaling complex. Science *355*, 1306-1311.

Contreras, P.S., Gonzalez-Zuniga, M., Gonzalez-Hodar, L., Yanez, M.J., Dulcey, A., Marugan, J., Seto, E., Alvarez, A.R., and Zanlungo, S. (2016). Neuronal gene repression in Niemann-Pick type C models is mediated by the c-Abl/HDAC2 signaling pathway. Biochimica et biophysica acta *1859*, 269-279.

Decressac, M., Mattsson, B., Weikop, P., Lundblad, M., Jakobsson, J., and Bjorklund, A. (2013). TFEB-mediated autophagy rescues midbrain dopamine neurons from alpha-synuclein toxicity. Proceedings of the National Academy of Sciences of the United States of America *110*, E1817-1826.

Druker, B.J., Tamura, S., Buchdunger, E., Ohno, S., Segal, G.M., Fanning, S., Zimmermann, J., and Lydon, N.B. (1996). Effects of a selective inhibitor of the Abl tyrosine kinase on the growth of Bcr-Abl positive cells. Nature medicine *2*, 561-566.

Ertmer, A., Huber, V., Gilch, S., Yoshimori, T., Erfle, V., Duyster, J., Elsasser, H.P., and Schatzl, H.M. (2007). The anticancer drug imatinib induces cellular autophagy. Leukemia *21*, 936-942.

Estrada, L.D., Chamorro, D., Yanez, M.J., Gonzalez, M., Leal, N., von Bernhardi, R., Dulcey, A.E., Marugan, J., Ferrer, M., Soto, C.*, et al.* (2016). Reduction of Blood Amyloid-beta Oligomers in Alzheimer's Disease Transgenic Mice by c-Abl Kinase Inhibition. Journal of Alzheimer's disease : JAD *54*, 1193-1205.

Estrada, L.D., Zanlungo, S.M., and Alvarez, A.R. (2011). C-Abl tyrosine kinase signaling: a new player in AD tau pathology. Current Alzheimer research *8*, 643-651.

Fraldi, A., Klein, A.D., Medina, D.L., and Settembre, C. (2016). Brain Disorders Due to Lysosomal Dysfunction. Annual review of neuroscience *39*, 277-295.

Gonzalez-Zuniga, M., Contreras, P.S., Estrada, L.D., Chamorro, D., Villagra, A., Zanlungo, S., Seto, E., and Alvarez, A.R. (2014). c-Abl stabilizes HDAC2 levels by tyrosine phosphorylation repressing neuronal gene expression in Alzheimer's disease. Molecular cell *56*, 163-173.

Gutknecht, M., Geiger, J., Joas, S., Dorfel, D., Salih, H.R., Muller, M.R., Grunebach, F., and Rittig, S.M. (2015). The transcription factor MITF is a critical regulator of GPNMB expression in dendritic cells. Cell communication and signaling : CCS *13*, 19.

Hantschel, O., Rix, U., and Superti-Furga, G. (2008). Target spectrum of the BCR-ABL inhibitors imatinib, nilotinib and dasatinib. Leukemia & lymphoma *49*, 615-619.

Hantschel, O., and Superti-Furga, G. (2004). Regulation of the c-Abl and Bcr-Abl tyrosine kinases. Nature reviews. Molecular cell biology *5*, 33-44.

Hebron, M.L., Lonskaya, I., and Moussa, C.E. (2013). Nilotinib reverses loss of dopamine neurons and improves motor behavior via autophagic degradation of alpha-synuclein in Parkinson's disease models. Human molecular genetics *22*, 3315-3328.

Iacob, R.E., Zhang, J., Gray, N.S., and Engen, J.R. (2011). Allosteric interactions between the myristate- and ATP-site of the Abl kinase. PloS one *6*, e15929.

Imam, S.Z., Trickler, W., Kimura, S., Binienda, Z.K., Paule, M.G., Slikker, W., Jr., Li, S., Clark, R.A., and Ali, S.F. (2013). Neuroprotective efficacy of a new brain-penetrating C-Abl inhibitor in a murine Parkinson's disease model. PloS one *8*, e65129.

Imamura, K., Izumi, Y., Watanabe, A., Tsukita, K., Woltjen, K., Yamamoto, T., Hotta, A., Kondo, T., Kitaoka, S., Ohta, A.*, et al.* (2017). The Src/c-Abl pathway is a potential therapeutic target in amyotrophic lateral sclerosis. Science translational medicine *9*.

Karuppagounder, S.S., Brahmachari, S., Lee, Y., Dawson, V.L., Dawson, T.M., and Ko, H.S. (2014). The c-Abl inhibitor, nilotinib, protects dopaminergic neurons in a preclinical animal model of Parkinson's disease. Scientific reports *4*, 4874.

Katsumata, R., Ishigaki, S., Katsuno, M., Kawai, K., Sone, J., Huang, Z., Adachi, H., Tanaka, F., Urano, F., and Sobue, G. (2012). c-Abl inhibition delays motor neuron degeneration in the G93A mouse, an animal model of amyotrophic lateral sclerosis. PloS one *7*, e46185.

Klein, A., Maldonado, C., Vargas, L.M., Gonzalez, M., Robledo, F., Perez de Arce, K., Munoz, F.J., Hetz, C., Alvarez, A.R., and Zanlungo, S. (2011). Oxidative stress activates the c-Abl/p73 proapoptotic pathway in Niemann-Pick type C neurons. Neurobiology of disease *41*, 209-218.

Kosten, J., Binolfi, A., Stuiver, M., Verzini, S., Theillet, F.X., Bekei, B., van Rossum, M., and Selenko, P. (2014). Efficient modification of alpha-synuclein serine 129 by protein kinase CK1 requires phosphorylation of tyrosine 125 as a priming event. ACS chemical neuroscience *5*, 1203-1208.

Kwiatkowska, K., Marszalek-Sadowska, E., Traczyk, G., Koprowski, P., Musielak, M., Lugowska, A., Kulma, M., Grzelczyk, A., and Sobota, A. (2014). Visualization of cholesterol deposits in lysosomes of Niemann-Pick type C fibroblasts using recombinant perfringolysin O. Orphanet journal of rare diseases *9*, 64.

Kwon, H.J., Abi-Mosleh, L., Wang, M.L., Deisenhofer, J., Goldstein, J.L., Brown, M.S., and Infante, R.E. (2009). Structure of N-terminal domain of NPC1 reveals distinct subdomains for binding and transfer of cholesterol. Cell *137*, 1213-1224.

Lawana, V., Singh, N., Sarkar, S., Charli, A., Jin, H., Anantharam, V., Kanthasamy, A.G., and Kanthasamy, A. (2017). Involvement of c-Abl Kinase in Microglial Activation of NLRP3 Inflammasome and Impairment in Autolysosomal System. Journal of neuroimmune

pharmacology : the official journal of the Society on NeuroImmune Pharmacology *12*, 624-660.

Li, L., Friedrichsen, H.J., Andrews, S., Picaud, S., Volpon, L., Ngeow, K., Berridge, G., Fischer, R., Borden, K.L.B., Filippakopoulos, P.*, et al.* (2018). A TFEB nuclear export signal integrates amino acid supply and glucose availability. Nature communications *9*, 2685.

Li, Y., Xu, M., Ding, X., Yan, C., Song, Z., Chen, L., Huang, X., Wang, X., Jian, Y., Tang, G.*, et al.* (2016). Protein kinase C controls lysosome biogenesis independently of mTORC1. Nature cell biology *18*, 1065-1077.

Lieberman, A.P., Puertollano, R., Raben, N., Slaugenhaupt, S., Walkley, S.U., and Ballabio, A. (2012). Autophagy in lysosomal storage disorders. Autophagy *8*, 719-730.

Lim, Y.M., Lim, H., Hur, K.Y., Quan, W., Lee, H.Y., Cheon, H., Ryu, D., Koo, S.H., Kim, H.L., Kim, J.*, et al.* (2014). Systemic autophagy insufficiency compromises adaptation to metabolic stress and facilitates progression from obesity to diabetes. Nature communications *5*, 4934.

Lloyd-Evans, E., Morgan, A.J., He, X., Smith, D.A., Elliot-Smith, E., Sillence, D.J., Churchill, G.C., Schuchman, E.H., Galione, A., and Platt, F.M. (2008). Niemann-Pick disease type C1 is a sphingosine storage disease that causes deregulation of lysosomal calcium. Nature medicine *14*, 1247-1255.

Lu, F., Liang, Q., Abi-Mosleh, L., Das, A., De Brabander, J.K., Goldstein, J.L., and Brown, M.S. (2015). Identification of NPC1 as the target of U18666A, an inhibitor of lysosomal cholesterol export and Ebola infection. eLife *4*.

Maekawa, T., Ashihara, E., and Kimura, S. (2007). The Bcr-Abl tyrosine kinase inhibitor imatinib and promising new agents against Philadelphia chromosome-positive leukemias. International journal of clinical oncology *12*, 327-340.

Manley, P.W., Drueckes, P., Fendrich, G., Furet, P., Liebetanz, J., Martiny-Baron, G., Mestan, J., Trappe, J., Wartmann, M., and Fabbro, D. (2010). Extended kinase profile and properties of the protein kinase inhibitor nilotinib. Biochimica et biophysica acta *1804*, 445-453.

Martina, J.A., Chen, Y., Gucek, M., and Puertollano, R. (2012). MTORC1 functions as a transcriptional regulator of autophagy by preventing nuclear transport of TFEB. Autophagy *8*, 903-914.

Martina, J.A., Diab, H.I., Brady, O.A., and Puertollano, R. (2016). TFEB and TFE3 are novel components of the integrated stress response. The EMBO journal *35*, 479-495.

Martina, J.A., and Puertollano, R. (2013). Rag GTPases mediate amino acid-dependent recruitment of TFEB and MITF to lysosomes. The Journal of cell biology *200*, 475-491.

Medina, D.L., Di Paola, S., Peluso, I., Armani, A., De Stefani, D., Venditti, R., Montefusco, S., Scotto-Rosato, A., Prezioso, C., Forrester, A.*, et al.* (2015). Lysosomal calcium signalling regulates autophagy through calcineurin and TFEB. Nature cell biology *17*, 288-299.

Medina, D.L., Fraldi, A., Bouche, V., Annunziata, F., Mansueto, G., Spampanato, C., Puri, C., Pignata, A., Martina, J.A., Sardiello, M.*, et al.* (2011). Transcriptional activation of lysosomal exocytosis promotes cellular clearance. Developmental cell *21*, 421-430.

Napolitano, G., and Ballabio, A. (2016). TFEB at a glance. Journal of cell science *129*, 2475-2481.

Napolitano, G., Esposito, A., Choi, H., Matarese, M., Benedetti, V., Di Malta, C., Monfregola, J., Medina, D.L., Lippincott-Schwartz, J., and Ballabio, A. (2018). mTOR-dependent phosphorylation controls TFEB nuclear export. Nature communications *9*, 3312.

Naureckiene, S., Sleat, D.E., Lackland, H., Fensom, A., Vanier, M.T., Wattiaux, R., Jadot, M., and Lobel, P. (2000). Identification of HE1 as the second gene of Niemann-Pick C disease. Science *290*, 2298-2301.

Pagan, F., Hebron, M., Valadez, E.H., Torres-Yaghi, Y., Huang, X., Mills, R.R., Wilmarth, B.M., Howard, H., Dunn, C., Carlson, A.*, et al.* (2016). Nilotinib Effects in Parkinson's disease and Dementia with Lewy bodies. Journal of Parkinson's disease *6*, 503-517.

Palmieri, M., Impey, S., Kang, H., di Ronza, A., Pelz, C., Sardiello, M., and Ballabio, A. (2011). Characterization of the CLEAR network reveals an integrated control of cellular clearance pathways. Human molecular genetics *20*, 3852-3866.

Palmieri, M., Pal, R., Nelvagal, H.R., Lotfi, P., Stinnett, G.R., Seymour, M.L., Chaudhury, A., Bajaj, L., Bondar, V.V., Bremner, L.*, et al.* (2017). mTORC1-independent TFEB activation via Akt inhibition promotes cellular clearance in neurodegenerative storage diseases. Nature communications *8*, 14338.

Parenti, G., Andria, G., and Ballabio, A. (2015). Lysosomal storage diseases: from pathophysiology to therapy. Annual review of medicine *66*, 471-486.

Patterson, M.C., Hendriksz, C.J., Walterfang, M., Sedel, F., Vanier, M.T., Wijburg, F., and Group, N.-C.G.W. (2012). Recommendations for the diagnosis and management of Niemann-Pick disease type C: an update. Molecular genetics and metabolism *106*, 330-344.

Pentchev, P.G., Boothe, A.D., Kruth, H.S., Weintroub, H., Stivers, J., and Brady, R.O. (1984). A genetic storage disorder in BALB/C mice with a metabolic block in esterification of exogenous cholesterol. The Journal of biological chemistry *259*, 5784-5791.

Polito, V.A., Li, H., Martini-Stoica, H., Wang, B., Yang, L., Xu, Y., Swartzlander, D.B., Palmieri, M., di Ronza, A., Lee, V.M.*, et al.* (2014). Selective clearance of aberrant tau proteins and rescue of neurotoxicity by transcription factor EB. EMBO molecular medicine *6*, 1142-1160.

Raben, N., and Puertollano, R. (2016). TFEB and TFE3: Linking Lysosomes to Cellular Adaptation to Stress. Annual review of cell and developmental biology *32*, 255-278.

Roczniak-Ferguson, A., Petit, C.S., Froehlich, F., Qian, S., Ky, J., Angarola, B., Walther, T.C., and Ferguson, S.M. (2012). The transcription factor TFEB links mTORC1 signaling to transcriptional control of lysosome homeostasis. Science signaling *5*, ra42.

Rojas, F., Gonzalez, D., Cortes, N., Ampuero, E., Hernandez, D.E., Fritz, E., Abarzua, S., Martinez, A., Elorza, A.A., Alvarez, A.*, et al.* (2015). Reactive oxygen species trigger motoneuron death in non-cell-autonomous models of ALS through activation of c-Abl signaling. Frontiers in cellular neuroscience *9*, 203.

Sardiello, M., and Ballabio, A. (2009). Lysosomal enhancement: a CLEAR answer to cellular degradative needs. Cell cycle *8*, 4021-4022.

Sardiello, M., Palmieri, M., di Ronza, A., Medina, D.L., Valenza, M., Gennarino, V.A., Di Malta, C., Donaudy, F., Embrione, V., Polishchuk, R.S.*, et al.* (2009). A gene network regulating lysosomal biogenesis and function. Science *325*, 473-477.

Schlatterer, S.D., Acker, C.M., and Davies, P. (2011). c-Abl in neurodegenerative disease. Journal of molecular neuroscience : MN *45*, 445-452.

Settembre, C., and Ballabio, A. (2011). TFEB regulates autophagy: an integrated coordination of cellular degradation and recycling processes. Autophagy *7*, 1379-1381.

Settembre, C., and Ballabio, A. (2014). Lysosomal adaptation: how the lysosome responds to external cues. Cold Spring Harbor perspectives in biology *6*.

Settembre, C., Di Malta, C., Polito, V.A., Garcia Arencibia, M., Vetrini, F., Erdin, S., Erdin, S.U., Huynh, T., Medina, D., Colella, P.*, et al.* (2011). TFEB links autophagy to lysosomal biogenesis. Science *332*, 1429-1433.

Settembre, C., Fraldi, A., Medina, D.L., and Ballabio, A. (2013). Signals from the lysosome: a control centre for cellular clearance and energy metabolism. Nature reviews. Molecular cell biology *14*, 283-296.

Settembre, C., and Medina, D.L. (2015). TFEB and the CLEAR network. Methods in cell biology *126*, 45-62.

Settembre, C., Zoncu, R., Medina, D.L., Vetrini, F., Erdin, S., Erdin, S., Huynh, T., Ferron, M., Karsenty, G., Vellard, M.C.*, et al.* (2012). A lysosome-to-nucleus signalling mechanism senses and regulates the lysosome via mTOR and TFEB. The EMBO journal *31*, 1095-1108.

Spampanato, C., Feeney, E., Li, L., Cardone, M., Lim, J.A., Annunziata, F., Zare, H., Polishchuk, R., Puertollano, R., Parenti, G.*, et al.* (2013). Transcription factor EB (TFEB) is a new therapeutic target for Pompe disease. EMBO molecular medicine *5*, 691-706.

Sturley, S.L., Patterson, M.C., Balch, W., and Liscum, L. (2004). The pathophysiology and mechanisms of NP-C disease. Biochimica et biophysica acta *1685*, 83-87.

Tanabe, A., Yamamura, Y., Kasahara, J., Morigaki, R., Kaji, R., and Goto, S. (2014). A novel tyrosine kinase inhibitor AMN107 (nilotinib) normalizes striatal motor behaviors in a mouse model of Parkinson's disease. Frontiers in cellular neuroscience *8*, 50.

Tsunemi, T., Ashe, T.D., Morrison, B.E., Soriano, K.R., Au, J., Roque, R.A., Lazarowski, E.R., Damian, V.A., Masliah, E., and La Spada, A.R. (2012). PGC-1alpha rescues Huntington's disease proteotoxicity by preventing oxidative stress and promoting TFEB function. Science translational medicine *4*, 142ra197.

Vargas, L.M., Cerpa, W., Munoz, F.J., Zanlungo, S., and Alvarez, A.R. (2018). Amyloid-beta oligomers synaptotoxicity: The emerging role of EphA4/c-Abl signaling in Alzheimer's disease. Biochimica et biophysica acta *1864*, 1148-1159.

Wang, W., Gao, Q., Yang, M., Zhang, X., Yu, L., Lawas, M., Li, X., Bryant-Genevier, M., Southall, N.T., Marugan, J.*, et al.* (2015). Up-regulation of lysosomal TRPML1 channels is essential for lysosomal adaptation to nutrient starvation. Proceedings of the National Academy of Sciences of the United States of America *112*, E1373-1381.

Xiao, Q., Yan, P., Ma, X., Liu, H., Perez, R., Zhu, A., Gonzales, E., Burchett, J.M., Schuler, D.R., Cirrito, J.R.*, et al.* (2014). Enhancing astrocytic lysosome biogenesis facilitates Abeta clearance and attenuates amyloid plaque pathogenesis. The Journal of neuroscience : the official journal of the Society for Neuroscience *34*, 9607-9620.

Xiao, Q., Yan, P., Ma, X., Liu, H., Perez, R., Zhu, A., Gonzales, E., Tripoli, D.L., Czerniewski, L., Ballabio, A.*, et al.* (2015). Neuronal-Targeted TFEB Accelerates Lysosomal Degradation of APP, Reducing Abeta Generation and Amyloid Plaque Pathogenesis. The Journal of neuroscience : the official journal of the Society for Neuroscience *35*, 12137-12151.

Xue, Y., Liu, Z., Cao, J., Ma, Q., Gao, X., Wang, Q., Jin, C., Zhou, Y., Wen, L., and Ren, J. (2011). GPS 2.1: enhanced prediction of kinase-specific phosphorylation sites with an algorithm of motif length selection. Protein engineering, design & selection : PEDS *24*, 255-260.

Yanez, M.J., Belbin, O., Estrada, L.D., Leal, N., Contreras, P.S., Lleo, A., Burgos, P.V., Zanlungo, S., and Alvarez, A.R. (2016). c-Abl links APP-BACE1 interaction promoting APP amyloidogenic processing in Niemann-Pick type C disease. Biochimica et biophysica acta *1862*, 2158-2167.

Yoshida, K., Yamaguchi, T., Natsume, T., Kufe, D., and Miki, Y. (2005). JNK phosphorylation of 14-3-3 proteins regulates nuclear targeting of c-Abl in the apoptotic response to DNA damage. Nature cell biology *7*, 278-285.

Supplemental information

ABL inhibition activates TFEB and promotes cellular clearance in a lysosomal disorder

Pablo S. Contreras, Pablo J. Tapia, Lila González-Hódar, Ivana Peluso, Chiara Soldati, Gennaro Napolitano, Maria Matarese, Macarena Las Heras, Alexis Martinez, Juan Castro, Nancy Leal, Frances M. Platt, Andrzej Sobota, Dominic Winter, Andrés D. Klein, Diego L. Medina, Andrea Ballabio, Alejandra R. Alvarez, Silvana Zanlungo.

Supplementary Figure 1

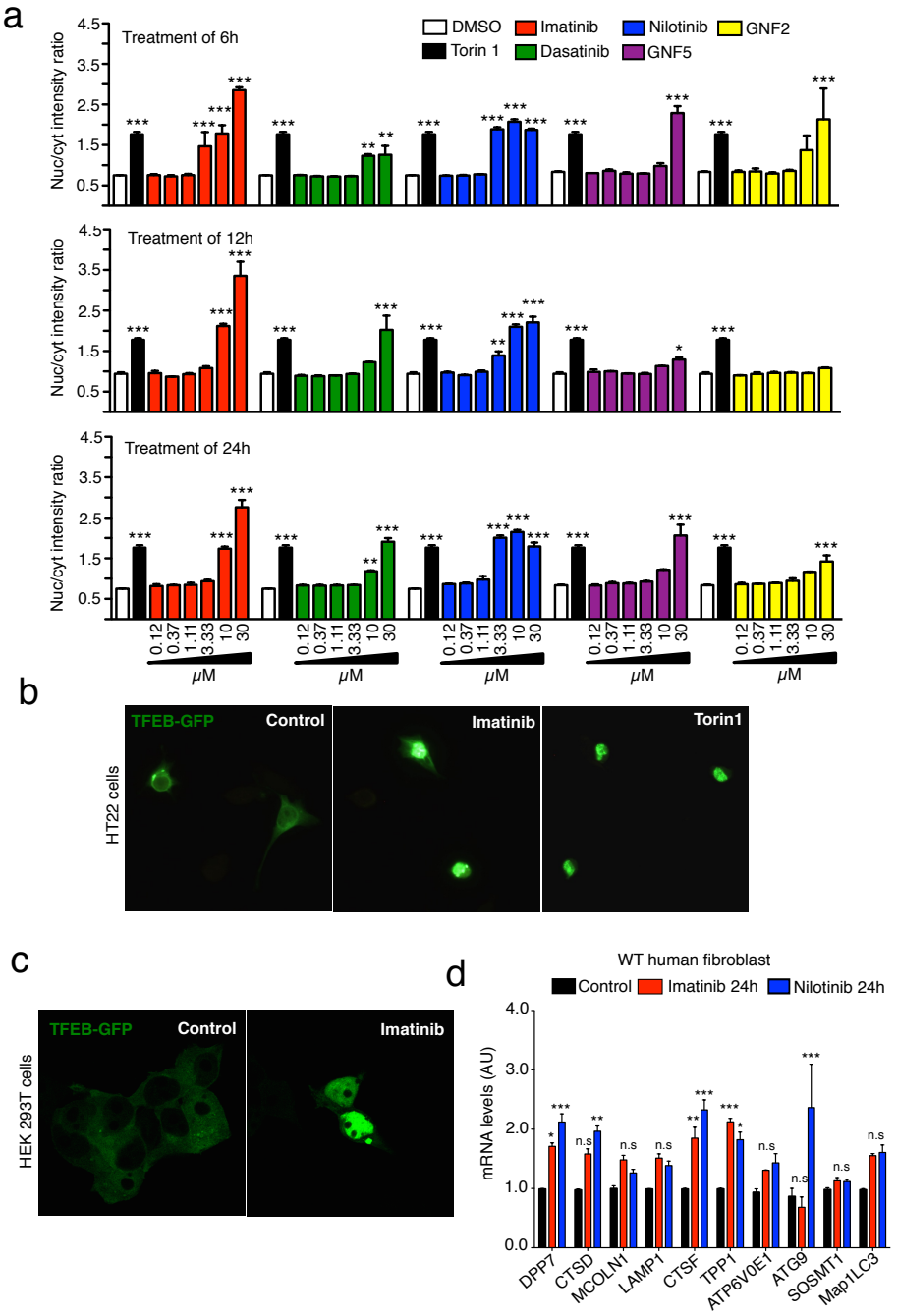

Supplementary Figure 1. ABL inhibitors promote TFEB nuclear translocation. HeLa TFEB-GFP cells were treated with DMSO (control), Torin1 0.3 μM (positive control) for 3h and ABL inhibitors at different concentrations for 6h, 12h and 24h. Then the cells were fixed and stained with DAPI. (a) The graph shows the ratio value resulting from the average intensity of nuclear TFEB–GFP fluorescence divided by the average intensity of cytosolic TFEB–GFP fluorescence. Black bars represent Torin1 treatment (positive control). Differences are statistically significant compared with the control conditions (DMSO). For each condition 450-800 cells were analyzed (two wells x 7 images). (b) Representative images of HT22 or HEK293T cells (c) transfected transiently with a TFEB-GFP plasmid for 24h and treated with Imatinib 10μM for 24h and Torin1 0.3 μM for 3h as a positive control. *n*=3 independent experiments. (d) The graph shows the results of q-PCR analysis of mRNA levels of different TFEB target genes in wild type human fibroblasts treated with Imatinib or Nilotinib 10μM for 24h. *n*=3 independent experiments. *$p < 0.05$, **$p < 0.01$,***$p < 0.001$. Data represent mean ± SEM.

Supplementary Figure 2

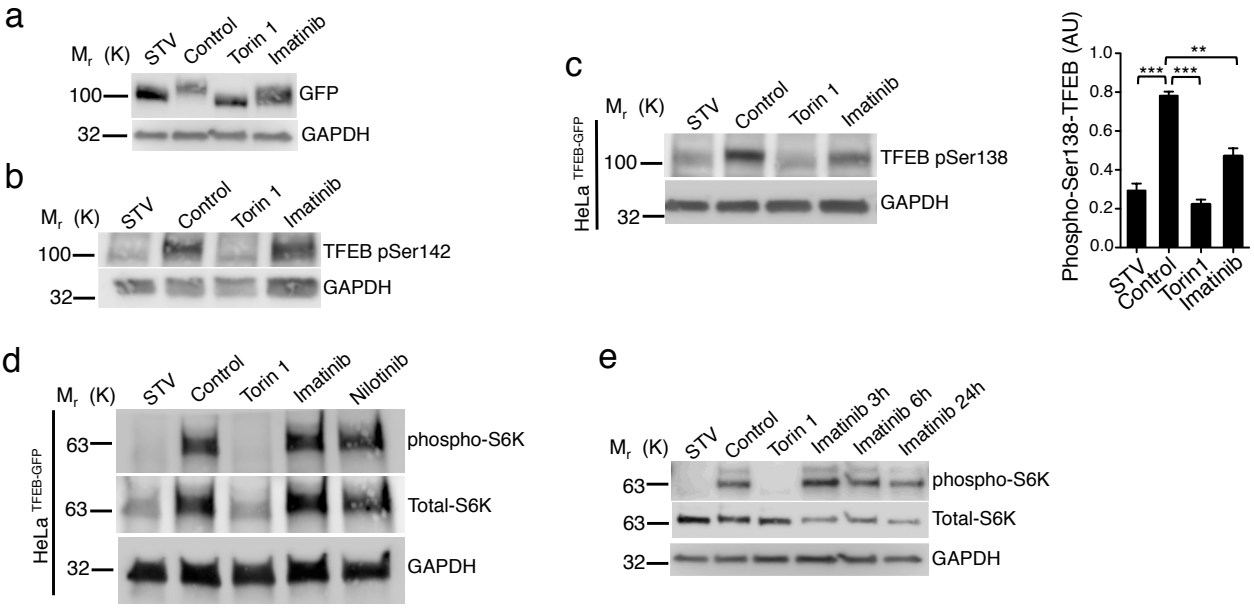

Supplementary Figure 2. ABL inhibition does not affect mTORC1 activity. (a) Representative Western blot showing TFEB-GFP in Hela TFEB-GFP cells treated with Imatinib 10μM for 3h. Torin1 0.3μM and starvation media (STV) for 3h was used as positive controls. (b) Representative Western blot showing TFEB phosphorylated on S142 in Hela TFEB-GFP cells treated with Imatinib 10μM for 3h. Torin1 0.3μM and starvation media (STV) for 3h was used as positive control. (c) Representative Western blot and quantification of TFEB phosphorylated on S138 in Hela TFEB-GFP cells treated with Imatinib 10μM for 3h and also in Hela TFEB-GFP cells treated with siRNA against ABL1 for 48h. Torin1 0.3μM and starvation media (STV) for 3h was used as positive control. *n*=3 independent experiments. (d) Representative Western blot of phospho p70-S6K in Hela TFEB-GFP cells treated with Imatinib and Nilotinib 10μM for 3h. Torin1 0.3μM and STV media for 3h were used as positive controls. *n*=3 independent experiments. (e) Representative western blot of phospho p70-S6K in Hela cells treated with Imatinib 10μM for 3h, 6h and 24h. Torin1 0.3μM and STV media for 3h were used as positive controls. *n*=3 independent experiments. *$p < 0.05$, **$p < 0.01$,***$p < 0.001$. Data represent mean ± SEM.

Supplementary Figure 3

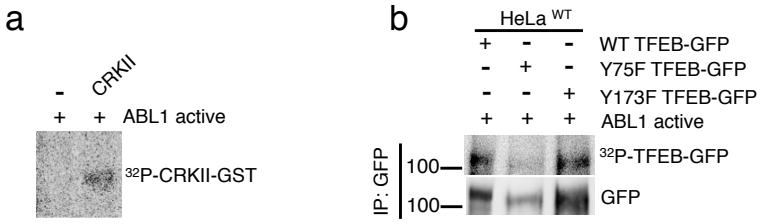

Supplementary Figure 3. *In vitro* tyrosine phosphorylation assay of TFEB mutants. Autoradiography of an *in vitro* phosphorylation assay. (a) Immunoprecipitated (IP) CRKII was incubated with human recombinant ABL1 active and ATP-γ-^{32}P for 2h. In (b) Site-directed Y75 and Y173 TFEB-GFP mutants were transfected into Hela cells. TFEB-GFP IP was incubated with human recombinant ABL1 active and ATP-γ-^{32}P for 2h.

Supplementary Figure 4

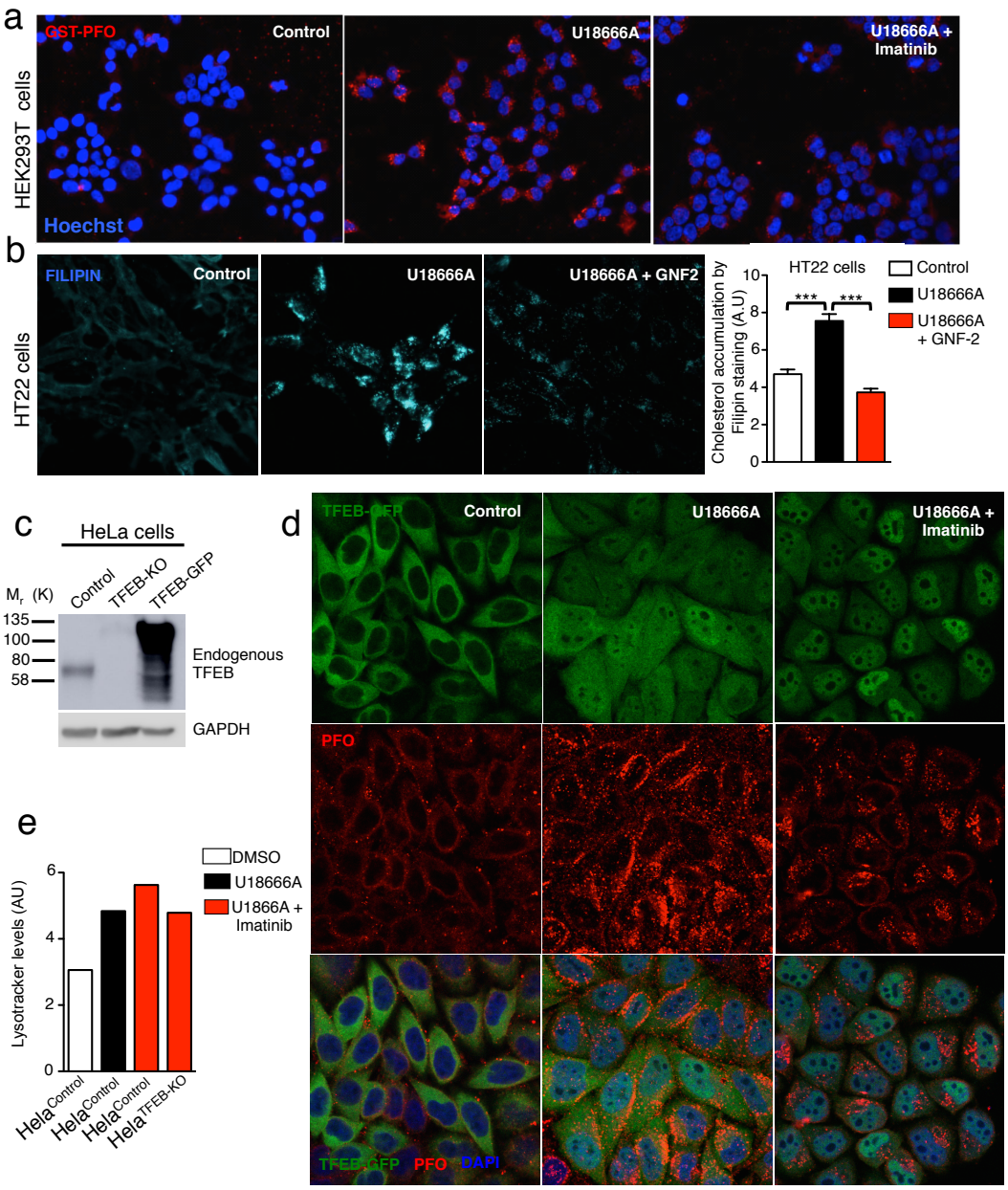

Supplementary Figure 4. ABL inhibitors reduce cholesterol accumulation in U18666A-treated cells. (a) Representative images of cholesterol accumulation. HEK293T cells were treated with U18666A 0.5μg/mL and/or Imatinib 10μM for 24h. Then GST-PFO (red) immunofluorescence and Hoechst (blue) staining were performed. (b) Representative images and quantification of cholesterol accumulation using filipin staining on HT22 cells treated with U18666A 0.5μg/mL and/or GNF2 10μM for 24h. *n*=3 independent experiments. (c) Representative western blot of endogenous in Hela cells (control), Hela TFEB-KO cells (TFEB-KO) and Hela TFEB-GFP cells (TFEB-GFP). GAPDH was used as loading control. (d) Representative confocal microscopy images showing cholesterol accumulation and TFEB-GFP localization. Hela TFEB-GFP cells were treated with U18666A 0.5μg/mL and/or Imatinib 10μM for 24h. Then GST-PFO immunofluorescence (red) and DAPI staining (blue) were performed. (e) Flow cytometry quantitative analysis of lysotracker in Hela cells, Hela TFEB-KO and Hela TFEB/TFE3 KO cells treated with U18666A and/or Imatinib and Nilotinib 10μM for 24h. *n*=10,000 cells per conditions. *$p < 0.05$, **$p < 0.01$,***$p < 0.001$. Data represent mean ± SEM.

Supplementary Figure 5

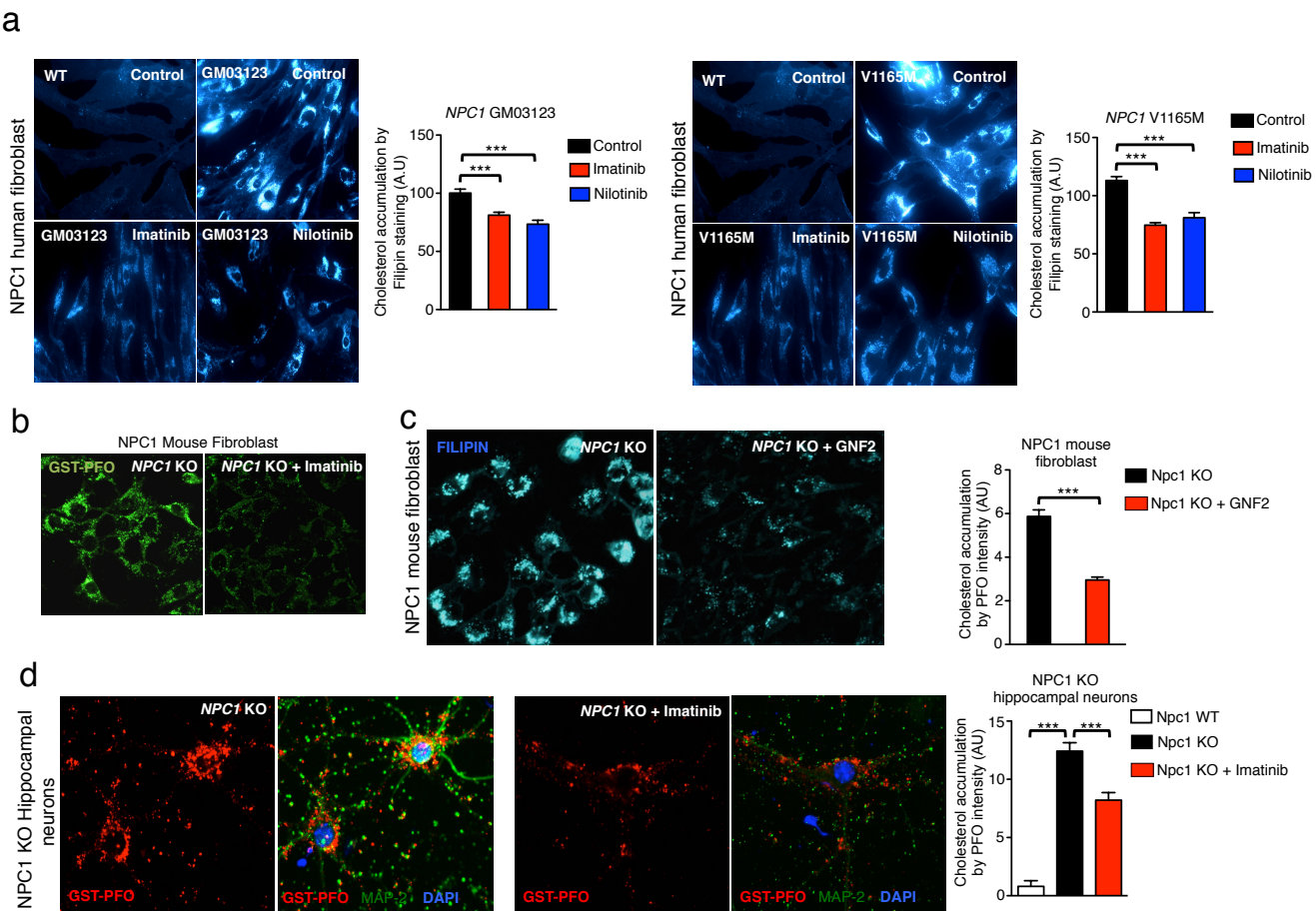

Supplementary Figure 5. Cholesterol-lowering effect of ABL inhibitors in different *in vitro* NPC1 models. (a) Representative images of NPC1 human fibroblast stained with filipin and quantification of cholesterol accumulation. NPC1 cells were treated with Imatinib 10μM and Nilotinib 10μM for 48h. *n*=3 independent experiments. (b) Representative images of cholesterol accumulation visualized by PFO staining (green) in NPC1 KO mice fibroblasts treated with Imatinib 10μM for 24h. (c) Representative images and quantification of cholesterol accumulation using filipin staining in NPC1 mouse fibroblast cells treated with GNF2 10μM for 24h. *n*=3 independent experiments. (d) Representative images and quantification of cholesterol accumulation using GST-PFO immunofluorescence, MAP2 (green) and DAPI (blue) on hippocampal neurons cultures (7 DIV) from NPC1 KO mice treated with Imatinib 10μM for 24h. *n*=3 independent experiments. *$p < 0.05$, **$p < 0.01$,***$p < 0.001$. Data represent mean ± SEM.

Supplementary Figure 6

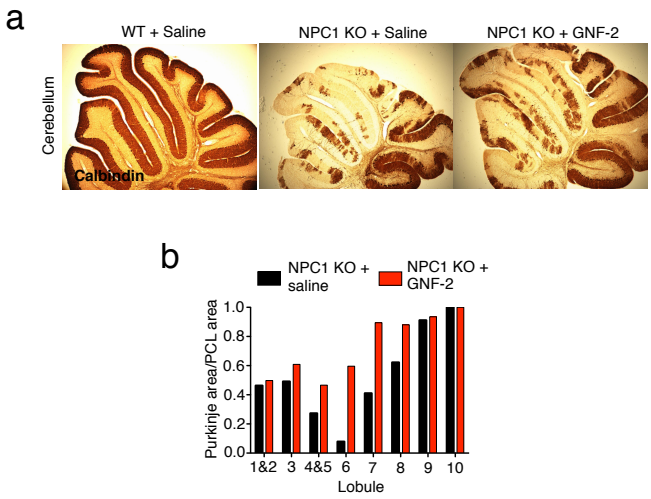

Supplementary Figure 6. GNF-2 improves Purkinje cell survival in NPC1 KO mice. GNF-2 (5 mg/kg in 40% water, 30% polyethylene glycol 300 and 30% propylene glycol) was given intraperitoneally to NPC1 KO mice in daily injections for four weeks starting at p28. (a) Cerebella from vehicle and GNF-2 treated female NPC1 KO mice were analyzed at 8 weeks of age for calbindin by immunohistochemistry. (b) Quantification of Purkinje cell area/Purkinje cell layer (PCL) area is shown.

3. Discussion

In recent years, TFEB has gathered great attention for playing a key role in lysosomal biogenesis and autophagy (Ballabio, 2016; Napolitano and Ballabio, 2016; Sardiello and Ballabio, 2009; Sardiello et al., 2009; Settembre and Ballabio, 2011; Settembre et al., 2011; Settembre et al., 2013; Settembre and Medina, 2015). The idea that the activation of TFEB could ameliorate diseases by promoting the degradation or clearance of molecules accumulated in the cell, especially in cells with lysosomal dysfunction, generates high expectations. Especially in rare diseases such as the lysosomal storage disorders (LSD), in which the development of treatments has been less successful. But also in more common diseases, in which lysosomes activity is compromised such as, Alzheimer disease, Parkinson disease, Huntington disease, etc.

Researchers have put a lot of effort in elucidating the mechanisms involved in TFEB regulation. In this sense, is already known that TFEB is mainly regulated by serine phosphorylations, being mTORC1 one of the key participating kinases. However, the relevance of this kind of regulation, by serine phosphorylation, has been shown under specific conditions, in which mTORC1 is activated or inhibited. But little is known about TFEB regulation in different cellular conditions, such as under oxidative stress, alterations in cholesterol homeostasis, lysosomal dysfunction and DNA stress, etc.

Our results identify a novel mTORC1-independent axis between TFEB and the tyrosine kinase ABL, and therefore a new potential therapeutic target for the treatment of lysosomal storage disorders. We demonstrated that the inhibition of this ABL/TFEB axis is critical to promote cellular clearance and plays a key role in the reduction of cholesterol accumulation in the Niemann Pick-type C lysosomal storage disorder. Remarkably, we

found that the inhibition of the tyrosine kinase ABL promotes a cholesterol-lowering effect in several NPC1 pharmacological and genetic models. Interestingly, the effect of the different ABL inhibitors was independent of the cellular type, including Hela, hepatic and neuronal cell lines.

3.1 ABL controls TFEB subcellular localization.

Our first finding was that the inhibition of the tyrosine kinase ABL promotes TFEB nuclear translocation. Previously, it was demonstrated that the serine/threonine kinase mTORC1 is the main regulator of TFEB, because in cells under mTORC1 inhibition, such as nutrient restriction or using a specific mTORC1-inhibitor, Torin1, TFEB translocates to the nucleus (Martina et al., 2012; Roczniak-Ferguson et al., 2012; Settembre et al., 2012). Nevertheless, our results show for the first time that the pharmacological inhibition of ABL, using different drugs including Imatinib, Nilotinib and Dasatinib, GNF2 and GNF5, produced the same result inducing TFEB nuclear translocation. Imatinib, Nilotinib and Dasatinib were designed to bind to the ATP binding site of ABL1 in the BCR-ABL1 fusion protein produced in patients with chronic myeloid leukemia (CML) (Capdeville et al., 2002; Druker et al., 1996; Hantschel et al., 2008; Maekawa et al., 2007), whereas both GNF2 and GNF5 bind to an allosteric site in ABL1 (Iacob et al., 2011). This result, suggested that TFEB sub-cellular localization is regulated by the tyrosine kinase ABL.

The next step was to demonstrate by genetic strategies that ABL regulates TFEB cellular localization. Thus, we used a siRNA against ABL1 and TFEB localization was analyzed. Concordantly with our pharmacological results, we observed an increase in TFEB nuclear

localization in cells with a decrease in ABL levels. Accordingly, we observed an increase in the mRNA levels of TFEB target genes in cells treated with a siRNA against ABL1.

These results altogether demonstrated that the inhibition of the tyrosine kinase ABL induces TFEB nuclear translocation and more importantly, the activation of TFEB.

3.2 ABL inhibition induces TFEB readouts.

Because ABL inhibition induces TFEB activation, we then evaluated what happens with the processes downstream of the activation of TFEB in these conditions.

It has been demonstrated that ABL inhibition promotes autophagy (Can et al., 2011; Ertmer et al., 2007; Lim et al., 2014), a biology process that is dysgregulated in different lysosomal storage disorders such as NPC, Pompe disease and MPSIIIA (Lieberman et al., 2012). Interestingly, we observed that ABL inhibition increases autophagy flux in the stable H4 LC3-GFP-mRFP cell line. In addition, the results showed an increased lysosome number in the HT22 cell line treated with ABL inhibitors. Concordantly, ABL inhibition by Imatinib or siRNA against ABL increased lysosomal protein levels and acidic organelles measured through Lamp1 and lysotracker in Hela cells and in human fibroblasts. In addition, we found an increase in lysosomes attached to the plasma membrane, suggesting an increase in lysosomal exocytosis.

Thus, our results support the idea that the increase in autophagy flux, quantity of lysosomes and lysosomal exocytosis, all of them biological process that are regulated by TFEB, are downstream events of the ABL inhibition and strongly support the idea that ABL

inhibition promotes TFEB activation. Nevertheless, we cannot discard the possibility that ABL inhibition is promoting this biological process through the activation of other signaling pathways that do not necessary involve TFEB. Indeed, our result showed that ABL inhibition promoted Map1LC3 gene expression, but neither ATG9 nor SQSTM1. This suggests that ABL inhibition promotes autophagy flux independent of the autophagy gene expression. However, gene expression of lysosomal genes, such as CTSD and MCOLN1 that also depend on TFEB activation were increased, suggesting that ABL inhibition could activate TFEB and the expression of a subset of TFEB target genes involved in lysosomal activity. Previously, has been described that TFEB can activate specific genes depending on the context. For example, under ER stress or starvation, TFEB may promote cell survival by enhancing pro-survival genes (genes implicated in autophagy, lysosomal biogenesis, metabolic regulators, etc). Nevertheless, under prolonged stress conditions, TFEB may increase expression of pro-apoptotic factors such as ATF4, PUMA or NOXA (Martina et al., 2016). In addition, we did not differentiate if the acidic organelles observed by lysotracker are the same population of lysosomes observed by Lamp1 when cells were treated with Imatinib. Probably, this difference on genes expression and the promotion of different pools of lysosomes is context-dependent. Under different stimulus, TFEB could be regulated by different kinases. In addition, and depending on the phosphorylation state, TFEB could be part of different protein complexes, that could impact differentially the expression of genes and affect different population of lysosomes in the cell.

As mentioned above, one of the best-known regulators of TFEB is MTORC1. For this reason, it was important to determine whether the regulation of TFEB by ABL is independent or not on MTORC1.

3.3 mTORC1-independent TFEB regulation by ABL.

Previously, it was described that mTORC1 inhibition promotes an electrophoretic shift in TFEB, due to a dephosphorylation in serine, mostly in Ser142 and Ser211 (Medina et al., 2015; Roczniak-Ferguson et al., 2012; Settembre et al., 2012). So, we first analyzed the electrophoretic mobility of TFEB in cells treated with ABL inhibitors. Interestingly, the inhibition of ABL promoted an electrophoretic shift on TFEB, which was different and smaller than the one obtained in cells treated with mTORC1 inhibitors. This result indicates that the TFEB translocated to the nucleus has a different phosphorylation profile depending on whether ABL or mTORC1 is inhibited.

Because the differences found in the TFEB electrophoretic shifts, the next step was to determine if the well-known TFEB phosphorylation in Ser142 or Ser211, were the responsible for TFEB nuclear translocation due to ABL inhibition. We observed that the levels of phosphorylated Ser142 on TFEB don´t decrease with ABL inhibition, compared to the control conditions in which mTORC1 was inhibited. This result was in accordance with the TFEB electrophoretic shifts results and indicates that ABL induces TFEB translocation to the nucleus phosphorylated in Ser142. A different scenario is produced by mTORC1 inhibition, in which TFEB translocate to the nucleus containing a dephosphorylated Ser142.

Recently, a nuclear export site (NES) on TFEB was described showing that TFEB can be exported to the cytoplasm from the nucleus depending on the phosphorylation on Ser138 (Li et al., 2018; Napolitano et al., 2018). This Ser138 phosphorylation depends on the Ser142. If TFEB is phosphorylated in Ser142 can be phosphorylated on Ser138. This mechanism ensures that only fully phosphorylated TFEB is completely cytosolic and

inactive. Interestingly, TFEB dephosphorylated in Ser211 translocate to the nucleus, but if is phosphorylated in the Ser138, TFEB will be re-exported to the cytoplasm (Li et al., 2018; Napolitano et al., 2018).

We observed that mTORC1 inhibition promotes a full dephosphorylation in Ser138, probably because Ser142 is dephosphorylated and then, Ser138 cannot be phosphorylated. Interestingly, ABL inhibition promotes a slightly decrease in Ser138 phosphoylation levels, but apparently these levels are not enough to determine TFEB re-exportation to the cytoplasm. This result opens the question of why TFEB fully phosphorylated in Ser142 and almost completely in Ser138 is retained in the nucleus. And most importantly, opens the possibility that TFEB could be regulated by ABL in a mTORC1-independent manner.

In regard to the status of Ser211 phosphorylation, TFEB was dephosphorylated in this serine under both conditions, ABL and mTORC1 inhibition. We were expecting this result because TFEB phosphorylated in Ser211 is anchor to its cytosolic chaperon 14-3-3. Therefore, TFEB dephosphorylated in Ser211, lose its anchor, and consequently is translocated to the nucleus.

Although we observed a different pattern of phosphorylation on TFEB nuclear import/export, differentiating ABL inhibition and mTORC1 inhibition, the question if ABL affects mTORC1 activity remains elusive.

We observed that mTORC1 target protein was phosphorylated in cells treated with ABL inhibitors, indicating that mTORC1 was active in these conditions. Interestingly, the inhibition of ABL was able to induce the translocation of TFEB to the nucleus under

conditions in which mTORC1 was fully active, including re-fed conditions after nutrients starvation and in cells deficient for TSC2, the negative regulator of mTORC1. This is of great relevance in pathological conditions in which mTORC1 signaling could be compromised, including mutants of NPC1, in which a negative feed-back is lost between NPC1 and mTORC1, which requires an intact sterol-sensing domain site in NPC1 (Castellano et al., 2017). Moreover, this result is encouraging in the sense that inhibiting mTORC1 is not a good strategy for the treatment of diseases with lysosomal compromise, since this kinase fulfills multiple cellular functions. Other recent studies have shown that the inhibition of the Akt kinase by compounds such as trehalose induces the nuclear translocation of TFEB independently of mTORC1 (Palmieri et al., 2017). Therefore, regulation of TFEB translocation seems to respond to more than one signaling system, increasing the possibilities of modulating it.

In summary and importantly, our results demonstrated that TFEB nuclear translocation, promoted by ABL inhibition, is independent of mTORC1.

3.4 TFEB is phosphorylated at tyrosine by ABL

Because our results indicate that ABL inhibition was promoting TFEB nuclear translocation independent of mTORC1, we decided to analyze if ABL could directly phosphorylate TFEB. Our study demonstrates, for the first time, that TFEB activity is negatively regulated by tyrosine phosphorylation. We found that the activity of ABL is enough to promote TFEB tyrosine phosphorylation. This is particularly interesting because until now, there are few

reports of novel post-traductional modifications on TFEB, such as deacetylations (Zhang et al., 2018).

Interestingly, by in silico analysis, we found that TFEB has two possible tyrosines to be phosphorylated by ABL, Y75 and Y173. We observed that the Y173F TFEB-GFP mutant present a constitutive nuclear localization, suggesting that the tyrosine 173 in TFEB is relevant for its retention in the cytoplasm. Next, we performed *in vitro* phosphorylation assays using active ABL1 and wild-type (WT) and mutant TFEBs. Although we expected a reduction of incorporated radioactivity on TFEB mutants, the Y173F TFEB-GFP and Y75F TFEB-GFP proteins incorporated radioactivity in a similar extent than the wild type TFEB-GFP by probably basal phosphorylation in other tyrosines. We cannot discard the possibility that ABL could phosphorylate other tyrosines, and regrettably with our approximation (in vitro phoshprylation assay) we cannot discriminates which tyrosine are relevant. Slightly less radioactivity was detected in the Y75F TFEB-GFP protein suggesting that ABL1 phosphorylates TFEB on Y75. However, the construct Y75F TFEB-GFP showed lower expression levels in cells transfected for the *in vitro* phosphorylation assays

The idea that phosphorylation on tyrosine by ABL could impact in the biology of this protein is not new. Previously, it was demonstrated that different transcription factors are phosphorylated by ABL, including p73 (Tsai and Yuan, 2003), Yap1 (Levy et al., 2008), c-Jun (Gao et al., 2006), etc. In addition, our laboratory also demonstrated in Alzheimer and NPC models that ABL can phosphorylate and regulate the activity of p73 or HDAC2 (Cancino et al., 2008; Contreras et al., 2016; Gonzalez-Zuniga et al., 2014; Klein et al., 2011).

We then analyze the serine phosphorylation on mutant TFEBs by western blot using

specific antibodies against TFEB S142, S138 and S211. Interestingly we observed that Y173F TFEB-GFP compared with the wild type TFEB-GFP and Y75F TFEB-GFP protein shown a reduction in S211, a slight decrease in S138, and S142 was unaffected. Interestingly, this pattern on serines phosphorylation was observed in cells treated with ABL inhibitors, suggesting that Y173 phosphorylation could be reduced when cells are treated with ABL1 inhibitors, transforming this Y173 of TFEB a target of ABL. In addition, we suggest a relevant role of Y173 on TFEB cellular localization by its impact on the S211 phosphorylation.

Altogether these results demonstrated that ABL phosphorylates TFEB in tyrosine, and suggest that Y173 could be relevant for TFEB translocation into the nucleus, raising the idea that tyrosine phosphorylation could impact in the phosphorylation status of serine in TFEB. More experiments are needed to demonstrate that tyrosine phosphorylations are impacting the serine phosphorylation status. Nevertheless, this phenomenon would not be novel since this priming phenomenon has been previously described in other contexts (Kosten et al., 2014).

3.5 Cholesterol-lowering effect promoted by ABL depends on TFEB

Active TFEB promotes clearance of molecules accumulated in the lysosomes (Napolitano and Ballabio, 2016). Since we observed that ABL phosphorylates TFEB on tyrosine, and that inhibition of this kinase promotes TFEB nuclear translocation, we decided to test if ABL inhibition can reduce the cholesterol accumulation promoted by U18666A drug.

Our results demonstrated that ABL inhibition mediated by pharmacological inhibitors, promotes a reduction in cholesterol accumulation in different cell lines in which cholesterol accumulation was induced by the U18666A drug. This drug is widely used in the NPC field, as a pharmacological inducer of a NPC phenotype in cells, since was discovered that this drug directly inhibits the NPC1 protein, promoting cholesterol accumulation in lysosomes (Lu et al., 2015). Importantly, this cholesterol accumulation was also corrected in ABL KO neurons culture.

Interestingly, the relevance of TFEB in NPC disease has not been totally explored yet. Previously, it was shown that the mTORC1 inhibitor Torin1 promotes clearance of cholesterol accumulation (Wang et al., 2015). Nevertheless, Torin1 has been shown to be toxic, probably due to the pleiotropic mTORC1 function in cells. In addition, mTORC1 has been shown to be over-activated in NPC cells, and TFEB preferentially localized in the cytoplasm in NPC null CHO cells (Castellano et al., 2017). Our results show that in Hela cells overexpressing TFEB, U18666A slightly increases TFEB nuclear translocation, but after Imatinib treatment, TFEB nuclear localization was even greater.

Remarkably, we demonstrated that the cholesterol-lowering effect obtained with the ABL inhibitors is abolished in Hela TFEB KO cells. Also, we observed an increase in lysotracker staining TFEB-dependent in Hela cells treated with U18666A. These results suggest that the increase in lysosomal levels observed under ABL inhibition depends on TFEB activation, being this result concordant with our previous ones and confirming the relevance of TFEB for cellular clearance in NPC cells.

3.6 ABL inhibition promotes cellular clearance in NPC models

The observation that the inhibition of ABL promotes a reduction of cholesterol accumulated in different cell lines, leads us to analyze if the inhibition of this novel ABL/TFEB axis could promotes cellular clearance in genetic NPC models such as NPC1 human fibroblast.

Previously, our laboratory demonstrated that the ABL kinase was active in cells treated with the U18666A drug (Klein et al., 2011). Here, we show that ABL was active in two different NPC1 human fibroblasts. Most importantly, in these NPC1 human fibroblasts, the ABL inhibitors promoted a reduction in cholesterol accumulation, independently of the specific NPC1 mutation. In addition, we observed similar results with the ABL inhibitors in NPC1 KO mouse fibroblast as well as in NPC1 KO hippocampal neurons cultures.

Further studies are required to evaluate the effect of ABL inhibition on *NPC2* mutants, which are responsible for 5% of NPC cases as well as in models of other lysosomal disorders, to find the relevance of this axis in other diseases (Patterson et al., 2012). In any case, inhibiting ABL seems to be a good therapeutic option not only for lysosomal storage disorders but also for other diseases such as Alzheimer's, Parkinson's and ALS, where lysosomal function is also compromised and ABL is activated (Cancino et al., 2011; Cancino et al., 2008; Estrada et al., 2016; Estrada et al., 2011; Hebron et al., 2013; Imam et al., 2013; Imamura et al., 2017; Karuppagounder et al., 2014; Katsumata et al., 2012; Pagan et al., 2016; Rojas et al., 2015; Tanabe et al., 2014; Vargas et al., 2018).

Remarkably, at basal conditions, NPC1 human fibroblasts show very low levels of TFEB at the nucleus, which are greatly increased after ABL inhibition, being this result in accordance with those obtained in cells treated with the U18666A drug. These

experiments demonstrate that in the context of NPC disease, ABL inhibition promotes TFEB nuclear translocation. Importantly, the mRNA levels of several TFEB-target genes, such as MCOLN1 (endosomal calcium channel), were recovered in the NPC1 human fibroblasts treated with Imatinib or Nilotinib and also promoted an increase in Lamp1 levels and lysotracker, suggesting that TFEB nuclear localization promotes the increase in lysosomal quantity. In addition, a previous report demonstrated that human cells that harbored loss-of-function of MCOLN1 failed to promote cellular clearance trough lysosomal exocytosis mediated by TFEB (Medina et al., 2011). Our data suggest that ABL inhibition could promote cellular clearance of cholesterol through the promotion of lysosomal exocytosis mediated by the recover of the TFEB-target gene MCOLN1. Nevertheless, the there is no information demonstrating that in NPC cells, the reduction of cholesterol accumulation is due to an increased secretion of the endo/lysosomal content dependent on MCOLN1. Because of that, we cannot discard the possibility that the cholesterol-lowering effect mediated by the ABL inhibition could be regulated by other processes.

3.7 ABL inhibition reduces cholesterol accumulation in *in vivo* NPC models

Our final step was to analyze this novel ABL/TFEB axis in *in vivo* models. We previously described that the ABL inhibitor, Imatinib, prevents the neuronal death and improves different behavioral test and lifespan of the NPC mice (Alvarez et al., 2008). However, the cholesterol-lowering effect of Imatinib in this mouse was not evaluated deeply.

Importantly, we observed concordantly results in *in vivo* models (Fig. 7). Imatinib treatment prevented cholesterol accumulation in NPC1 KO mice. Nevertheless, the poor BBB

penetrance of Imatinib, lead us to taste novel ABL inhibitors with better brain penetrance. We choose GNF-2, because although it is not an approved drug by the FDA, previous analysis of our laboratory show that this compound presents a better pass of the BBB than Imatinib. We first corroborated our previously data obtained with Imatinib and observed that NPC1 KO mice treated with GNF-2 present a better performance in the behavioral tests. Importantly, we found that this improvement correlated with a decrease in cholesterol accumulation.

To strengthen our results, we decided to treat ABL1 KO mice with the U18666A drug to homologate the NPC disease in an *in vivo* ABL1 KO genetic background. First, we observed that wild type mice treated with the U18666A drug show increased cholesterol accumulation in the cerebellum compared with wild type mice treated with a saline solution. To our knowledge, this is the first time that a mice treated with U18666A is presented as a NPC *in vivo* model. Remarkably, in the ABL1 KO mice treated with U18666A we did not observed a clear cholesterol accumulation such as is in the wild type mice treated with the drug. These results suggest that the absence ABL1 prevents cholesterol accumulation in these mice.

Interestingly and in accordance with our *in vitro* results, endogenous-TFEB localization in Purkinje cells of the wild type mice treated with U18666A drug was slightly more nuclear than in the wild type mice treated with the saline solution. Remarkably, the nuclear localization of endogenous-TFEB was more evident in the ABL1 KO mice treated with U18666A. These results confirm our previous *in vitro* results and also suggest that TFEB is involved in the clearance of accumulated cholesterol mediated by ABL inhibition in *in vivo* NPC models.

In summary, our results show that ABL is a very good target for the treatment of neurodegenerative lysosomal diseases such as NPC, since its inhibition promotes the activation of TFEB and cellular clearance (Figure 16). Interestingly, because ABL is a tyrosine kinase that participates through several signaling pathways inducing neuronal dysfunction and death, its inhibition generates other beneficial responses for neurodegenerative diseases. These include, decreasing the activation of the proapoptotic p73 transcription factor and HDAC2 and of APP processing, as it has been shown in AD and NPC models (Cancino et al., 2008; Contreras et al., 2016; Estrada et al., 2016; Gonzalez-Zuniga et al., 2014; Klein et al., 2011; Yanez et al., 2016). In addition, ABL inhibition decreases misfolded α-synuclein and mutant SOD1 protein accumulation in Parkinson and ALS (Imamura et al., 2017), respectively. Remarkably, Imatinib and Nilotinib are FDA approved drugs, and their chronic use in patients with CML is quite safe and has little side effects. Moreover, the results in a small group of patients with Parkinson's disease and Dementia with Lewy bodies treated for 24 weeks with Nilotinib, suggested a possible beneficial effect on clinical outcomes (Pagan et al., 2016). Altogether, these information position ABL inhibitors as novel strategies to treat diseases in which lysosomes and TFEB have been proposed as therapeutic targets, such as Pompe disease, Gaucher disease, MPSIV and Batten disease, among others (Ballabio, 2016; Napolitano and Ballabio, 2016)

4. CONCLUSIONS

The results presented in this work allow us to formulate the following conclusions:

1. ABL inhibition promotes TFEB activation, inducing its nuclear localization and activity.
2. ABL inhibition promotes an increase in TFEB-dependent cell biology process, including autophagy flux, lysosomal biogenesis and exocytosis.
3. TFEB regulation by ABL is independent of mTORC1 activity and NES phosphorylation.
4. ABL phosphorylates TFEB on tyrosine, being a novel post-translational modification for TFEB. We suggest that Y173 on TFEB is phosphorylated by ABL and that phosphorylated Y173 promotes TFEB localization in the cytoplasm.
5. ABL inhibition promotes, in a TFEB-dependent manner, the clearance of accumulated cholesterol in NPC cells. Also ABL inhibition induces TFEB massive nuclear localization in NPC cells.
6. The ABL/TFEB axis is relevant in *in vivo* NPC models, promoting both a reduction in the cholesterol accumulation in cerebellum and TFEB nuclear localization.
7. Finally, our data reveal a novel ABL/TFEB mechanism mTORC1-independent that controls lysosomal homeostasis. Inhibition of the tyrosine kinase ABL promotes lysosomal clearance through TFEB activation. This mechanism is relevant in the context of the NPC lysosomal storage disorder in which this kinase is active. The inhibition of this kinase using FDA approved drugs, opens the possibility to treat NPC patients as well as other neurodegenerative lysosomal storage disorders.

Figure 16

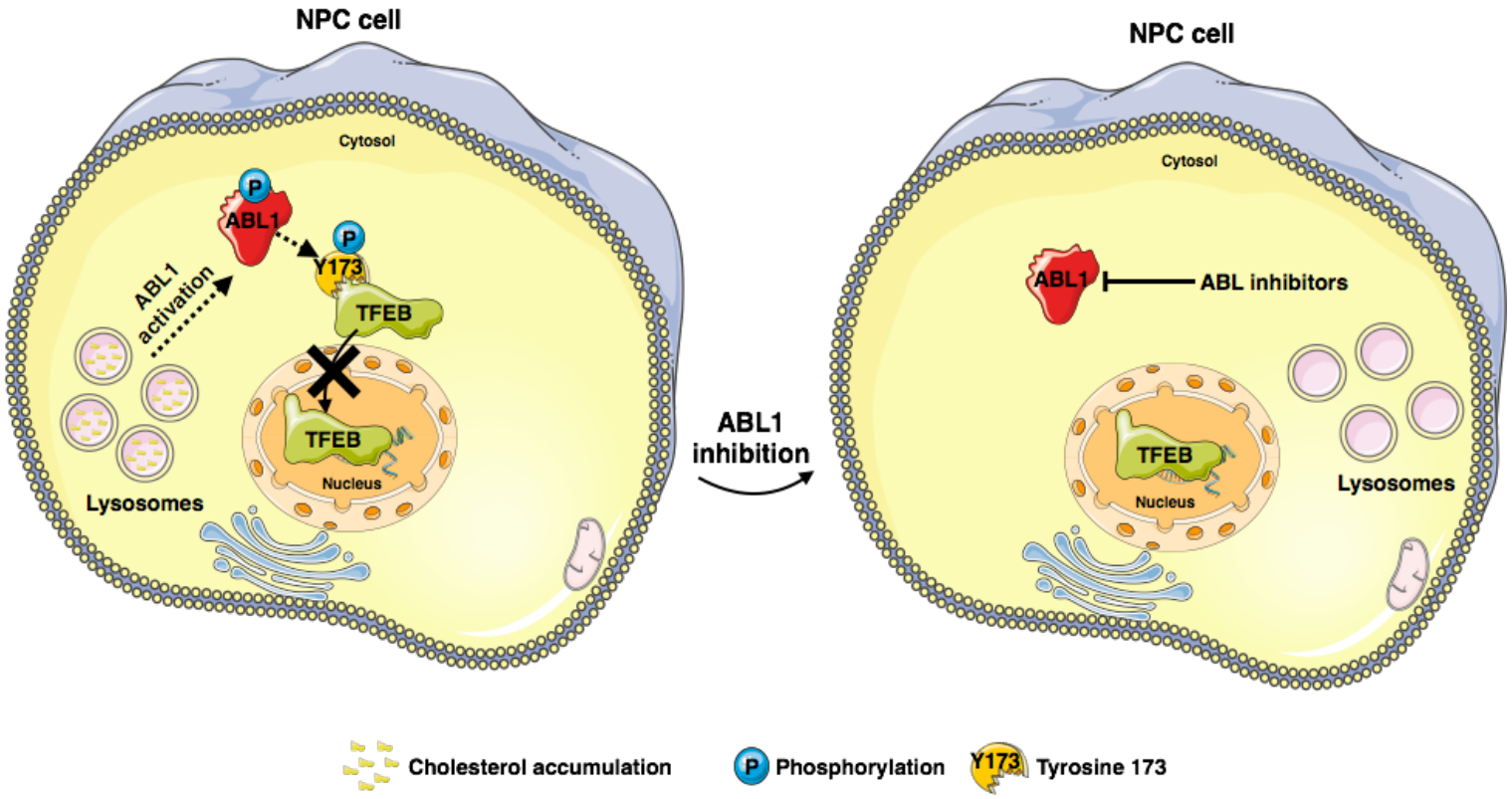

Figure 16. Proposal model of ABL role on TFEB regulation in NPC cells. The cellular stress induced by cholesterol accumulation in NPC disease, promotes the ABL activation, which phoshorylates TFEB on tyrosine 173. This phosphorylation on tyrosine retains TFEB in the cytoplasm. The inhibition of ABL, reverts this tyrosine phoshorylation promoting TFEB activation and as a consequence, promoting cholesterol-lowering effects.

5. REFERENCES

Alam, M.S., Getz, M., and Haldar, K. (2016). Chronic administration of an HDAC inhibitor treats both neurological and systemic Niemann-Pick type C disease in a mouse model. Science translational medicine *8*, 326ra323.

Alvarez, A.R., Klein, A., Castro, J., Cancino, G.I., Amigo, J., Mosqueira, M., Vargas, L.M., Yevenes, L.F., Bronfman, F.C., and Zanlungo, S. (2008). Imatinib therapy blocks cerebellar apoptosis and improves neurological symptoms in a mouse model of Niemann-Pick type C disease. FASEB journal : official publication of the Federation of American Societies for Experimental Biology *22*, 3617-3627.

Alvarez, A.R., Sandoval, P.C., Leal, N.R., Castro, P.U., and Kosik, K.S. (2004). Activation of the neuronal c-Abl tyrosine kinase by amyloid-beta-peptide and reactive oxygen species. Neurobiology of disease *17*, 326-336.

Ballabio, A. (2016). The awesome lysosome. EMBO molecular medicine *8*, 73-76.

Ben-Neriah, Y., Daley, G.Q., Mes-Masson, A.M., Witte, O.N., and Baltimore, D. (1986). The chronic myelogenous leukemia-specific P210 protein is the product of the bcr/abl hybrid gene. Science *233*, 212-214.

Brasher, B.B., and Van Etten, R.A. (2000). c-Abl has high intrinsic tyrosine kinase activity that is stimulated by mutation of the Src homology 3 domain and by autophosphorylation at two distinct regulatory tyrosines. The Journal of biological chemistry *275*, 35631-35637.

Butters, T.D., Mellor, H.R., Narita, K., Dwek, R.A., and Platt, F.M. (2003). Small-molecule therapeutics for the treatment of glycolipid lysosomal storage disorders. Philosophical transactions of the Royal Society of London. Series B, Biological sciences *358*, 927-945.

Calias, P. (2017). 2-Hydroxypropyl-beta-cyclodextrins and the Blood-Brain Barrier: Considerations for Niemann-Pick Disease Type C1. Current pharmaceutical design *23*, 6231-6238.

Can, G., Ekiz, H.A., and Baran, Y. (2011). Imatinib induces autophagy through BECLIN-1 and ATG5 genes in chronic myeloid leukemia cells. Hematology *16*, 95-99.

Cancino, G.I., Perez de Arce, K., Castro, P.U., Toledo, E.M., von Bernhardi, R., and Alvarez, A.R. (2011). c-Abl tyrosine kinase modulates tau pathology and Cdk5 phosphorylation in AD transgenic mice. Neurobiology of aging *32*, 1249-1261.

Cancino, G.I., Toledo, E.M., Leal, N.R., Hernandez, D.E., Yevenes, L.F., Inestrosa, N.C., and Alvarez, A.R. (2008). STI571 prevents apoptosis, tau phosphorylation and behavioural impairments induced by Alzheimer's beta-amyloid deposits. Brain : a journal of neurology *131*, 2425-2442.

Capdeville, R., Buchdunger, E., Zimmermann, J., and Matter, A. (2002). Glivec (STI571, imatinib), a rationally developed, targeted anticancer drug. Nature reviews. Drug discovery *1*, 493-502.

Carstea, E.D., Morris, J.A., Coleman, K.G., Loftus, S.K., Zhang, D., Cummings, C., Gu, J., Rosenfeld, M.A., Pavan, W.J., Krizman, D.B.*, et al.* (1997). Niemann-Pick C1 disease gene: homology to mediators of cholesterol homeostasis. Science *277*, 228-231.

Castellano, B.M., Thelen, A.M., Moldavski, O., Feltes, M., van der Welle, R.E., Mydock-McGrane, L., Jiang, X., van Eijkeren, R.J., Davis, O.B., Louie, S.M.*, et al.* (2017). Lysosomal cholesterol activates mTORC1 via an SLC38A9-Niemann-Pick C1 signaling complex. Science *355*, 1306-1311.

Contreras, P.S., Gonzalez-Zuniga, M., Gonzalez-Hodar, L., Yanez, M.J., Dulcey, A., Marugan, J., Seto, E., Alvarez, A.R., and Zanlungo, S. (2016). Neuronal gene repression in Niemann-Pick type C models is mediated by the c-Abl/HDAC2 signaling pathway. Biochimica et biophysica acta *1859*, 269-279.

David-Cordonnier, M.H., Payet, D., D'Halluin, J.C., Waring, M.J., Travers, A.A., and Bailly, C. (1999). The DNA-binding domain of human c-Abl tyrosine kinase promotes the interaction of a HMG chromosomal protein with DNA. Nucleic acids research *27*, 2265-2270.

Decressac, M., Mattsson, B., Weikop, P., Lundblad, M., Jakobsson, J., and Bjorklund, A. (2013). TFEB-mediated autophagy rescues midbrain dopamine neurons from alpha-

synuclein toxicity. Proceedings of the National Academy of Sciences of the United States of America *110*, E1817-1826.

Druker, B.J., Tamura, S., Buchdunger, E., Ohno, S., Segal, G.M., Fanning, S., Zimmermann, J., and Lydon, N.B. (1996). Effects of a selective inhibitor of the Abl tyrosine kinase on the growth of Bcr-Abl positive cells. Nature medicine *2*, 561-566.

Ertmer, A., Huber, V., Gilch, S., Yoshimori, T., Erfle, V., Duyster, J., Elsasser, H.P., and Schatzl, H.M. (2007). The anticancer drug imatinib induces cellular autophagy. Leukemia *21*, 936-942.

Estrada, L.D., Chamorro, D., Yanez, M.J., Gonzalez, M., Leal, N., von Bernhardi, R., Dulcey, A.E., Marugan, J., Ferrer, M., Soto, C.*, et al.* (2016). Reduction of Blood Amyloid-beta Oligomers in Alzheimer's Disease Transgenic Mice by c-Abl Kinase Inhibition. Journal of Alzheimer's disease : JAD *54*, 1193-1205.

Estrada, L.D., Zanlungo, S.M., and Alvarez, A.R. (2011). C-Abl tyrosine kinase signaling: a new player in AD tau pathology. Current Alzheimer research *8*, 643-651.

Gao, B., Lee, S.M., and Fang, D. (2006). The tyrosine kinase c-Abl protects c-Jun from ubiquitination-mediated degradation in T cells. The Journal of biological chemistry *281*, 29711-29718.

Goff, S.P., Gilboa, E., Witte, O.N., and Baltimore, D. (1980). Structure of the Abelson murine leukemia virus genome and the homologous cellular gene: studies with cloned viral DNA. Cell *22*, 777-785.

Gonzalez-Zuniga, M., Contreras, P.S., Estrada, L.D., Chamorro, D., Villagra, A., Zanlungo, S., Seto, E., and Alvarez, A.R. (2014). c-Abl stabilizes HDAC2 levels by tyrosine phosphorylation repressing neuronal gene expression in Alzheimer's disease. Molecular cell *56*, 163-173.

Greuber, E.K., Smith-Pearson, P., Wang, J., and Pendergast, A.M. (2013). Role of ABL family kinases in cancer: from leukaemia to solid tumours. Nature reviews. Cancer *13*, 559-571.

Gutknecht, M., Geiger, J., Joas, S., Dorfel, D., Salih, H.R., Muller, M.R., Grunebach, F., and Rittig, S.M. (2015). The transcription factor MITF is a critical regulator of GPNMB expression in dendritic cells. Cell communication and signaling : CCS *13*, 19.

Hantschel, O., Nagar, B., Guettler, S., Kretzschmar, J., Dorey, K., Kuriyan, J., and Superti-Furga, G. (2003). A myristoyl/phosphotyrosine switch regulates c-Abl. Cell *112*, 845-857.

Hantschel, O., Rix, U., and Superti-Furga, G. (2008). Target spectrum of the BCR-ABL inhibitors imatinib, nilotinib and dasatinib. Leukemia & lymphoma *49*, 615-619.

Hebron, M.L., Lonskaya, I., and Moussa, C.E. (2013). Nilotinib reverses loss of dopamine neurons and improves motor behavior via autophagic degradation of alpha-synuclein in Parkinson's disease models. Human molecular genetics *22*, 3315-3328.

Iacob, R.E., Zhang, J., Gray, N.S., and Engen, J.R. (2011). Allosteric interactions between the myristate- and ATP-site of the Abl kinase. PloS one *6*, e15929.

Imam, S.Z., Trickler, W., Kimura, S., Binienda, Z.K., Paule, M.G., Slikker, W., Jr., Li, S., Clark, R.A., and Ali, S.F. (2013). Neuroprotective efficacy of a new brain-penetrating C-Abl inhibitor in a murine Parkinson's disease model. PloS one *8*, e65129.

Imamura, K., Izumi, Y., Watanabe, A., Tsukita, K., Woltjen, K., Yamamoto, T., Hotta, A., Kondo, T., Kitaoka, S., Ohta, A.*, et al.* (2017). The Src/c-Abl pathway is a potential therapeutic target in amyotrophic lateral sclerosis. Science translational medicine *9*.

Jacobs, W.B., Kaplan, D.R., and Miller, F.D. (2006). The p53 family in nervous system development and disease. Journal of neurochemistry *97*, 1571-1584.

Jing, Z., Caltagarone, J., and Bowser, R. (2009). Altered subcellular distribution of c-Abl in Alzheimer's disease. Journal of Alzheimer's disease : JAD *17*, 409-422.

Karuppagounder, S.S., Brahmachari, S., Lee, Y., Dawson, V.L., Dawson, T.M., and Ko, H.S. (2014). The c-Abl inhibitor, nilotinib, protects dopaminergic neurons in a preclinical animal model of Parkinson's disease. Scientific reports *4*, 4874.

Katsumata, R., Ishigaki, S., Katsuno, M., Kawai, K., Sone, J., Huang, Z., Adachi, H., Tanaka, F., Urano, F., and Sobue, G. (2012). c-Abl inhibition delays motor neuron

degeneration in the G93A mouse, an animal model of amyotrophic lateral sclerosis. PloS one *7*, e46185.

Kim, S.J., Lee, B.H., Lee, Y.S., and Kang, K.S. (2007). Defective cholesterol traffic and neuronal differentiation in neural stem cells of Niemann-Pick type C disease improved by valproic acid, a histone deacetylase inhibitor. Biochemical and biophysical research communications *360*, 593-599.

Klein, A., Maldonado, C., Vargas, L.M., Gonzalez, M., Robledo, F., Perez de Arce, K., Munoz, F.J., Hetz, C., Alvarez, A.R., and Zanlungo, S. (2011). Oxidative stress activates the c-Abl/p73 proapoptotic pathway in Niemann-Pick type C neurons. Neurobiology of disease *41*, 209-218.

Ko, D.C., Milenkovic, L., Beier, S.M., Manuel, H., Buchanan, J., and Scott, M.P. (2005). Cell-autonomous death of cerebellar purkinje neurons with autophagy in Niemann-Pick type C disease. PLoS genetics *1*, 81-95.

Ko, H.S., Lee, Y., Shin, J.H., Karuppagounder, S.S., Gadad, B.S., Koleske, A.J., Pletnikova, O., Troncoso, J.C., Dawson, V.L., and Dawson, T.M. (2010). Phosphorylation by the c-Abl protein tyrosine kinase inhibits parkin's ubiquitination and protective function. Proceedings of the National Academy of Sciences of the United States of America *107*, 16691-16696.

Kosten, J., Binolfi, A., Stuiver, M., Verzini, S., Theillet, F.X., Bekei, B., van Rossum, M., and Selenko, P. (2014). Efficient modification of alpha-synuclein serine 129 by protein kinase CK1 requires phosphorylation of tyrosine 125 as a priming event. ACS chemical neuroscience *5*, 1203-1208.

Kwon, H.J., Abi-Mosleh, L., Wang, M.L., Deisenhofer, J., Goldstein, J.L., Brown, M.S., and Infante, R.E. (2009). Structure of N-terminal domain of NPC1 reveals distinct subdomains for binding and transfer of cholesterol. Cell *137*, 1213-1224.

Lachmann, R.H., te Vruchte, D., Lloyd-Evans, E., Reinkensmeier, G., Sillence, D.J., Fernandez-Guillen, L., Dwek, R.A., Butters, T.D., Cox, T.M., and Platt, F.M. (2004).

Treatment with miglustat reverses the lipid-trafficking defect in Niemann-Pick disease type C. Neurobiology of disease *16*, 654-658.

Lawana, V., Singh, N., Sarkar, S., Charli, A., Jin, H., Anantharam, V., Kanthasamy, A.G., and Kanthasamy, A. (2017). Involvement of c-Abl Kinase in Microglial Activation of NLRP3 Inflammasome and Impairment in Autolysosomal System. Journal of neuroimmune pharmacology : the official journal of the Society on NeuroImmune Pharmacology *12*, 624-660.

Levy, D., Adamovich, Y., Reuven, N., and Shaul, Y. (2008). Yap1 phosphorylation by c-Abl is a critical step in selective activation of proapoptotic genes in response to DNA damage. Molecular cell *29*, 350-361.

Li, L., Friedrichsen, H.J., Andrews, S., Picaud, S., Volpon, L., Ngeow, K., Berridge, G., Fischer, R., Borden, K.L.B., Filippakopoulos, P*., et al.* (2018). A TFEB nuclear export signal integrates amino acid supply and glucose availability. Nature communications *9*, 2685.

Lieberman, A.P., Puertollano, R., Raben, N., Slaugenhaupt, S., Walkley, S.U., and Ballabio, A. (2012). Autophagy in lysosomal storage disorders. Autophagy *8*, 719-730.

Lim, Y.M., Lim, H., Hur, K.Y., Quan, W., Lee, H.Y., Cheon, H., Ryu, D., Koo, S.H., Kim, H.L., Kim, J*., et al.* (2014). Systemic autophagy insufficiency compromises adaptation to metabolic stress and facilitates progression from obesity to diabetes. Nature communications *5*, 4934.

Lloyd-Evans, E., Morgan, A.J., He, X., Smith, D.A., Elliot-Smith, E., Sillence, D.J., Churchill, G.C., Schuchman, E.H., Galione, A., and Platt, F.M. (2008). Niemann-Pick disease type C1 is a sphingosine storage disease that causes deregulation of lysosomal calcium. Nature medicine *14*, 1247-1255.

Lopez, M.E., Klein, A.D., Dimbil, U.J., and Scott, M.P. (2011). Anatomically defined neuron-based rescue of neurodegenerative Niemann-Pick type C disorder. The Journal of neuroscience : the official journal of the Society for Neuroscience *31*, 4367-4378.

Lopez, M.E., and Scott, M.P. (2013). Genetic dissection of a cell-autonomous neurodegenerative disorder: lessons learned from mouse models of Niemann-Pick disease type C. Disease models & mechanisms *6*, 1089-1100.

Lu, F., Liang, Q., Abi-Mosleh, L., Das, A., De Brabander, J.K., Goldstein, J.L., and Brown, M.S. (2015). Identification of NPC1 as the target of U18666A, an inhibitor of lysosomal cholesterol export and Ebola infection. eLife *4*.

Maekawa, T., Ashihara, E., and Kimura, S. (2007). The Bcr-Abl tyrosine kinase inhibitor imatinib and promising new agents against Philadelphia chromosome-positive leukemias. International journal of clinical oncology *12*, 327-340.

Marin, T., Contreras, P., Castro, J.F., Chamorro, D., Balboa, E., Bosch-Morato, M., Munoz, F.J., Alvarez, A.R., and Zanlungo, S. (2014). Vitamin E dietary supplementation improves neurological symptoms and decreases c-Abl/p73 activation in Niemann-Pick C mice. Nutrients *6*, 3000-3017.

Martina, J.A., Chen, Y., Gucek, M., and Puertollano, R. (2012). MTORC1 functions as a transcriptional regulator of autophagy by preventing nuclear transport of TFEB. Autophagy *8*, 903-914.

Martina, J.A., Diab, H.I., Brady, O.A., and Puertollano, R. (2016). TFEB and TFE3 are novel components of the integrated stress response. The EMBO journal *35*, 479-495.

Medina, D.L., Di Paola, S., Peluso, I., Armani, A., De Stefani, D., Venditti, R., Montefusco, S., Scotto-Rosato, A., Prezioso, C., Forrester, A.*, et al.* (2015). Lysosomal calcium signalling regulates autophagy through calcineurin and TFEB. Nature cell biology *17*, 288-299.

Medina, D.L., Fraldi, A., Bouche, V., Annunziata, F., Mansueto, G., Spampanato, C., Puri, C., Pignata, A., Martina, J.A., Sardiello, M.*, et al.* (2011). Transcriptional activation of lysosomal exocytosis promotes cellular clearance. Developmental cell *21*, 421-430.

Mengel, E., Klunemann, H.H., Lourenco, C.M., Hendriksz, C.J., Sedel, F., Walterfang, M., and Kolb, S.A. (2013). Niemann-Pick disease type C symptomatology: an expert-based clinical description. Orphanet journal of rare diseases *8*, 166.

Munkacsi, A.B., Chen, F.W., Brinkman, M.A., Higaki, K., Gutierrez, G.D., Chaudhari, J., Layer, J.V., Tong, A., Bard, M., Boone, C.*, et al.* (2011). An "exacerbate-reverse" strategy in yeast identifies histone deacetylase inhibition as a correction for cholesterol and sphingolipid transport defects in human Niemann-Pick type C disease. The Journal of biological chemistry *286*, 23842-23851.

Muralidhar, A., Borbon, I.A., Esharif, D.M., Ke, W., Manacheril, R., Daines, M., and Erickson, R.P. (2011). Pulmonary function and pathology in hydroxypropyl-beta-cyclodextin-treated and untreated Npc1(-)/(-) mice. Molecular genetics and metabolism *103*, 142-147.

Napolitano, G., and Ballabio, A. (2016). TFEB at a glance. Journal of cell science *129*, 2475-2481.

Napolitano, G., Esposito, A., Choi, H., Matarese, M., Benedetti, V., Di Malta, C., Monfregola, J., Medina, D.L., Lippincott-Schwartz, J., and Ballabio, A. (2018). mTOR-dependent phosphorylation controls TFEB nuclear export. Nature communications *9*, 3312.

Naureckiene, S., Sleat, D.E., Lackland, H., Fensom, A., Vanier, M.T., Wattiaux, R., Jadot, M., and Lobel, P. (2000). Identification of HE1 as the second gene of Niemann-Pick C disease. Science *290*, 2298-2301.

Nunes, M.J., Moutinho, M., Gama, M.J., Rodrigues, C.M., and Rodrigues, E. (2013). Histone deacetylase inhibition decreases cholesterol levels in neuronal cells by modulating key genes in cholesterol synthesis, uptake and efflux. PloS one *8*, e53394.

Pagan, F., Hebron, M., Valadez, E.H., Torres-Yaghi, Y., Huang, X., Mills, R.R., Wilmarth, B.M., Howard, H., Dunn, C., Carlson, A.*, et al.* (2016). Nilotinib Effects in Parkinson's disease and Dementia with Lewy bodies. Journal of Parkinson's disease *6*, 503-517.

Palmieri, M., Pal, R., Nelvagal, H.R., Lotfi, P., Stinnett, G.R., Seymour, M.L., Chaudhury, A., Bajaj, L., Bondar, V.V., Bremner, L.*, et al.* (2017). mTORC1-independent TFEB activation via Akt inhibition promotes cellular clearance in neurodegenerative storage diseases. Nature communications *8*, 14338.

Park, W.D., O'Brien, J.F., Lundquist, P.A., Kraft, D.L., Vockley, C.W., Karnes, P.S., Patterson, M.C., and Snow, K. (2003). Identification of 58 novel mutations in Niemann-Pick disease type C: correlation with biochemical phenotype and importance of PTC1-like domains in NPC1. Human mutation *22*, 313-325.

Patterson, M.C., Hendriksz, C.J., Walterfang, M., Sedel, F., Vanier, M.T., Wijburg, F., and Group, N.-C.G.W. (2012). Recommendations for the diagnosis and management of Niemann-Pick disease type C: an update. Molecular genetics and metabolism *106*, 330-344.

Paul, C.A., Boegle, A.K., and Maue, R.A. (2004). Before the loss: neuronal dysfunction in Niemann-Pick Type C disease. Biochimica et biophysica acta *1685*, 63-76.

Pentchev, P.G., Boothe, A.D., Kruth, H.S., Weintroub, H., Stivers, J., and Brady, R.O. (1984). A genetic storage disorder in BALB/C mice with a metabolic block in esterification of exogenous cholesterol. The Journal of biological chemistry *259*, 5784-5791.

Pipalia, N.H., Cosner, C.C., Huang, A., Chatterjee, A., Bourbon, P., Farley, N., Helquist, P., Wiest, O., and Maxfield, F.R. (2011). Histone deacetylase inhibitor treatment dramatically reduces cholesterol accumulation in Niemann-Pick type C1 mutant human fibroblasts. Proceedings of the National Academy of Sciences of the United States of America *108*, 5620-5625.

Platt, F.M., Neises, G.R., Dwek, R.A., and Butters, T.D. (1994). N-butyldeoxynojirimycin is a novel inhibitor of glycolipid biosynthesis. The Journal of biological chemistry *269*, 8362-8365.

Polito, V.A., Li, H., Martini-Stoica, H., Wang, B., Yang, L., Xu, Y., Swartzlander, D.B., Palmieri, M., di Ronza, A., Lee, V.M.*, et al.* (2014). Selective clearance of aberrant tau proteins and rescue of neurotoxicity by transcription factor EB. EMBO molecular medicine *6*, 1142-1160.

Roczniak-Ferguson, A., Petit, C.S., Froehlich, F., Qian, S., Ky, J., Angarola, B., Walther, T.C., and Ferguson, S.M. (2012). The transcription factor TFEB links mTORC1 signaling to transcriptional control of lysosome homeostasis. Science signaling *5*, ra42.

Rojas, F., Gonzalez, D., Cortes, N., Ampuero, E., Hernandez, D.E., Fritz, E., Abarzua, S., Martinez, A., Elorza, A.A., Alvarez, A.*, et al.* (2015). Reactive oxygen species trigger motoneuron death in non-cell-autonomous models of ALS through activation of c-Abl signaling. Frontiers in cellular neuroscience *9*, 203.

Sardiello, M., and Ballabio, A. (2009). Lysosomal enhancement: a CLEAR answer to cellular degradative needs. Cell cycle *8*, 4021-4022.

Sardiello, M., Palmieri, M., di Ronza, A., Medina, D.L., Valenza, M., Gennarino, V.A., Di Malta, C., Donaudy, F., Embrione, V., Polishchuk, R.S.*, et al.* (2009). A gene network regulating lysosomal biogenesis and function. Science *325*, 473-477.

Schlatterer, S.D., Acker, C.M., and Davies, P. (2011a). c-Abl in neurodegenerative disease. Journal of molecular neuroscience : MN *45*, 445-452.

Schlatterer, S.D., Tremblay, M.A., Acker, C.M., and Davies, P. (2011b). Neuronal c-Abl overexpression leads to neuronal loss and neuroinflammation in the mouse forebrain. Journal of Alzheimer's disease : JAD *25*, 119-133.

Schulze, H., and Sandhoff, K. (2011). Lysosomal lipid storage diseases. Cold Spring Harbor perspectives in biology *3*.

Settembre, C., and Ballabio, A. (2011). TFEB regulates autophagy: an integrated coordination of cellular degradation and recycling processes. Autophagy *7*, 1379-1381.

Settembre, C., Di Malta, C., Polito, V.A., Garcia Arencibia, M., Vetrini, F., Erdin, S., Erdin, S.U., Huynh, T., Medina, D., Colella, P.*, et al.* (2011). TFEB links autophagy to lysosomal biogenesis. Science *332*, 1429-1433.

Settembre, C., Fraldi, A., Medina, D.L., and Ballabio, A. (2013). Signals from the lysosome: a control centre for cellular clearance and energy metabolism. Nature reviews. Molecular cell biology *14*, 283-296.

Settembre, C., and Medina, D.L. (2015). TFEB and the CLEAR network. Methods in cell biology *126*, 45-62.

Settembre, C., Zoncu, R., Medina, D.L., Vetrini, F., Erdin, S., Erdin, S., Huynh, T., Ferron, M., Karsenty, G., Vellard, M.C.*, et al.* (2012). A lysosome-to-nucleus signalling mechanism senses and regulates the lysosome via mTOR and TFEB. The EMBO journal *31*, 1095-1108.

Spampanato, C., Feeney, E., Li, L., Cardone, M., Lim, J.A., Annunziata, F., Zare, H., Polishchuk, R., Puertollano, R., Parenti, G.*, et al.* (2013). Transcription factor EB (TFEB) is a new therapeutic target for Pompe disease. EMBO molecular medicine *5*, 691-706.

Steingrimsson, E., Copeland, N.G., and Jenkins, N.A. (2004). Melanocytes and the microphthalmia transcription factor network. Annual review of genetics *38*, 365-411.

Sturley, S.L., Patterson, M.C., Balch, W., and Liscum, L. (2004). The pathophysiology and mechanisms of NP-C disease. Biochimica et biophysica acta *1685*, 83-87.

Sturley, S.L., Patterson, M.C., and Pentchev, P. (2009). Unraveling the sterol-trafficking defect in Niemann-Pick C disease. Proceedings of the National Academy of Sciences of the United States of America *106*, 2093-2094.

Tanabe, A., Yamamura, Y., Kasahara, J., Morigaki, R., Kaji, R., and Goto, S. (2014). A novel tyrosine kinase inhibitor AMN107 (nilotinib) normalizes striatal motor behaviors in a mouse model of Parkinson's disease. Frontiers in cellular neuroscience *8*, 50.

Treiber, A., Morand, O., and Clozel, M. (2007). The pharmacokinetics and tissue distribution of the glucosylceramide synthase inhibitor miglustat in the rat. Xenobiotica; the fate of foreign compounds in biological systems *37*, 298-314.

Tsai, K.K., and Yuan, Z.M. (2003). c-Abl stabilizes p73 by a phosphorylation-augmented interaction. Cancer research *63*, 3418-3424.

Tsunemi, T., Ashe, T.D., Morrison, B.E., Soriano, K.R., Au, J., Roque, R.A., Lazarowski, E.R., Damian, V.A., Masliah, E., and La Spada, A.R. (2012). PGC-1alpha rescues Huntington's disease proteotoxicity by preventing oxidative stress and promoting TFEB function. Science translational medicine *4*, 142ra197.

Van Etten, R.A., Jackson, P.K., Baltimore, D., Sanders, M.C., Matsudaira, P.T., and Janmey, P.A. (1994). The COOH terminus of the c-Abl tyrosine kinase contains distinct F- and G-actin binding domains with bundling activity. The Journal of cell biology *124*, 325-340.

Vance, J.E., and Peake, K.B. (2011). Function of the Niemann-Pick type C proteins and their bypass by cyclodextrin. Current opinion in lipidology *22*, 204-209.

Vanier, M.T. (2010). Niemann-Pick disease type C. Orphanet journal of rare diseases *5*, 16.

Vargas, L.M., Cerpa, W., Munoz, F.J., Zanlungo, S., and Alvarez, A.R. (2018). Amyloid-beta oligomers synaptotoxicity: The emerging role of EphA4/c-Abl signaling in Alzheimer's disease. Biochimica et biophysica acta *1864*, 1148-1159.

Walkley, S.U., and Suzuki, K. (2004). Consequences of NPC1 and NPC2 loss of function in mammalian neurons. Biochimica et biophysica acta *1685*, 48-62.

Walterfang, M., Fahey, M., Desmond, P., Wood, A., Seal, M.L., Steward, C., Adamson, C., Kokkinos, C., Fietz, M., and Velakoulis, D. (2010). White and gray matter alterations in adults with Niemann-Pick disease type C: a cross-sectional study. Neurology *75*, 49-56.

Wang, W., Gao, Q., Yang, M., Zhang, X., Yu, L., Lawas, M., Li, X., Bryant-Genevier, M., Southall, N.T., Marugan, J.*, et al.* (2015). Up-regulation of lysosomal TRPML1 channels is essential for lysosomal adaptation to nutrient starvation. Proceedings of the National Academy of Sciences of the United States of America *112*, E1373-1381.

Xiao, Q., Yan, P., Ma, X., Liu, H., Perez, R., Zhu, A., Gonzales, E., Burchett, J.M., Schuler, D.R., Cirrito, J.R.*, et al.* (2014). Enhancing astrocytic lysosome biogenesis facilitates Abeta clearance and attenuates amyloid plaque pathogenesis. The Journal of neuroscience : the official journal of the Society for Neuroscience *34*, 9607-9620.

Xiao, Q., Yan, P., Ma, X., Liu, H., Perez, R., Zhu, A., Gonzales, E., Tripoli, D.L., Czerniewski, L., Ballabio, A.*, et al.* (2015). Neuronal-Targeted TFEB Accelerates Lysosomal Degradation of APP, Reducing Abeta Generation and Amyloid Plaque

Pathogenesis. The Journal of neuroscience : the official journal of the Society for Neuroscience *35*, 12137-12151.

Yanez, M.J., Belbin, O., Estrada, L.D., Leal, N., Contreras, P.S., Lleo, A., Burgos, P.V., Zanlungo, S., and Alvarez, A.R. (2016). c-Abl links APP-BACE1 interaction promoting APP amyloidogenic processing in Niemann-Pick type C disease. Biochimica et biophysica acta *1862*, 2158-2167.

Yang, X.J., and Seto, E. (2003). Collaborative spirit of histone deacetylases in regulating chromatin structure and gene expression. Current opinion in genetics & development *13*, 143-153.

Yang, X.J., and Seto, E. (2008). Lysine acetylation: codified crosstalk with other posttranslational modifications. Molecular cell *31*, 449-461.

Yevenes, L.F., Klein, A., Castro, J.F., Marin, T., Leal, N., Leighton, F., Alvarez, A.R., and Zanlungo, S. (2012). Lysosomal vitamin E accumulation in Niemann-Pick type C disease. Biochimica et biophysica acta *1822*, 150-160.

Yoshida, K., Yamaguchi, T., Natsume, T., Kufe, D., and Miki, Y. (2005). JNK phosphorylation of 14-3-3 proteins regulates nuclear targeting of c-Abl in the apoptotic response to DNA damage. Nature cell biology *7*, 278-285.

Zervas, M., Somers, K.L., Thrall, M.A., and Walkley, S.U. (2001). Critical role for glycosphingolipids in Niemann-Pick disease type C. Current biology : CB *11*, 1283-1287.

Zhang, J., Wang, J., Zhou, Z., Park, J.E., Wang, L., Wu, S., Sun, X., Lu, L., Wang, T., Lin, Q.*, et al.* (2018). Importance of TFEB acetylation in control of its transcriptional activity and lysosomal function in response to histone deacetylase inhibitors. Autophagy *14*, 1043-1059.

Zhou, S.Y., Xu, S.J., Yan, Y.G., Yu, H.M., Ling, S.C., and Luo, J.H. (2011). Decreased purinergic inhibition of synaptic activity in a mouse model of Niemann-Pick disease type C. Hippocampus *21*, 212-219.